Ο ρόλος της ιντερλευκίνης-33 στους μηχανισμούς φυσικής ανοσίας που επάγουν την αυτοανοσία στον Συστηματικό Ερυθηματώδη Λύκο (ΣΕΛ)

Σπύρος Γεωργάκης

Εργαστήριο Ρευματολογίας, Αυτοανοσίας και Φλεγμονής

Ιατρική σχολή, Πανεπιστήμιο Κρήτης

Επιβλέπων Δρ. Γεώργιος Μπερτσίας

Ηράκλειο, 2021

«Το έργο συγχρηματοδοτείται από την Ελλάδα και την Ευρωπαϊκή Ένωση (Ευρωπαϊκό Κοινωνικό Ταμείο) μέσω του Επιχειρησιακού Προγράμματος «Ανάπτυξη Ανθρώπινου Δυναμικού, Εκπαίδευση και Διά Βίου Μάθηση», στο πλαίσιο της Πράξης «Ενίσχυση του ανθρώπινου ερευνητικού δυναμικού μέσω της υλοποίησης διδακτορικής έρευνας» (MIS-5000432), που υλοποιεί το Ίδρυμα Κρατικών Υποτροφιών (ΙΚΥ)»

Interleukin-33 and its contribution on innate immune mechanisms that mediate autoimmune manifestations of Systemic Lupus Erythematosus (SLE)

Spiros Georgakis

Laboratory of Rheumatology, Autoimmunity and Inflammation

School of Medicine, University of Crete

Supervised by Dr. George Bertsias

Heraklion,2021

«This research is co-financed by Greece and the European Union (European Social Fund- ESF) through the Operational Programme «Human Resources Development, Education and Lifelong Learning» in the context of the project "Strengthening Human Resources Research Potential via Doctorate Research" (MIS-5000432), implemented by the State Scholarships Foundation (IKY)»

Ευχαριστίες

Πάγια άποψη μου είναι οτι οι ευχαριστίες δεν θα έπρεπε να εκφράζονται λεκτικά αλλα με πράξεις. Παρολαυτά, μετα απο μια περιπέτεια σαν αυτή της διδακτορικής δατριβής θα ήταν άδικο και άκομψο να μην εκφράσω την ευγνωμοσύνη σε όλους αυτούς που με στήριξαν άμεσα ή έμμεσα.

Αρχικά θα ήθελα να ευχαριστήσω τον επιβλέποντα μου κ. Γιώργο Μπερτσία για την εμπιστοσύνη που μου έδειξε, για ότι μου έμαθε και για την όμορφη συνεργασία που είχαμε. Ο κ. Παναγιώτης Βεργίνης, που επίσης επέβλεψε την ερευνητική μου περιπέτεια κατα την διάρκεια του διδακτορικού, με βοήθησε ιδαίτερα με τις υποδείξεις του, τις συμβουλές του και τον ειλικρινή του επιστημονικό σκεπτικισμό. Ειλικρινείς ευχαριστίες και στον καθηγητή κ. Πρόδρομο Σιδηρόπουλο για την συνεισφορά του στο να μάθω να τοποθετώ την επιστημονική σκέψη στο σωστό εννοιολογικό πλαίσιο αλλα και για την στήριξη του. Ευχαριστώ τέλος και τον καθηγητή κ. Δημήτριο Μπούμπα για την πάντα εύστοχη επιστημονική κριτική και για την βοήθεια του.

Ευχαριστώ, επίσης, και την οικογένεια μου . Όλοι σας με στηρίξατε με κάθε τρόπο έστω και απο χιλιόμετρα μακριά. Ο πατέρας μου, Άγγελος, πάντα ηταν το πρότυπο μου και μου μετέδωσε είτε γενετικά είτε επιγενετικά την αστείρευτη του λατρεία για την γνώση, το διάβασμα αλλα και την αυτοπειθαρχία. Η μητέρα μου, Μαριατένα, με την ανιδιοτελή της αγάπη και φροντίδα με έκανε καλύτερο άνθρωπο και ικανό να ανταπεξέλθω σε οτιδήποτε προκύπτει. Οι αδελφές μου , Φωτεινή και Βασιλιάνα, είναι τα άτομα για τα οποία νιώθω εγω ανιδιοτελή και αστείρευτη αγάπη και τις ευχαριστώ που υπάρχουν και με στηρίζουν. Δεν θα μπορούσα να μην αναφερθώ και στην οικογένεια που διάλεξα, τους φίλους και τις φίλες μου απο το Ηράκλειο, την Αθήνα , τα Γιάννενα κλπ. ‘Ολοι έχετε συνδράμει με τον τρόπο σας στο να γίνω αυτο που είμαι και όποια μελλοντική μικρή ή μεγάλη επιτυχία οφείλεται σε εναν βαθμό σε εσάς και στην αγάπη που μου δείξατε.Θα ήθελα όμως να κάνω ειδική μνεία σε τρία άτομα: τους αδελφικούς μου φίλους , Γιώργο και Γιάννη και την σύντροφο μου Εύα. Ο Γιώργος και ο Γιάννης αποτελούν τους συνοδοιπόρους μου τα τελευταία 13 χρόνια και έχουμε μοιραστεί τα πάντα: σπίτι , φαγητό, φοβερές εμπειρίες. Οι συζητήσεις μας και οι κοινές εμπειρίες μας με έχουν διαμορφώσει και θα συνεχίσουν να με διαμορφώνουν στο μέλλον. Είστε απο τους λίγους ανθρώπους που γνωρίζετε ποίος πραγματικά είμαι και με τιμάτε με την φιλία σας.

Η σύντροφος μου Εύα αποτέλεσε το πιο ισχυρό στήριγμα μου κατα την περίοδο της διδακτορικής μου διατριβής. Αποτελεί την αυστηρότερη κριτή αλλα ταυτόχρονα και θαυμάστρια όσων πράττω. Η τρυφερότητα και η στηριξή της αποτελούσαν και αποτελούν κινητήριο δύναμη στο να ανταπεξέλθω σε ότι μου προέκυψε και προκύπτει και την ευχαριστώ απο τα βάθη της καρδιάς μου.

Ευχαριστώ θερμά και τις φανταστικές συνεργάτιδες μου που έκαναν όμορφη την καθημερινότητα μου και με την παρουσία τους αλλα και με την συντροφιά τους. Λυπάμαι αν κάποια στιγμη σας στεναχώρησα με την απότομη συμπεριφορά μου αλλα μετα απο τόσα χρόνια φαντάζομαι γνωρίζετε ότι αν αυτό συνέβη δεν ήταν σε καμία περίπτωση λόγω εμπάθειας. Η βοήθεια σας, ψυχολογική ή πρακτική, ήταν καθοριστική. Σας εύχομαι κάθε επιτυχία σε όλους τους τομείς.

Τέλος, θέλω να ευχαριστήσω θερμά όλους τους περιφερειακούς συνεργάτες που βοήθησαν και διευκόλυναν την ζωή μου κατα την διάρκεια της διαδακτορικής μου διατριβής. Το προσωπικό της αιμοδοσίας και της Ρευματολογικής κλινικής του ΠΑΓΝΗ, το προσωπικό του εργαστηρίου Παθολογο-Ανατομίας της Ιατρικής Σχολης Ηρακλείου και τον αν. Καθηγητή κ. Ηλία Δράκο για την τεχνική βοήθεια και τις συμβουλές, αντίστοιχα.

Table of contents

1) Abstract

Systemic Lupus erythematosus (SLE) is the prototypic systemic autoimmune disease characterized by aberrant immune activation, defective clearance mechanisms, autoantibody formation, immune complexes accumulation and a profound type I IFN gene signature. One of the primary sources of IFN-α are plasmacytoid dendritic cells (pDCs) especially in response to Toll-like receptor(TLR)-7/9- and nucleic acid cytoplasmic sensors-mediated signaling. Additionally, transcriptomic and functional assays indicated that SLE neutrophils exhibit an over-activated status and enhanced capacity to form chromatin extracellular traps (NETs) which are considered key players in SLE pathogenesis. Pathogenic vicious feedback loops taking place in SLE can subsequently lead to end organ damage.

Interleukin-33 (IL-33), a nuclear alarmin released mainly during necrotic cell death, exerts context-specific effects on adaptive and innate immune cells eliciting potent inflammatory or anti-inflammatory responses. The soluble regulatory receptor of IL-33, sST2, was monitored to display up-regulated levels in SLE patients' sera and was correlated to disease severity and renal involvement. IL-33 is mainly expressed by non-hematopoietic cells of barrier tissues while recent findings suggest it is also released by immune cells upon inflammatory or damage/death-related stimuli. Until now, the role of neutrophil-derived IL-33 in autoimmunity has not been investigated. The main research questions addressed in this study are a) if SLE neutrophils exhibit differential expression levels of IL-33, b) If SLE-relevant stimuli promote the release of IL-33 decorated NETs, c) if SLE NETs display their inflammatory effects in an IL-33-dependent manner and, d) if IL-33 decorated NETs exhibit in vivo significance regarding SLE pathogenesis.

Herein, we demonstrated that SLE neutrophils exhibit relatively increased *IL-33* mRNA levels and the ability to release IL-33 decorated NETs both spontaneously and after IC-stimulation. IC-mediated NETs enhance IFN-α response by pDCs in a IL33R- (ST2L-) and IRF-7-dependent manner. *IL33*-silenced neutrophil-like cells cultured under lupus-inducing conditions generated NETs with diminished interferogenic effect. Notably, a focused proteomic analysis (PRM) and ex vivo functional aasays

revealed that SLE patient-derived NETs are enriched in mature bioactive isoforms of IL-33 processed by the neutrophil proteases elastase and cathepsin G. Pharmacological inhibition of these proteases neutralized IL-33-dependent IFN-α production elicited by NETs. Regarding their in vivo significance in SLE, IL-33 decorated NETs were found up-regulated in SLE patients' peripheral blood and were also detected at relevant inflamed tissues (kidneys, skin).

To conclude, by using a combination of molecular, imaging and proteomic approaches, we revealed that SLE neutrophils -activated by disease immunocomplexes- release bioactive IL-33-bearing NETs exhibiting potent interferogenic capacity. These data support a novel role for cleaved IL-33 alarmin decorating NETs in human SLE, linking neutrophil activation, IFN-α production and end-organ inflammation.

Keywords: neutrophils, proteases, alarmins, IL-1 family, interferon-α, autoimmunity, Neutrophil extracellular traps (NETs), Systemic Lupus Erythematosus, plasmacytoid dendritic cells (pDCs)

1) Περίληψη

Ο Συστηματικός Ερυθηματώδης Λύκος (ΣΕΛ) αποτελεί την πρωτότυπη συστηματική ασθένεια και χαρακτηρίζεται απο ανοσιακή ενεργοποίηση, ανεπάρκεια των μηχανισμών καθαρισμού της φλεγμονής, παραγωγή αυτοαντισωμάτων , σχηματισμό και συσσώρευση ανοσοσυμπλεγμάτων αλλά και απο την χαρακτηριστική γονιδιακή ‘’σφραγίδα’’ ιντερφερόνης-α. Μια από τις κύριες πηγές ιντερφερόνης-α είναι τα πλασματοκυτταροειδή δενδριτικά κύτταρα μετά απο ενεργοποίηση των σηματοδοτικών μονοπατιών των υποδοχέων τύπου Toll 7 και 9 (TLR7/9) και των κυτταροπλασματικών υποδοχέων νουκλεικών οξέων. Πρόσφατες γονιδιακές και άλλες λειτουργικές μελέτες προτείνουν οτι τα ουδετερόφιλα ασθενών με ΣΕΛ χαρακτηρίζονται απο αυξημένη ενεργοποίηση και τάση να απελευθερώνουν εξωκυττάριες παγίδες χρωματίνης (NETs) αποτελώντας έτσι ρυθμιστές της παθογένειας της νόσου.Οι επιζήμιοι ανατροφοδοτικοί βρόχοι που λαμβάνουν χώρα στον ΣΕΛ οδηγούν συχνά σε ιστική βλάβη τελικού σταδίου.

Η ιντερλευκίνη-33, μια πυρηνική πρωτείνη κινδύνου που απελευθερώνεται κατα την διάρκεια του νεκρωτικού κυτταρικού θανάτου, έχει ποικίλες επιδράσεις στα κύτταρα της επίκτητης και της φυσικής ανοσίας ανάλογα με το πλαίσιο στο οποίο μελετάται. Ο διαλυτός υποδοχέας της IL-33, sST2, έχει αυξημένα επίπεδα στον ορό ασθενών με ΣΕΛ που συσχετίζονται με την ενεργότητα της ασθένειας και με την εκδήλωση νεφρίτιδας. Η ιντερλευκίνη-33 εκφράζεται κυρίως απο κύτταρα της μη αιμοποιητικής σειράς των ιστών φραγμού αλλα πρόσφατα δεδομένα υποδεικνύουν πως μπορεί και να εκκριθεί απο κύτταρα του ανοσοποιητικού συστήματος αν ενεργοποιηθούν με φλεγμονώδη ερεθίσματα ή ερεθίσματα που σχετίζονται με βλάβη ή θάνατο. Μέχρι σήμερα, ο ρόλος της προερχόμενης απο ουδετερόφιλα IL-33 στην ανάπτυξη αυτοανοσιας δεν έχει ερευνηθεί. Τα κύρια ερευνητικά ερωτήματα που τίθενται σε αυτήν την έρευνα είναι: α) αν τα ΣΕΛ ουδετερόφιλα χαρακτηρίζονται απο σχετικά αυξημένη έκφραση της IL-33 β) αν διεγερτικά μόρια που σχετίζονται με τον ΣΕΛ μπορούν να προκαλέσουν απελευθέρωση εξωκυττάριων παγίδων ουδετεροφίλων (NETs) διακοσμημένων με IL-33 γ) αν τα ΣΕΛ NETs παρουσιάζουν φλεγμονώδεις επιδράσεις που εξαρτώνται απο την IL-33 δ) αν τα NETs που διακοσμούνται με IL-33 έχουν κάποια in vivo σημασία που σχετίζεται με την παθογένεια του ΣΕΛ.

Σε αυτήν την έρευνα, αποδείξαμε ότι τα ΣΕΛ ουδετερόφιλα παρουσιάζουν συγκριτικά αυξημένα επίπεδα *IL-33* mRNA και έχουν την ικανότητα να απελευθερώνουν εξωκυττάριες παγίδες διακοσμημένες με IL-33

αυθόρμητα ή μετά απο ενεργοποίηση με χρήση ανοσοσυμπλεγμάτων. Οι επαγόμενες απο ανοσοσυμπλέγματα- εξωκυττάριες παγίδες επάγουν την παραγωγή ιντερφερόνης-α (IFN-α) απο τα πλασματοκυτταροειδή δενδριτικά κύτταρα (pDCs) μέσω του υποδοχέα της IL-33 (ST2L) ενεργοποιώντας τον μεταγραφικό παράγοντα IRF-7. Οταν αποσιωπήθηκε το γονίδιο της *IL-33* σε κυτταρική σειρά που προσομοιάζει τα ουδετερόφιλα κάτω απο συνθήκες πάρομοιες με αυτές που υπάρχουν στο περιβάλλον του ΣΕΛ, οι εξωκυττάριες παγίδες που δημιουργήθηκαν είχαν μειωμένη ικανότητα να προάγουν την έκκριση IFN-α. Μια στοχευμένη πρωτεομική μελέτη (PRM) και ex vivo λειτουργικά πειράματα αποκάλυψαν οτι στις εξωκυττάριες παγίδες των ασθενών με ΣΕΛ εντοπίζονται βιοενεργές ισομορφές της IL-33 που προέρχονται απο την επεξεργασία μέσω πρωτεασών των ουδετεροφίλων, όπως είναι η ελαστάση και η καθεψίνη G. Φαρμακευτική αναστολή αυτών των πρωτεασών εξουδετέρωσαν την επαγόμενη απο IL-33 παραγωγή IFN-α που προκαλείται μέσω των NETs. Όσον αφορά την in vivo σημασία τους στον ΣΕΛ, εξωκυττάριες παγίδες διακοσμημένες με IL-33 παρουσίασαν αυξημένα επίπεδα στο περιφερικό αίμα ασθενών ΣΕΛ ενω εντοπίστηκαν και σε χαρακτηριστικούς φλεγμαίνοντες ιστούς (νεφροί,δέρμα).

Συνοψίζοντας, επιστρατεύοντας εναν συνδυασμό απο μοριακές ,απεικονιστικές και πρωτεομικές προσεγγίσεις αποκαλύψαμε ότι τα ΣΕΛ ουδετερόφιλα – όταν ενεργοποιούνται με ανοσοσυμπλέγματα σχετιζόμενα με την ασθένεια- απελευθερώνουν εξωκυττάριες παγίδες που φέρουν βιοδραστική IL-33 και διακρίνονται απο την ικανότητα τους να επάγουν την παραγωγή IFN-α. Αυτά τα δεδομένα υποδεικνύουν ένα σημαντικό ρόλο για την βιοδραστικη πρωτείνη κινδύνου IL-33 που διακοσμεί τα NETs των ανθρώπων με ΣΕΛ, συνδέοντας την ενεργοποίηση των ουδετεροφίλων , την παραγωγή IFN-α και την τελικού σταδίου ιστική φλεγμονή.

2) Abbreviations

NETs	Neutrophil extracellular traps
SLE	Systemic Lupus Erythematosus
IL-33	Interleukin-33
IFN-α	Interferon-α
PAD4	Peptidylarginine deiminase-4
RA	Rheumatoid arthritis
LDGs	Low density granulocytes
pDCs	Plasmacytoid dendritic cells
ICs	Immune complexes
HMGB-1	High mobility group box-1
CitH3	Citrullinated histone-3
ST2	Suppression of tumorigenicity -2
IL-1a	Interleukin-1a
PRM	Parallel Reaction Monitoring
Th1-2-17	T helper cells-1-2-17
Tregs	T regulatory cells
TNF-α	Tumor necrosis factor-α
ISGs	Interferon Stimulated genes
IRF5-7-9	Interferon regulatory factor5-7-9
MPO	Myeloperoxidase

3) Introduction

3.1 Autoimmunity

Self-destructive behavior

The psychologic burden that people carry and which is created by living in a world of speed, economic violence, social repression and impersonal relationships, can drive to self-destructive behavior. Self-destructive behavior is any behavior that is harmful or potentially harmful towards the person who engages it. This ‘abnormal’ reaction was first studied in 1895 by Freud and Ferenczi (Weiss H., 2020). Freud concluded later that self destructive behaviors are fueled by one's superego and his/her aggression potential. The superego is the ethical base of someone’s personality and provides the moral standards by which the ego operates. To make it more simple, the superego describes how we believe that an ideal person would act regarding on our point of view of what is ethical. So, self-destructive behavior can be triggered mainly by the environment (that shapes superego in our early years) combined with a genetic background that provides susceptibility (genetic predisposition to aggression appears to be deeply affected by the polymorphic genetic variants of the serotoninergic system that influences serotonin levels in the central and peripheral nervous system (Pavlov et al., 2012)). Self-destructive behaviour can also take place in cell-level and not only in a person-level. Human body is consisted of different cell-based systems which operate simultaneously in an elegant manner. It is not surprising that those systems can react abnormally during stress. To be more specific, **immune system works in a perfectly accurate manner but in a predisposed genetic background combined with environmental pressure our delicate immune mechanisms can be self-destructive**.

Defining autoimmunity

Autoimmunity is a pathologic condition in which a misdirected immune response against self-antigens is developed leading to various of deleterious symptoms. In most of the autoimmune comorbidities, a variety of environmental factors act in genetically susceptible individuals leading to loss of immune tolerance and

aberrant immune activation against self- body components and tissues. Autoimmune-based pathologies affect nearly 8% of western world population lowering significantly the life quality of patients, augmenting the financial burden of national health care systems and/or individuals and resulting in a significant amount of deaths yearly although the 10-year survival rate has significantly increased the last 50 years (Singh R. et al.,2018)

3.2 Systemic lupus erythematosus

Autoimmune diseases can be classified according to several criteria. One of them is the location of the autoimmune attack. Based on this criterion, autoimmune diseases are distinguished into systemic or organ-specific. Systemic lupus erythematosus (SLE) is the prototypic systemic autoimmune disease although it took almost 100 years for physicians to realize that it was not just a skin entity. The aberrant immune response occurring in SLE patients is characterized by the production of autoantibodies against cell nuclear components in association with a diverse array of clinical manifestations the exact patho-aetiology of which still remains elusive. Except skin tissue, the deleterious immune activation of SLE patients may affect multiple vital organs and tissues such as the brain, blood and the kidney (Tsokos G., 2020).

SLE & organ involvement

SLE-associated morbidity is inevitably correlated with end-organ damage. One of the most severe and frequent implication of SLE is Lupus Nephritis (LN) in which activated immune cells infiltrate the kidney. Immune cell derivatives and immune complexes deposition in the glomerulus lead to kidney failure. One additional well-described tissue manifestation related to SLE is this of skin (Cutaneous Lupus). UV radiation promotes keratinocytes' cell death which leads to an abnormal immune response against nuclear self-antigens resulting in the characteristic skin lesions of patients. Except of kidneys and skin the deleterious immune system activation of SLE can affect the central nervous system (Neuropsychiatric Lupus) and the cardiovascular system, the clinical manifestations of which are quite diverse among patients (Tsokos et al., 2020).

SLE: Environmental stress and Genetic predisposition

In SLE, a complex multifactorial contribution of environmental factors, genetic susceptibility and sex hormones orchestrate the immune dysregulation. SLE prevalence ranges from 20 to 150 cases per 100,000 people while it exhibits a strong female of childbearing age-bias (9:1 female to male ratio) (Mok C., 2003). The increased SLE prevalence of women is of great interest and until now it is mainly explained by estrogen-dependent signaling and double dosage of immune-related genes due to X-chromosome inactivation escape that is reported taking place in SLE patients (Syrret C. et al,2019). Moreover, racial or ethnic groups of African, Hispanic and Asian ancestry display an increased prevalence of SLE and end-organ damage as compared to Caucasians (Lanata C. et al.,2019).

Environmental factors and life-quality contribute to initiation and development of SLE. More specifically, air pollution, ultraviolet light, infections, vaccinations, smoking, pesticides, and heavy metals such as mercury, were reported to be related to SLE risk. Those distinct factors modulate the systemic immune response leading to inflammatory cytokine secretory burst, by increasing oxidative stress as well as by altering epigenetic modifications of immune-related genes (Barbhaiya M. et al., 2016). Additionally, alterations in intestinal and oral microbiota were correlated with SLE development or flare in lupus-prone mice and human patients. while SLE patients' gut microbiota was reported to br characterized by decreased diversity (Silverman G. et al., 2019). In any case, the role of altered microbiome in SLE has to be further investigated.

Genetic susceptibility is also a pivotal factor of SLE prevalence. The concordance of the disease in twins (in identical twins the concordance is approximately 25–50% while in dizygotic twins is around 5%) and the increased SLE risk of SLE patients' siblings imply a polygenic inheritance of the disease. Genome Wide Association Studies (GWAS) had monitored many genes that contribute to disease susceptibility while only in a small proportion of SLE patients (<5%) a single gene is responsible. Expectedly, most of the single nucleotide polymorphisms (SNPs) reported in SLE fall within noncoding DNA regions of immune response–related genes regulating thus their transcription indirectly. There are some genes associated with predisposition for several autoimmune diseases (like *STAT4* and *PTPN22*) but there are also others that appear to increase the risk for SLE specifically (*IRF5, TREX1, ITGAM, C1QA, C4, FCGR3A, PRDM1,*

TNFAIP3, TNIP1, IL10 etc). (Tsokos G.,2011). Additionally, a proportion of heritability in SLE cannot be explained by GWAS data alone, epigenetic mechanisms, such as DNA methylation and post-translational histone modification regulating the gene expression appear to display a role in lupus pathogenesis. Therefore, future epigenome-centered studies will probably reveal the exact mechanism of abnormal gene regulation that drives to SLE (Rose T. et al., 2017).

To sum up, a combination of genetic susceptibility, environmental factors and hormones promote immune dysregulation, aberrant immune activation and end-organ damage that characterize SLE pathogenesis (**figure 1**). The question arose was about which are the key cells that drive SLE progression. Considering that SLE terminology is governed by the terms autoantigen, autoantibody and autoreactive T, B cells, someone could argue that the adaptive immune system is mainly responsible for SLE deleterious symptoms. On the contrary, innate immune cells also significantly contribute to SLE-related sterile inflammation by exerting their own pro-inflammatory functions or by activating adaptive immune cells (Paulson J., 2007). Notably, deficient apoptotic cell- and immune complex- clearance mechanisms strongly affect SLE pathogenesis. Additionally, non-hematopoietic cells were also described as mediators of SLE initiation and SLE-related end organ damage (Der A. et al.,2019, Psarras A. et a., 2020).

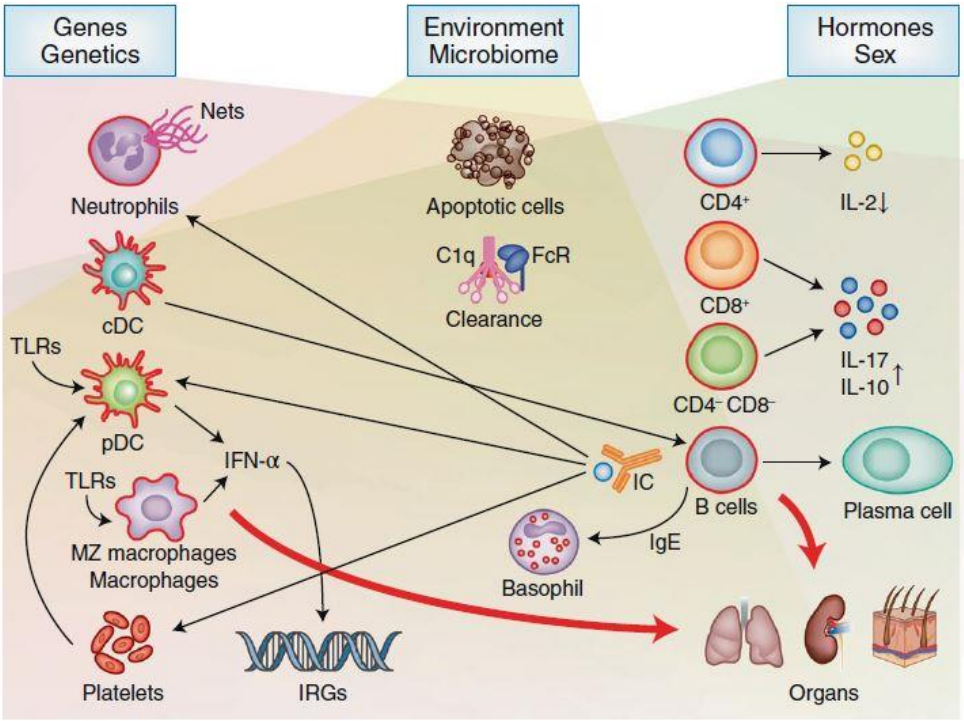

Figure 1: The pathogenetic landscape of SLE. Genetic, environmental and hormonal factors act on various elements of the innate and adaptive immune responses (Tsokos et al., Nature Immunology, 2020)

3.3 Adaptive immunity in SLE pathogenesis

SLE B cells

Autoantibodies against a variety of self-antigens is a hallmark of lupus-related pathogenesis. ANA positivity is an important criterion for the classification of SLE. Additionally, immune complexes formed by autoantibodies are potent mediators of SLE pathogenesis and end-organ damage. Normally, autoreactive B cells are deleted from the B-cell repertoire in the bonne marrow during their development or in the periphery. In SLE patients, self-reactive naïve B cells are not depleted, and increased numbers of circulating mature autoreactive B cells are detectable in the periphery. B cell antigen receptor (BCR)–sequencing studies in SLE pediatric patients revealed that defects at distinct checkpoints in early B cell development accounted for autoantibody production while peripheral tolerance (taking place in peripheral lymphoid organs and extrafollicular sites of B cell maturation) was also reported to be defective (Yurasov J. et al.,2005).

Plasmablasts and IgD- CD27- B cells are expanded in SLE periphery, associated to autoantibody production and tightly correlated to disease severity. Interestingly, both mature (CD27+) and naïve (CD27-) B cells contribute to over-activated SLE-humoral response. Importantly, IgD- CD27- B cells were found to be hyperresponsive to TLR7 ligands and IL-21 (Jenks s. et al., 2018). Memory B cells are also increased in SLE patients (Nakano M. et al., 2021) while IL-10-producing CD24+CD38hi B regulatory cells (Bregs) generation is disturbed in SLE (Menon M. et., 2016). To sum up, B cells are of high significance regarding SLE pathogenesis, a notion that is further confirmed by the plasmablast gene signature which characterizes the blood and kidneys of active SLE and LN patients respectively (Panousis N. et al., 2019, Arazi A. et al., 2019). Of note, B cells are used as therapeutic targets for SLE amelioration (rituximab, belimumab) while additional CAR-T cell-related approaches are designed in order to deplete them (Kansal R., 2019).

SLE T cells

T-cells are key players in promoting autoimmunity of SLE mainly by helping B-cell dependent responses or by exerting pro-inflammatory cytokine-mediated properties. It is well-established that T cells are consisted of different subsets. Autoreactive CD4+ T cells were described to respond to nucleosomal antigens and to augment the production of IgG autoantibodies against histone-DNA complex in vitro (Mohan C. et al.,1993).

Although CD8+ T cells are not the most potent mediators of SLE pathogenesis, they are the main cause of SLE patients' increased infection rate due to their reduced cytotoxic capacity and decreased production of granzymes and perforin. Interestingly, those cytotoxic cells express increased levels of CD38 in SLE patients which is a marker of T cell exhaustion associated to reduced expression of cytotoxicity- related molecules (Katsuyama E. et al., 2020). SLE T follicular cells (Tfh), expressing CXCR5 and PD-1, drive B-cell proliferation, isotype-switching and somatic hypermutation in an IL-21-dependent fashion (Craft J., 20212). Notably, a recently described CXCR5–CXCR3+PD-1+ extrafollicular T cell population is present in the periphery and in kidney tissues of SLE patients, and provides help to B cells by producing IL-10 and succinate (Caielli S. et al., 2019). T regulatory cells (Tregs) are potent anti-inflammatory mediators which were reported to display decreased percentage at the early stages of SLE (Sharabi A. et al., 2018).

Taking into consideration that Tregs express high affinity IL-2 receptor, an IL-2 low dose administration-based therapeutic approach was used in lupus prone mice. In those mice, Tregs were expanded while Th17 cells, which are crucial mediators of Lupus Nephritis in SLE murine models, were significantly decreased (Mizui M. et al., 2014). This approach seems to be clinically beneficial also in human SLE (He J. e al., 2016).

.

3.4 Innate Immunity in SLE pathogenesis

SLE is typically defined as an aberrant response of lymphocytes against self-antigens that ultimately leads to tissue damage. It is well-established, that SLE is a complex multifactorial autoimmune condition so it was not surprising that innate immune cells were found to contribute also to lupus pathogenesis both as antigen presenting cells and as effector cells that mediate tissue damage. Additionally, SLE myeloid cells were found to exhibit deficient apoptotic cells- and immune complexes-clearance capacity augmenting thus the source of potential autoantigens. Innate immunity importance was proved initially by investigating the phenotype of *motheaten* (tyrosine phosphatase SHP1 deficient) and *αM-II* (a-mannosidase deficient) mouse models. Those mice developed a characteristic lupus-like phenotype which was not rescued when they were crossed with *Rag1-/-* mice (unable to develop adaptive immune response due to lack of T, B cells). So, in both cases, the lupus-like phenotype was developed due to innate immune cells aberrant activation (Paulson J., 2007). Regarding human SLE, multiple high throughput genetic studies revealed that SLE is governed mainly by two gene signatures, IFNa and granulopoiesis signature, confirming thus the pivotal contribution of innate immunity on its pathogenic mechanisms (Bennet L. et al.,2003, Panousis N. et al., 2019). Innate immunity is consisted of several cell types, like dendritic cells macrophages, monocytes, basophils and neutrophils each of which can promote SLE-related symptoms using distinct mechanisms.

SLE macrophages / SLE monocytes / SLE dendritic cells / SLE basophils

To begin with, macrophages and monocytes promote SLE pathogenesis either by secreting pro-inflammatory cytokines or by exhibiting impaired clearance capacity increasing thus the potential

autoantigen pool. Macrophages are categorized into two main subgroups: the pro-inflammatory M1 subtype and the M2 subtype which is mainly implicated in homeostasis and tissue repair –related mechanisms.

In SLE, M1/M2 ratio was found to be altered in favor of M1 phenotype (Labonte AC. Et al., 2018). Splenic marginal zone murine macrophages exhibit decreased phagocytic potential in a TRL7- and IFN- dependent fashion leading to impaired clearance of apoptotic cells and immune complexes of lupus prone mice (Li H. et al.,2015). It should also be noted that IFN type I and tumor necrosis factor (TNFa) cooperate to create an inflammatory gene signature in monocytes, and such cooperation also occurs in monocytes from SLE patients (Park S. et al., 2017). Recent findings, described a distinct cytotoxic subset of monocytes (CD14+CD16+) that exhibit increased levels in the periphery and infiltrated in kidneys of active SLE patients correlating with disease severity (Mukherjee R. et al.,2015, Arazi A. et al., 2019). Moreover, in vitro stimulation of monocytes with SLE serum strongly enhances their antigen presenting capacity in an IFN-dependent manner (Blanco P. et al., 2001). Dendritic cells (DCs) link innate and adaptive immune responses and their hyper-activated profile may trigger autoimmune responses. In some cases, dendritic cells exhibit decreased levels in SLE peripheral blood but this can be explained by the increased levels monitored in inflamed tissues where they are accumulated, secreting pro-inflammatory cytokines and helping T and B cells to exert their autoantigen-specific responses. Stimulation of dendritic cells using RNA-containing immune complexes leads to OX40L overexpression which subsequently drives Tfh generation inducing thus autoimmune humoral responses (Jacquemin C. et al., 2015). Basophils activated status in periphery and IgE immune complexes deposited in LN patient kidneys revealed that those polymorphonuclear cells, despite their low abundance, are involved in SLE progression (Charles N. et al., 2010). As it is already mentioned, SLE peripheral blood and tissues are characterized by IFN-α and granulopoiesis gene signatures. Taking into consideration that this dissertation is focused on pDCs and neutrophils pathogenic interaction occurring in SLE, those innate immune cells and their interesting pathogenic features will be examined in depth separately.

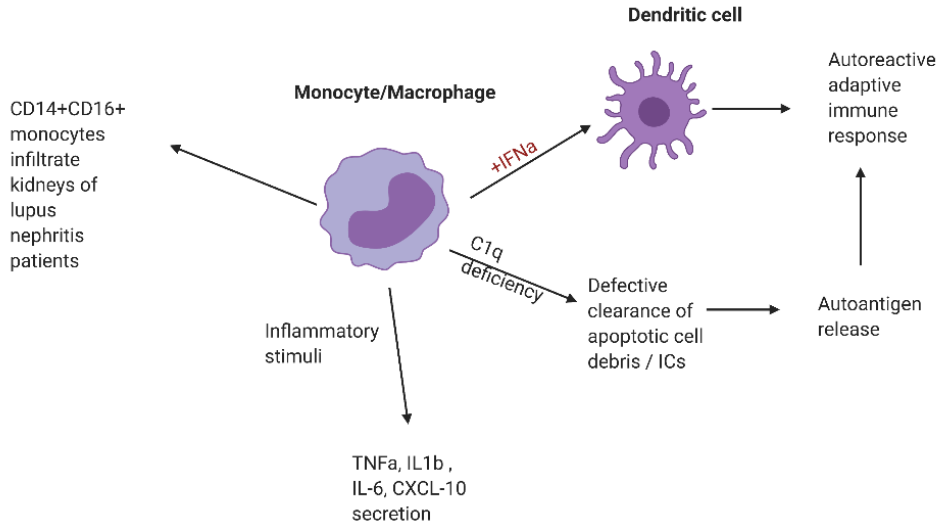

Figure 2: Monocytic lineage SLE cells contribute significantly to SLE progression

SLE Neutrophils

SLE Neutrophils' inflammatory properties

Neutrophils — the most abundant white blood cell type in humans — display crucial roles in innate immune response and act in the first line of defense against invading microorganisms. Neutrophils secrete pro-inflammatory cytokines and chemokines but their contribution in innate immune response is mainly exerted from their capacity to phagocytose, release the content of their granules, generate reactive oxygen species (ROS) and exocytose filamentous complexes of chromatin decorated with numerus proteins, also known as neutrophil extracellular traps (Gupta S. et al., 2016). As already mentioned, one of the two most characteristic gene signatures of SLE patients' blood is this of granulopoiesis. That can be explained by the increased neutrophil activation status and the existence of a highly proinflammatory neutrophil-like population (low density granulocytes, LDGs) in peripheral blood mononuclear cells (PBMCs) (Bennet L. et al.,2003, Panousis N. et al., 2019). Neutrophils develop in the bonne marrow and enter the circulation as terminally differentiated cells.

They are characterized by their multilobulated nucleus, short lifespan, as well as by distinct types of cytoplasmicgranules packed with microbicidal molecules. Neutrophil granules have been classified into three types: azurophilic (primary) granules, specific (secondary) granules and gelatinase (tertiary) granules. Each type contains different microbicidal agents which combined with NADPH-derived ROS equip neutrophils armamentarium against infectious microorganisms (Burn G. et al., 2021).

Despite their role in innate immunity, neutrophils have the capacity to regulate also adaptive immune responses. More specifically, neutrophils can both stimulate and suppress T-cell responses. Indeed, neutrophils prime CD8+ T-cells in a MHC-I dependent manner and activate γδ T cells through cross-presentation of bacterial antigens (Tvinnereim A. et al., 2004). Conversely, granular proteases like elastase and cathepsin G, inhibit the production of T-cell stimulating cytokines, including IL-2 and IL-6 (Minns D. et al., 2019). Additionally, human neutrophils express PD-L1 which upon ligation can promote PD-1-mediated T-cell apoptosis (Luo Q. et al., 2016). Regarding B cells, neutrophils are able regulate their development by expressing B-cell activating factor (BAFF) and A proliferation-inducing ligand (APRIL) while they also display B-cell helper properties in spleen (Parsa R. et al., 2016).

Neutrophil extracellular traps (NETs)

Neutrophils extracellular traps were firstly described as DNA-protein complexes released from dying neutrophils (during a distinct process of cell death called NETosis which differs from necrosis and apoptosis) which can trap and immobilize pathogens in order to encounter them (Brinkmann V. et al., 2004). Extensive investigation of this magnificent immune weapon revealed that NETs can exert distinct functions by activating other immune cells while their uncontrolled release can result in autoimmunity. Additionally, vital NETosis from neutrophils that continue to be functional after releasing NETs was also reported (Jorsch L.et al., 2017). Several NET-inducing stimuli have been reported like phorbol myristate acetate (PMA), Monosodium Urate Crystals (MSU), the calcium ionophore A23817, lipopolysaccharide (LPS), immune complexes relevant to SLE or RA etc. Until now, there are two main mechanisms of NET generation that act separately or simultaneously, the NOX-dependent and the NOX-independent mechanism. NOX-dependent NETotic process is related to NADPH-derived ROS which mediate the translocation of elastase in the nucleus in a MPO- and actin- dependent manner.

Elastase promotes chromatin decondensation by cleaving histones and leads to chromatin swelling, subsequent nuclear- and plasma- membrane passive rupture and NETs release (Papayannopoulos V. et al., 2010, Neubert E. et al., 2018). NOX-independent mechanism is mainly orchestrated by increased calcium influx (via SK3 channel),

release of mitochondrial ROS and translocation of PAD4 enzyme (protein arginine deiminase 4) in the nucleus where it citrullinates histone arginine residues leading to chromatin decondensation and subsequent NETs release (Douda D. et al., 2015). Those mechanisms differ regarding the process (speed, ROS source, different decondensating enzymes etc.) and the protein cargo of NETs (Chapman E. et al., 2019). **Notably, as previously reported, NOX-independent NETs are more cytotoxic than NOX-dependent while characterization of in vivo circulating NETs revealed the presence of NOX-independent NETs in RA, SLE and sepsis, but NOX-dependent NETs in PsA** (Pieterse E. et al., 2018).

NETs in autoimmunity

Neutrophils or neutrophil-like cells (LDGs) display a significant role in autoimmune diseases initiation and perpetuation mainly by releasing NETs providing thus a rich source of autoantigens (DNA, RNA, histones or other proteins) while they also perpetuate deleterious immune responses by potently activating both the adaptive and the innate immunity. Specifically, autoantibodies to dsDNA and to RNA-binding proteins are characteristic of SLE, autoantibodies that target MPO and proteinase-3 (PR3) are predominantly observed in patients with AAV while individuals with rheumatoid arthritis develop autoantibodies (anti-citrullinated protein antibodies; ACPAs) that target citrullinated intracellular and extracellular antigens, such as vimentin, enolase, and fibrinogen (Kaplan MJ, 2011). Additionally, in a murine model of RA, NETs were reported to activate Th1-autoimmune responses by promoting DC maturation (Papadaki G. et al., 2016). Similarly, NETs consisted of citrullinated peptides were internalized by human RA fibroblasts leading to MHC-II upregulation. NET-activated fibroblast exhibited increased capacity to present cit-peptides to Ag-specific T cells leading to RA exacerbation (Carmona-Rivera C. et., 2017). NET formation is also increased in peripheral blood and lesional skin of psoriasis patients and correlates with disease severity while they enhanced the pro-inflammatory potential of keratinocytes by triggering HBD-2 expression (Hu et al., 2016).

In diabetes, high glucose milieu promotes NET generation which impairs wound healing mechanisms (Wong L. et al., 2015). Notably, NETs can also mediate atherosclerotic effects in patients suffering from autoimmune diseases. Using a murine model of atherosclerosis, Warnatch and colleagues reported that cholesterol crystals can trigger neutrophils to release neutrophil extracellular traps (NETs). Subsequently, NETs primed macrophages for cytokine release (mainly IL-1b in an inflammasome-dependent manner), activating thus T helper 17 (TH17) cells that amplify immune cell recruitment in atherosclerotic plaques (Warnatch et al., 2015). On the contrary, NETs were reported to exert an anti-inflammatory effect in gouty arthritis where they served as platforms for the pro-inflammatory cytokines to aggregate and to be degraded (Schauer C. et al., 2014). In general, NETs are crucial mediators of autoimmunity and their most profound effects were reported in SLE.

NETs in SLE

NETs mediate SLE pathogenesis both by direct and indirect activation of immune cells or by promoting cytotoxic effects in tissue resident cells. Interestingly, SLE neutrophils were described to display increased NETotic potential when cultured in vitro while NET levels in sera of SLE patients are significantly increased compared to those of healthy donors and correlated with renal involvement (Hakim A. et al., 2010). Moreover, NETs were also detected in inflamed tissues of SLE patients like skin and kidneys (Frangou E. et al., 2019). SLE neutrophils characteristic NETotic potential was mainly attributed to IFNα-priming (or alternative SLE milieu factors) of SLE neutrophils rather than to genetic predisposition (Garcia-Romo G. et al., 2011). Notably, SLE NETs trigger autoantibody production from B cells (Gestermann N. et al., 2018), promote pro-inflammatory cytokine secretion from macrophages in an inflammasome-dependent manner (Kahlenberg J. et al., 2013), exert cytotoxic effects on epithelial endothelial cells and most importantly enhance pDCs' type I IFN production in a TLR7,9 and cGAs-STING-dependent manner (Garcia-Romo G. et al., 2011, Caielli S. et al., 2016, Lood C. et al., 2016) leading to disease exacerbation **(Figure 2)**. As already mentioned, SLE NETs-mediated activation of pDCs can also promote the generation of extrafollicular T-cell subsets that help B cells in an IL-10 and succinate-dependent manner (Caielli S. et al., 2019). NETs' immunogenicity is mediated by the inflammatory potential of oxidized DNA and the pro-inflammatory capacity of NET-decorating alarmins like LL-37, HMGB1 and histones

(Garcia-Romo G. et al., 2011, Caielli S. et al., 2016, Lood C. et al., 2016). In addition to the presence of neutrophils and LDGs with enhanced capacity to undergo NETosis, NETs are not properly cleared from the circulation in a substantial proportion of patients with SLE. Deficient complement activation or non-functional alleles of DNAse1, DNAse1L3 and RNAseH2 were proposed to interfere with NETs efficient clearance (Leffler J. et al., 2012, Hakim A. et al., 2010, Al-Mayouf S. et al., 2011, Gunther S. et al., 2015). Moreover, NETs were also proposed to be protected by anti-NET antibodies, NET-decorating DNAse inhibitors like actin, alarmins that stabilize NET-structure like LL-37 and post transcriptional modifications of NET-DNA like oxidation (Hakim A. et al., 2010, Gehrke N. et al., 2013, Garcia-Romo G. et al., 2011, Lande R. et al., 2011).

As previously noted a neutrophil-like population named as low density granulocytes due to their decreased granularity, is of high importance regarding SLE pathogenesis. Those cells exhibit a characteristic activated phenotype and upregulated levels in SLE patients peripheral blood PBMC fraction. They also display an enhanced potential to release highly interferogenic and cytotoxic NETs consisted of both genomic and mitochondrial DNA decorated with immunogenic protein cargo. They are distinguished by increased CD10 expression and exhibit the capacity to secrete significant levels of IFN-α (Lood C. et al., 2016, Mistry P. et al., 2019). Complete characterization of this pathogenic neutrophil subtype will pressumably provide with efficient cell-targeted therapeutic approaches.

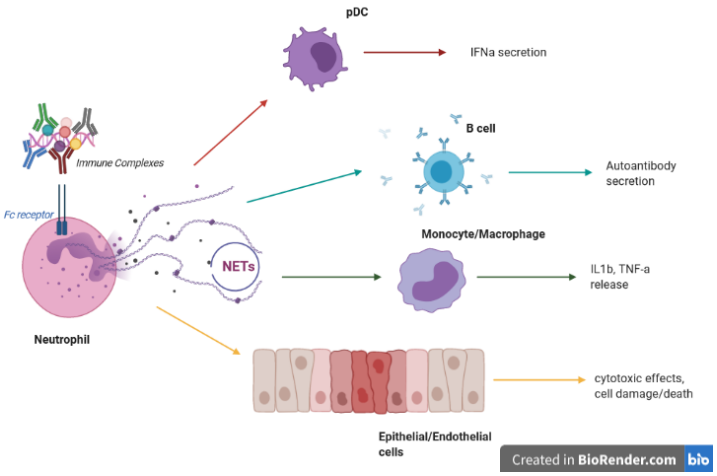

Figure 3: Neutrophil extracellular traps-mediated signaling modulates both hematopoietic and non-hematopoietic cell responses exacerbating thus SLE pathogenesis (created using Biorender.com)

3.4.2 SLE plasmacytoid dendritic cells (pDCs)

Phenotypic identification & inflammatory properties of pDCs

Dendritic cells are the link between innate and adaptive immunity and their main function is antigen presentation. Notably, there is also a dendritic cell subtype of low abundance (0,2-0,5% of PBMCs) that invest its energy stock mainly in producing type I IFNs. Those dendritic cells were named as plasmacytoid due to their plasma cell morphology. PDCs are mainly differentiated within the myeloid lineage but there also reports of pDCs exhibiting lymphoid origin. Their specialization in producing type I IFNs in response to viruses, bacteria or extracellular DNA-derived from dead cells (apoptotic, necrotic, NETotic) is based on their nucleic acid sensor expression (TRL7, TLR9, cGAs e.t.c) and their constitutive expression of interferon regulatory factors (IRF7, IRF5, IRF9 e.t.c). However, pDCs can also secrete other pro-inflammatory cytokines and chemokines, including tumour necrosis factor (TNFa), interleukin-6 (IL-6), IL-12, CXC-chemokine ligand 8 (CXCL8), CXCL10, CC-chemokine ligand 3 (CCL3) and CCL4. Human pDCs lack expression of the lineage-associated markers CD3, CD19, CD14, CD16 and CD11c, and they selectively express the C-type lectin BDCA2, BDCA4, the immunoglobulin superfamily receptor immunoglobulin-like transcript 7 (ILT7) and elevated levels of IL3R (CD123) which mediates their survival. As pDCs express MHC class II molecules and the co-stimulatory molecules CD40, CD80 and CD86, they are capable of presenting antigens to CD4+ T cells, albeit not as efficiently as cDCs. Antigen presentation by pDCs can lead to CD4+ T cell activation or tolerance, depending on the context (Swiecki M. et al., 2015). Moreover, human pDCs were reported to exhibit cross-presentation of viral antigens to CD8+ T cell in a MHC-I-dependent and proteasome-independent manner (Di Pucchio T. et al., 2008). The multifaceted biology of pDCs is extensively investigated with a view to understanding their potential roles in the pathogenesis of autoimmune diseases, cancer and viral infections.

pDCs as professional interferon producing cells

As already mentioned, the most prominent gene signature of SLE peripheral blood and tissues is this of IFN. IFN-mediated signaling promote enhanced transcription of several characteristic genes that are mainly

related to antiviral immune response and IFN signaling axis and consist the aforementioned IFN signature which is present in a large proportion of SLE patients (especially pediatric) and which is tightly associated to disease severity and end-organ damage. There are three different types of IFNs (I–III), and the type I IFNs are the largest family. It can be divided into five classes (IFN-α, β, ε, κ and ω), of which IFN-α can be further divided into 12 subtypes. Several (hematopoietic or non-hematopoietic) cells can produce IFNb or negligible amounts of IFN-α and other IFNs. In contrast to the universality of IFN production, the main IFN-α producing cell among human leukocytes is the pDC. IFN-α is the most crucial cytokine regarding SLE initiation and perpetuation due to its proinflammatory effect on multiple immune cell types while both type II (IFNγ) and type III (IFNλ) were also reported to exert pathogenic pro-inflammatory effects both in murine and human lupus (Harigai M. et al., 2008, Goel R. et al.,2020, Tsokos G., 2020). Specifically, IFN-α enhance antigen presenting capacity of SLE monocytes enabling thus autoantigen-dependent activation of T cells while it significantly induces BLyS, expressionthereby providing support for B cell differentiation, and supports immunoglobulin class switching to generate potentially pathogenic autoantibodies (Blanco P. et al., 2001, Ittah M. et al.,2006+ unpublished data from our lab). Additionally, IFN-α act as a priming factor for extracellular traps release by neutrophils (Garcia-Romo G. et al., 2011) **(Figure 3)**. This pleiotropic cytokine can also contribute to deleterious organ-related manifestations. For example, IFN-α exerts cytotoxic effects on renal podocytes exacerbating thus lupus nephritis while it primes keratinocytes to secrete proinflammatory cytokines that promote skin SLE manifestations (Migliorini A. et al., 2013 Stannard J. et al., 2017). To conclude, IFNs are pivotal for SLE pathogenesis and this is why it is important to describe what triggers their secretion and which cells are directly or indirectly responsible for their excessive signaling in SLE milieu.

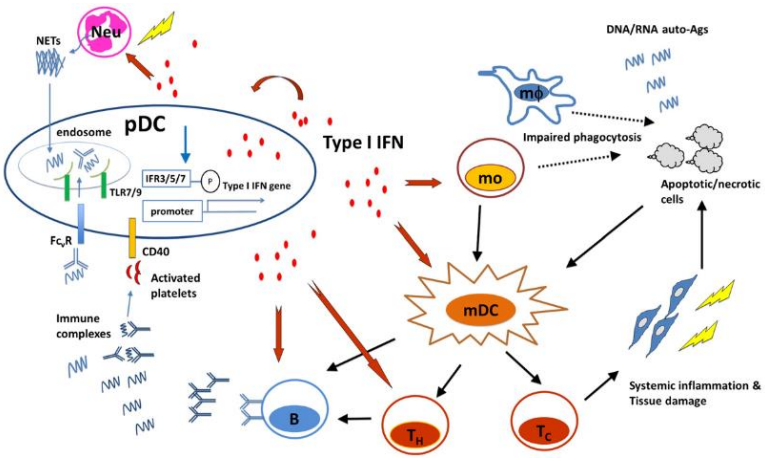

Figure 4: pDC-derived Type I IFNs promote SLE progression by activating multiple cells of both adaptive and innate immunity (V.S.-F. Chan et al., Autoimmunity Reviews 11, 2012)

SLE-relevant mediators of pDCs' IFN production

In SLE, pDCs were reported to be one of the main IFN-producers both in peripheral blood and tissues like skin and kidney where they infiltrate to exert their pathogenic effects. There are multiple conceivable inducers of pDCs-derived type I IFNs. During SLE initiation or flare, the most crucial inducers are nuclear material from apoptotic or necrotic cells combined or not with autoantibodies (immune complexes, ICs) and NETotic chromatin combined with damage associated molecular patterns (DAMPs or alarmins). ICs are endocytosed via FcγRIIa in pDCs, transported to the endosome where their nucleic acid part binds to TLR7 or TLR9 with subsequent activation of transcription factors and IFN-α production (Eloranta ML et al., 2009)]. NETs are endocytosed in a FcγRIIa-independent manner and can stimulate both endosomal (TLR7, TLR9) and cytoplasmic (cGas) nucleic acid receptors leading to IFN-α secretion. It was also reported that NET uptake from pDCs could be facilitated by their decorating DAMPs (or alarmins) like HMGB1 or LL-37 (Tian J. et al., 2007, Lande R. et al., 2011). After nucleic acid receptor sensing a signaling cascade is triggered that leads to phosphorylation and subsequent translocation of IRF proteins in the nucleus where they promote IFN transcription. SLE pDCs can also sense bacterial DNA and viral DNA or RNA leading to SLE flares or SLE periodic infections which can be deleterious for immunosuppressed patients (Banchereau J. et al., 2006). To gain insights on the pathogenic neutrophil interaction with pDCs taking place in SLE milieu

which is investigated in this research project, the exact mechanism of NET-dependent stimulation of pDCs will be analyzed. So, during SLE progression immune complexes consisted of nuclear material and autoantibodies (especially anti-RNP ICs) promote generation of NETs from neutrophils and LDGs in a FcγRIIa-, TLR7- , NADPH- and mitochondrial ROS dependent-manner (Garcia-Romo G. et al., 2011, Caielli S. et al., 2016). Those extracellular chromatin structures are consisted of both genomic and mitochondrial DNA combined with various immunomodulatory alarmins. The interferogenicity of IC-SLE NETs is highly augmented due to its increased oxidation status (Caielli S. et al., 2016). Then, those complex structures are endocytosed or phagocytosed from pDCs and localized in endosomes or just vesicle-free in the cytoplasm. Endosomes-localized NETs trigger TRL9 or TLR7 while cytoplasm NETs activate cytoplasmic nucleic acid sensors (cGas-STING pathway). **Nucleic acid –mediated activation of pDCs trigger the release of copious amounts of type I IFNs which are capable of priming neutrophils to release more NETs creating thus a vicious feedback loop**.

Targeting pDCs as a therapeutic approach for SLE amelioration

Considering the pathogenic IFN-dependent phenotype of pDCs in SLE, those cells of low abundance had been targeted therapeutically both in lupus mouse models and SLE patients. Specifically, early and transient depletion of pDCs in BXSB lupus-prone mice resulted in reduced splenomegaly and lymphadenopathy, impaired expansion and activation of T and B cells, reduced antibodies against nuclear autoantigens and improved kidney pathology (Rowland S.L et al., 2014). Furthermore, Tcf4 haplodeficiency (reduced differentiation of myeloid cells to pDCs due to genetically reduced E2-2 dosage) in the B6. Sle1.Sle3 multigenic model of SLE nearly abolished key disease manifestations including anti-DNA antibody production and glomerulonephritis (Sisirak V. et al., 2014). Of note, pDC-targeting was also found to be efficient in ameliorating cutaneous lupus patients. More specifically, anti-BDCA-2 specific antibody administration in patients with SLE decreased expression of IFN response genes in blood, normalized MxA expression, reduced immune infiltrates in skin lesions, and decreased CLASI-A score (Furie R. et al.,2019).

3.5 Alarmins: Self-derived orchestrators of deleterious inflammation

PAMPs & DAMPs

Recent studies indicate that nucleic acid-mediated SLE pathogenic immune responses are tightly associated with alarmin decoration. **Both immune complexes and NETs are consisted of immunogenic nucleic acids and highly pro-inflammatory proteins**. Several of these proteins belong to the alarmin (or DAMP) family. Generally, inflammation is triggered by pathogen associated molecular patterns (PAMPs), conserved microbe molecules, which warn the immune system that something foreign and possibly infectious has entered the body. On the other hand, damage-associated molecular patterns (DAMPs), or alarmins, are host biomolecules that can initiate and perpetuate both infectious and noninfectious inflammatory response during cell or tissue stress, damage, and non-physiologic cell death. Both PAMPs and alarmins stimulate pattern recognition receptors (PRRs) leading to inflammatory responses while alarmins can also promote wound healing.

Non-apoptotic cell death and damage are the most well-described triggers of alarmin release which can act both separately or simultaneously with PAMPs. Alarmin function evolved possibly because infectious microorganisms had found ways to avoid detection by our immune system but at the same time they have not managed to avoid inducing cell death within their hosts. Several alarmins that are normally contained within the cell interior and hidden from the immune system have been characterized. Protein molecules (like HMGB-1, S100 proteins, HSPs, LL-37, IL-33 etc), nucleic acids (DNA and RNA), and metabolites (ATP, uric acid) consist this heterogenous group of inflammation boosting signals. Considering that alarmins are pro-inflammatory self-biomolecules, their contribution on autoimmunity has been thoroughly investigated (Martin S.J, 2016, Gallo P. et al., 2013).

Alarmins' contribution in autoimmunity

High mobility group protein 1 (HMGB1), one of the most well-described alarmins, recruit immature DCs, which take up autoantigens and home to secondary lymphoid organs where they stimulate adaptive immune responses (Yang D. et al., 2007). In RA, targeting HMGB1/RAGE axis successfully inhibited the development of synovial inflammation and joint swelling in animal models of arthritis (Ostberg T. et al.,2010). In SLE, HMGB-1 was detected decorating IC-induced NETs facilitating their uptake by pDCs and the subsequent IFN-α production in a RAGE-dependent manner (Caielli S. et al., 2016).

Another alarmin, LL-37, was also decorated on SLE-NETs preventing NET-DNA from degradation. Immune complexes consisted of NET-DNA, LL-37 and autoantibodies promote a strong type I IFN response by pDCs (Lande R. et al., 2011). Moreover, NET-derived LL-37 stimulates inflammasome activation resulting in IL-1β and IL-18 production (Kahlenberg j. et al.,2013). Anti-native LL37 and anti-cit-LL37-specific antibody reactivity correlates with SLEDAI and declines in inactive SLE patients (Lande R. et al., 2020). Notably, LL-37 is up-regulated on psoriatic skin and it contributes to disease pathogenesis mainly by generating, once again, stable DNA-LL37 complexes that promote pDCs' IFN-α production (Lande R., 2007). Another group of alarmins, S100 proteins (S100A8, S100A9, and S100A12), are highly expressed by human phagocytes within the affected joints in inflammatory arthritis. S100 proteins can activate the endothelium; recruit and stimulate immune cells such as macrophages to produce proinflammatory cytokines, including TNF-α and IL-1β; and demonstrate cytotoxic effects, leading to tissue destruction (Van lent P. et al., 2008). Uric acid is the primary cause of gout arthritis, an IL-1b mediated autoimmune disorder (Busso N. et al., 2010). The immunogenic properties of extracellular DNA of genomic or mitochondrial origin has already been thoroughly described in this text. Heat shock proteins (HSPs) are responsible for maintaining the correct folding of nascent and misfolded proteins and contribute in murine autoimmune diabetes (and other autoimmune disorders) by acting as chaperones that physically deliver autoantigens to APCs (Liu B. et al., 2003). Furthermore, autoantibodies against HSPs were found in SLE patients and allelic variants of the Hsp70 genes are significantly associated with SLE (Furnrohr et al., 2010).

ATP can also promote autoimmune responses via its abundantly expressed receptor P2X7. Notably, lack of ATP/P2X7axis signaling decreases the severity of EAE (Sharp A. et al., 2008), and oxidized ATP (oxATP), an antagonist of the ATP receptor P2XR7, ameliorated autoimmune type I diabetes and autoimmune encephalitis in mice (Lang P. et al., 2010). IL1a, that belongs to the famous IL-1 family and which is released upon cell stress or death, was found upregulated in SLE monocytes (unpublished data from our lab) while it also contributes to autoimmunity mainly by promoting the generation of IL-17-producing γδ T cells (Sutton CE et al., 2009).

IL-33, a multifaceted IL-1 family cytokine

IL-33/ST2L axis

IL-33, another cytokine that belongs to the IL-1 family, is a characteristic alarmin. Under steady/healthy state, it resides in the nucleus associated to chromatin while upon stress, damage or inflammatory stimuli and necrotic cell death IL-33 is released both as a nuclear protein, which retains moderate signaling capacity, and as a cleaved-cytokine (18kd) which exerts pleiotropic immunomodulatory effects. Specifically, human IL33 consists of seven coding exons (there is also one non coding exon located 25.8 kb upstream of exon 1) located in chromosome 9, which are translated into a 31 kD protein of 270 amino acids. Exons 1–3 encode the N-terminal domains required for IL-33 nuclear localization, whereas exons 4–7 encode the C-terminal IL-1-like cytokine domain. The nuclear localization domain includes a chromatin binding domain which mediates interaction of IL-33 with histone dimers (acidic patch of H2A-H2B) and promotes chromatin compaction. The IL-1-like cytokine domain, a 12-stranded b-trefoil fold similar to IL-1a, IL-1b, IL-1Ra, and IL-18, binds to the IL-33 receptor ST2, thus facilitating recruitment of IL-1RAcP to form the heterotrimeric signaling complex. ST2L includes the extracellular immunoglobulin (Ig)-like domain, a short extracellular spacer, the transmembrane domain, and an intracellular TIR domain. The formation of the heterotrimeric signaling complex IL-33-ST2L- IL-1RAcP recruits the receptor complex of MyD88, IRAK1, IRAK4, and TRAF6; leads to activation of MAP kinases Erk1/2, p38, and JNK, activation of AP-1 transcription factors and degradation of IkBa promoting the translocation of NF-kB to the nucleus **(figure 4)** (Molofsky A. et al., 2015, Cayol C. et al., 2018).

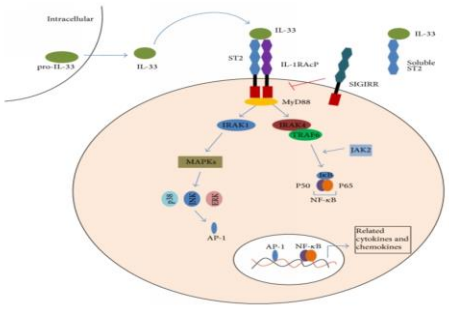

Figure 4: IL-33/ST2L axis-mediated intracellular signaling and regulation (Zhao Q. et al., 2014)

IL-33's expression and secretion

IL-33 is mainly expressed in the nucleus of epithelial and endothelial cells of barrier tissues but recent findings indicate that IL-33 can also be expressed and released both in its nuclear or its cytokine-isoform by various immune cells upon inflammatory, stress or necrosis-related stimuli. Specifically, in myeloid cells, Il33 transcription can be induced by allergic challenge and TLR signaling. Additionally, IL-33 can be expressed under specific conditions in lymphoid cells also, exerting mainly intrinsic effects as a transcription regulator via its nuclear isoform (Hatzioannou et al., 2020, Stier M. et al., 2019). Interestingly, IL-33 lacks a classic secretory signal so it is released via unconventional active or passive death-related pathways. Recently, an interesting secretory mechanism in which the pore-forming protein perforin-2 functions as a conduit on the plasma membrane facilitating thus IL-33 export, had been described in murine DCs (Hung L. et al.,2020). **However, characterizing of IL-33 secretory pathways needs further investigation**. On the other hand, both non-hematopoietic and hematopoietic cells, express ST2L in a constitutive or inducible-fashion. Many tissue-resident immune cells express ST2L constitutively. These include mast cells, group 2 innate lymphoid cells and tissue regulatory T cells (Tregs). On the other hand, in a murine model of COPD, ST2L was monitored to be induced on NK cells and macrophages that don't express it at steady state. Induction of ST2 expression has also been observed on Th1 cells and CD8+ T cells after activation (Molofsky A. et al., 2015, Cayrol C. et al., 2018).

Regulation of IL-33's activity

The significance of IL-33/ST2L signaling axis is revealed by its strict regulatory mechanisms. For example, under normal apoptotic cell death, caspase-3 and caspase-7 cleave and inactivate IL-33 at a conserved residue, Asp178, within the IL-1-like domain (Luthi A. et al., 2009). Moreover, post-translational modifications like oxidation, reduce IL-33 signaling capacity by disrupting its binding to ST2L (Cohen E. et al., 2015). The most potent and abundant regulator of IL-33 is the soluble isoform of ST2L, sST2. This soluble isoform is generated via alternative splicing of *IL1RL1(ST2)* gene and it is detected in human sera in relatively high levels despite the fact that IL-33 levels are negligible or completely absent (Molofsky A. et al., 2015). Intracellularly, IL-33/ST2L signaling pathway can be inhibited by single Ig IL-1-related receptor (SIGIRR) protein which was reported to antagonize under circumstances IL-1R-mediated signaling

(Wald D. et al., 2003). Notably, the nuclear localization signal of IL-33 could be considered as a negative regulator of IL-33's potent proinflammatory capacity and that was revealed using a mouse model that exhibited altered subcellular localization (from nuclear to cytoplasmic) of IL-33 that led to non-resolving lethal inflammation (Bessa J. et al., 2014). Besides its regulation or inhibition, IL-33's bioactivity can be profoundly enhanced via cleavage-dependent enzymatic mechanisms **(figure 5)**. Specifically, inflammatory serine proteases from neutrophils and mast cells can cleave full length IL-33 precursor to release shorter mature forms of 18-21 kD. Proteomic studies revealed that the cleavage site was within the central part of IL-33, upstream of the IL-1-like cytokine domain. Six distinct inflammatory serine proteases were reported to cleave human full length IL-33 including neutrophil cathepsin G, elastase and proteinase 3 (PR3), as well as mast cell chymase, tryptase and granzyme B. Human IL-33$^{(95\text{-}270)}$ and IL-33$^{(109\text{-}270)}$ has to be major mature forms of IL-33 in vivo because they can be generated by both activated neutrophils and IgE-activated mast cells. In mice, mature forms of IL-33 of 19-20 kD have been detected in BAL fluids after acute lung injury or exposure to fungal aeroallergen *Alternaria alternata* and in the lungs in response to chitin or migratory helminths. **Of note, all of this cleaved isoforms, both in mice and humans, were found to exhibit significantly increased biological activity** (Lefrancais E. et al.2012, Cayrol C. et al., 2018)

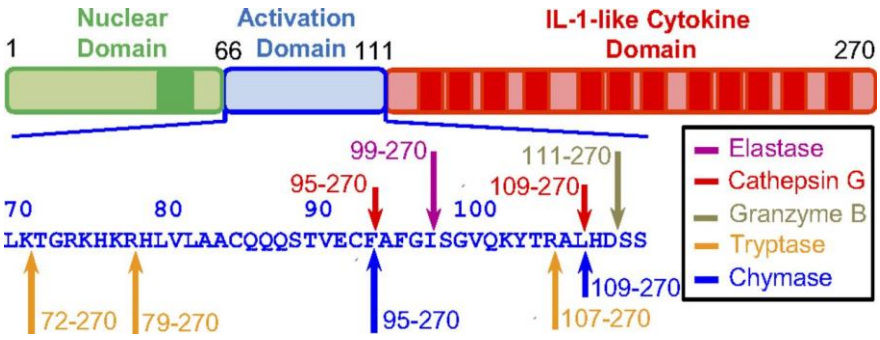

Figure 5: Primary structure of human IL-33. The nuclear (amino acids 1–65), cleavage/activation (amino acids 66–111), and IL-1–like cytokine (amino acids 112–270) domains are indicated. The different mature forms of IL-33 and the sequences surrounding the cleavage sites for inflammatory proteases are shown (Lefrancais E. et al.,2012)

IL-33 shapes adaptive immune responses

IL-33, both as a nuclear protein and as a cytokine, can promote distinct context-specific effects. Depending on its source, its target and the surrounding milieu, IL-33 can promote both inflammatory and anti-inflammatory effects regarding adaptive immune responses. To begin with, IL-33 was initially described as a mediator of type II inflammation. Specifically, IL-33 acts as a chemoattractant for Th2 CD4+ T cells and promotes IL-4, IL-5 and IL-13 secretion. Moreover, IL-33 promotes Th2-type responses by signaling on other immune cells rather than CD4+ T cells like mast cells, basophils and eosinophils (Carrasco T. et al., 2015). Additionally, by using mouse models of EAE, RA or models of viral infection, an alternative Th1 and Th17 response-promoting role for IL-33 were revealed (Jiang H. et al., 2012, Palmer G. et al., 2009, Bonilla W. et al., 2012, Baumann C. et., 2015). Regarding the tolerance-related effect of IL-33, it is reported that it can also expand and promote Tregs accumulation in different contexts.

In an ongoing-colitis model, IL-33 administration promotes the expansion of Tregs and Foxp3 expression (Schiering C. et al., 2014). In a cancer mouse model, Treg-conditional knock-out of IL-33 reprograms Tregs into T cells that exhibit potent cytotoxic properties (T effector cells) unravelling its important intrinsic function (Hatzioannou et al., 2020). IL-33-dependent T effector polarization was also reported in perinatal mice (Tuncel J. et al., 2019). B cells are also targeted by IL-33.

In a delayed-hypersensitivity mouse model, IL-33 markedly activated B1 (IgM-secreting) cell proliferation and enhanced IgM, IL-5, and IL-13 production in vitro and in vivo (Komai-Koma M. et al., 2011). Additionally, a cell-intrinsic, ST2-independent role for IL-33 in early B cell development was described by Stier and colleagues (Stier M. et al., 2019). Of note, IL-33 was also found to shape adaptive immune responses in a dendritic cell-dependent fashion. More specifically, Rank and colleagues found that DCs express high levels of intracellular ST2, and that the in vitro treatment of DCs with IL-33 triggers the secretion of IL-6, upregulates the expression levels of MHC-II and CD86, and shapes the polarization of naïve T cells toward a Th2 phenotype (Rank M. et al., 2009). Similarly, Besnard and colleagues described that IL-33 exposure induces the recruitment and activation of DCs in the lung, and their posterior migration

to lymph nodes for antigen presentation in an allergic airway inflammation model (Besnard A.G et al., 2012). Similarly, allergen-specific IgG-ICs, formed upon re-exposure to allergen, promoted Th2 responses by inducing IL-33 expression of DCs (Tjota M. et al., 2013).

IL-33 modulates innate immune responses

Except, its role in shaping adaptive immune responses, IL-33 was described to modulate also innate immunity. As it is already mentioned many tissue-resident and circulating innate immune cells can respond to IL-33. Per example, after infection with the helminth *Nippostrongylus brasiliensis* and in response to IL33, ILC2s expanded robustly and produced large amounts of IL13, which led to goblet cell hyperplasia in the intestine and worm expulsion. Activation of lung ILC2s by IL-33 was also shown to mediate influenza-induced airway hyper-reactivity. Regarding allergen-mediated immune responses, IL-33 was reported to induce allergic airway inflammation by stimulating lung ILC2s to secrete IL-5 and IL-13 promoting thus eosinophilic lung inflammation (Cayrol C. et al., 2014). In murine models of allergic airway inflammation, the IL-33 mediated ILC2 pathogenic responses were dependent on IRF7 (He J. et al., 2019). Additionally, IL-33/ST2L axis also promotes MCs activation and maturation mediating thus hypersensitivity-related responses. IL-33 acts both alone and in combination with thymic stromal lymphopoietin to accelerate the maturation of CD34+ MCs precursors in vitro and induce the secretion of IL-5, IL-13, GM-CSF, CXCL8, CCL17, CCL22, and CCL2.

Except of the DC-focused adaptive immunity-related effects, IL-33 can also modulate macrophages inflammatory potential. Specifically, IL-33 has a significant role in regulation of chemokine secretion on macrophages. IL-33 favors M1 chemokines such as CCL3 generation in cultures of naïve human macrophages. Conversely, IL-33 promotes or amplifies the expression of M2 chemokine markers such as CCL18 in either M1 or M2-polarized macrophages. This observation is consistent with the results from mouse macrophages, which suggests that IL-33 amplifies the polarization of alternatively activated or M2 macrophages (Lu J. et al., 2015). Regarding tissue resident macrophages, IL-33 changes the quiescent phenotype of alveolar macrophages toward an AAM phenotype that expresses mannose receptor, IL-4R, and produces high levels of CCL24 and CCL17 in an IL-13-dependent manner

(Kurowska-Stolarska M. et al., 2009). Among others, IL-33 has been a general mediator of neutrophil recruitment in tissues like lungs and liver while it can also regulate their inflammatory properties mainly indirectly (Liang M. et al.,2019, Lefrancais E. et al., 2012). Moreover, IL-33 exacerbates liver sterile inflammation by amplifying neutrophil extracellular trap formation (Yazdani H. et al., 2017).

IL-33 as a mediator of autoimmunity

Regarding its role in autoimmunity, IL-33 may confer to autoimmune initiation or progression also by augmenting innate immune responses in murine models of dextran-induced colitis (Oboki K. et al., 2010) while its contribution in RA and EAE is mainly mediated by adaptive immunity (Jiang H. et al., 2012, Palmer G. et al., 2009). In SLE, elevated serum concentrations of IL-33 and the soluble form of ST2L have been reported (Mok MY et al, 2010, Moreau A. et al., 2021). Genetic studies have also implicated IL33 gene polymorphisms in susceptibility to SLE (Guo J et al., 2016).

In animal studies, exogenous IL-33 induces the B-cell activating factor (BAFF) (Rose WA et al., 2018), a growth factor implicated in SLE, and MRL/l*pr* lupus-prone mice treated with anti-IL-33 antibody show reduced renal inflammation and serum autoantibodies (Li P. et al., 2014). **However, the in vivo expression and function of IL-33, as well as its contribution to immune cell activation and tissue inflammation in SLE, remain ill-defined.**

Collectively, IL-33 was reported as a potent mediator of autoimmunity by enhancing both innate and adaptive immune responses. However, the exact mechanism of how IL-33 can affect SLE pathogenesis has not been thoroughly addressed. Moreover, the potential IL-33 decoration of SLE NETs and if such complexes display in vivo significance has not been investigated. Notably, neutrophil protease-mediated activation of IL-33 has not, until now, been described taking place in SLE milieu. This dissertation is focused on unravelling the potential contribution of IL-33 decorated NETs regarding the characteristic pDC-driven IFN signature of SLE peripheral blood and tissues that leads to disease exacerbation and end-organ damage.

4) Objectives

The present study seeks to delineate the role of IL-33-decorated neutrophil extracellular traps (NETs) in the pathogenesis of Systemic Lupus Erythematosus (SLE). Specifically, the objectives of the study are:

1) to evaluate the capacity of SLE neutrophils (derived from SLE patients) to release IL-33 decorated NETs, spontaneously or upon immune complex administration
2) to characterize the distinct features and immunostimulatory properties of IL-33 decorated SLE NETs regarding pDC-mediated IFN-α production
3) to address the in vivo significance of IL-33 decorated NETs in SLE pathogenesis

Preliminary results indicated that SLE neutrophils release IL-33-decorated NETs spontaneously and in a larger extent upon IC-administration. Intriguingly, IL-33 decorated NETs promote pDCs' IFN-α production in an ST2L-dependent manner. Additionally, IL-33 decorated NETs are accumulated in both blood and non-blood (skin, kidney) SLE inflamed tissues. Taking into consideration that SLE is characterized by a profound type I IFN signature which, until now, cannot be ameliorated pharmaceutically, we set the following questions to delineate how IL-33 mediates the interferogenic potential of SLE NETs:

- What's the exact mechanism of IL-33-decorating NETs-mediated IFN-α production?
- Do IL-33-null NETs abolish its interferogenicity?
- Are they any NET-decorating factors that could potentiate IL-33's bioactivity?

To address those questions, we pursued a combination of molecular, imaging and proteomic approaches using human SLE-relevant biologic material and primary cells in order to better characterize the contribution of IL-33 in NET-mediated exacerbation of human SLE. Our aim to provide with new drugable targets to reinforce the relatively-poor SLE-related armamentarium of physicians.

5) Materials & Methods

Human Subjects

We included SLE patients followed at the Rheumatology Clinic, University Hospital of Heraklion, who met the 1997 American College of Rheumatology revised classification criteria (Hochberg M., 1997) (Supplementary Table S1). Active SLE was defined according to a SLE Disease Activity Index-2000 score (SLEDAI-2K) equal or higher than 6 (74) at the day of sampling. Clinical response to treatment was evaluated according to the SLE Responder Index-4 (SRI-4) (Moska M. et al., 2006). Patients were abstained fromtheir medications for at least 12 hours prior to blood drawing.

Isolation and culture of blood neutrophils

Human peripheral blood neutrophils were isolated as previously described (Papadaki G. et al., 2016). Cell viability wasmeasured at 99% by trypan blue dye exclusion. Neutrophils were cultured with no phenol red RPMImedium (Gibco, 11835030) supplemented with 1% v/v heat-inactivated FBS and 10mm Hepes (Gibco,15630080) in a humidified 37°C/5% CO2 incubator. Serum from SLE and healthy individuals was used at 10% v/v final concentration. To inhibit serum IC-mediated effects, neutrophils were pre-treated for 45 minutes with FcR blocking reagent (Miltenyi Biotec) or the TLR-7 antagonist oligonucleotide IRS661 (1μM, 5′-TGCTTGCAAGCTTGCAAGCA-3′, Invitrogen).

HL-60 differentiation and gene silencing

The HL-60 promyelotic cell line was cultured in RPMI-1640/L-glutamine (Gibco, 21875-034), supplemented with 10% v/v heat-inactivated FBS, 100IU/mL penicillin, 100μg/mL streptomycin and 10mm Hepes (Gibco) in a humidified 37°C/5% CO2 incubator. Exponentially growing cells (1×106) were incubated with 1μM ATRA (Sigma Aldrich, R2625). After 6 days, flow cytometry was used to monitor the expression of neutrophil markers (CD11b, CD66b, CD16). For gene silencing, we collected 4×106 cells/sample on day 4 of differentiation, which were electroporated with 25nM ONTARGETplusIL-33 siRNA (Dharmacon, L-HUMAN-XX-0005) and ON-TARGETplus Nontargeting

siRNA (Dharmacon, D-001810-01-05) using the Amaxa Nucleofector kit V (Lonza Bioscience, VCA-1003) and program T019. Cells were incubated in serum-free medium for 6 hours to recover and then cultured in complete medium plus 1μM ATRA for 2 days. Immunofluorescence and western immunoblotting were used to evaluate silencing efficiency on day 6.

Generation, isolation and quantification of NETs

SLE neutrophils (1×106) or differentiated HL-60 cells were seeded in 12-well tissue culture plates and cultured with no phenol red RPMI (Gibco) supplemented with 1% v/v heat-inactivated FBS, 5μM 2-mercaptethanol (Gibco, 31350010) and 10mm Hepes (Gibco), for 3 hours in a humidified 37°C/5% CO2 incubator. ICs were prepared as previously described (Lovgren M., 2004). Differentiated HL-60 cells wereprimed with 2000U/ml Universal IFNa (PBL, PBL11200-2) for 1 hour prior to stimulation with lupus ICs. Supernatants were discarded, cells were carefully washed once with pre-warmed medium, and NETs-containing supernatants were vigorously collected and spun at 150g for 5 minutes at 4°C to obtain cell-free supernatants. Inhibitors of elastase (2μM sivelestat, Sigma Aldrich, S7198) or Cathepsin G (20 μM CGi, Calbiochem, 219372) were added after 75 minutes of neutrophil stimulation. In NET-mediated cleavage experiments, recombinant GST-tagged full-length IL-33 (100nM, Abnova, H00090865) was added after 2 hours of neutrophil stimulation for 1 hour. PMA (100nM Sigma Aldrich, P1585) and Monosodium Urate Crystals (MSU, 100μg/ml, Invivogen, tlrl-msu) were used as controls. Both cell supernatants and NETs were precipitated for Western blot analysis. To quantify NET-containing supernatants, we used the SYTOX green Nucleic Acid Stain kit (Invitrogen, S7020) according to the manufacturer instructions. NETs were quantified as previously described (Papadaki G. et al., 2016). Briefly, decondensed nuclei or filamentous DNA structures stained for both DAPI and MPO were considered as NETs. We used the FIJI software and assessed 5 randomly selected coverslip fields for each treatment and n=3 biological replicates (independent experiments), to calculate the proportion of NETs-releasing cells out of the total number of cells.

Isolation and culture of pDCs

Buffy coats from healthy donors were used for isolation of peripheral blood mononuclear cells (PBMCs) by density-gradient centrifugation (Lymphosep, MST00T41004). pDCs were obtained by the BDCA-4 isolation kit (Miltenyi Biotec,130-090-532) at a purity >95%. pDCs were cultured in RPMI-1640/L-glutamine supplemented with 10% v/v heat-inactivated FBS, 100IU/mL penicillin, 100µg/mL streptomycin and 10mm Hepes (Gibco) for up to 18 hours. Prior to stimulation with NETs (25% v/v of NET-containing supernatants or cleaved IL-33-containing supernatants) and CpG-A (0.1µM, Invivogen, tlrl-2216), pDCs were pre-treated with anti-ST2L antibody (3µg/ml, R&D, AF523) and FcR blocking reagent (Miltenyi Biotec, 130-090532) to minimize any IC carry-over effect and non-specific binding of anti-ST2L. IC SLE NETs-containing supernatants were pre-treated with goat anti-human IL-33 antibody (4µg/ml, R&D, AF3625) or left untreated at 37°C for 45 minutes before their administration to pDCs cultures. pDCs were also pre-treated with cytochalasin D (5µg/ml, Sigma-Aldrich, C2618) or chloroquine (4µM, Plaquenil [Sanofi Aventis], ATC code 8P01BA02) for 30 minutes in order to block endocytosis and TLR trafficking, respectively.

In vitro cleavage of full-length IL-33

Bioactive IL-33–containing supernatants were generated as previously described (Clancy D. et al., 2018). Specifically, reactions consisting of recombinant elastase (50ng/ml, Calbiochem, 324681) and recombinant full lengthIL-33 (1.8µg/ml, Abnova) were carried out (15µL final volume) in protease reaction buffer (50mM HEPES [pH 7.4], 75 mM NaCl, 0.1% CHAPS, 5µM 2-mercaptethanol) for 2 hours at 37°C. The reaction was stopped by adding sivelestast (2 µM). As control, recombinant full-length IL-33 was incubated for 2 hours at 37°C in protease reaction buffer without recombinant elastase.

Immunofluorescence

Neutrophils or differentiated HL-60 cells were seeded on coverslips coated with 0.001% poly-l-lysine (Sigma-Aldrich, P8920) and cultured for 3 hours at 37°C/5% CO2. Cells were fixed with 4% paraformaldehyde (PFA), blocked with 5% w/v BSA/PBS buffer and permeabilized with 0.2% triton X-100 for 6 minutes. DNA was stained with 300nM DAPI (Sigma Aldrich, D9542). IL-33 protein

staining (R&D goat antibody/AF3625 [1:50 dilution], mouse “Nessy” antibody for verification [Enzo, ALX-804-840-C100, 1:250 dilution]) was performed at 4°C overnight. NET protein staining was performed using anti-citH3 (Abcam, ab5103, 1:200 dilution), anti-NE (Abcam, ab21595, 1:200 dilution) and anti-MPO (Dako, A0398, 1:350 dilution) primary antibody for 1 hour at room temperature, followed by 1-hour incubation with Alexa488-conjugated (Molecular probes, A-11008), CF555-conjugated (Biotium, 20039) and CF633-conjugated (Biotium, 20121) secondary antibodies (1:750 dilution). Anti-TOMM20 (NovusBio, NBP1-81556, 1:150 dilution) and anti-8-OHdG (Santa Cruz Biotechnology, sc-393871, 1:150 dilution) were also used. Three washes with 0.5% w/v BSA/PBS were performed in-between all stainings. After staining, coverslips were mounted on Mowiol 4-88 (Sigma-Aldrich, 81381) and were observed with confocal microscopy (40X objective, Leica SP8). Confocal images were analyzed with the FIJI software.

Paraffin-embedded renal and skin sections from active SLE patients and healthy donors were cut at 3μm, mounted and dried on Superfrost Plus slides (Thermo Scientific). After dewaxing and rehydration, the sections were incubated in citrate-based HIER buffer at 60°C in a water bath for 60 minutes. After antigen retrieval, they were left in the respective citrate buffer at room temperature to cool below 30°C, rinsed with deionized water three times, TBS pH7.4 one time, and permeabilized for 8 minutes with 0.2% Triton X100 in TBS, followed by three rinsing steps with TBS and blocking with 5% w/v BSA/TBS. Immunostaining was conducted as detailed above. The same tissue sections were also stained with hematoxylin & eosin (H&E) and evaluated by a Nikon Eclipse E-400 light microscope (400X magnification).

Western blot

Cells or NETs-precipitated proteins were lysed on ice in SDS lysis buffer (2% Sodium Dodecyl sulfate-SDS, 62.5mM Tris pH 6.8, 5% 2-Mercaptoethanol, 10% glycerol) supplemented with Complete Protease inhibitor cocktail (Roche) and centrifuged at 13,000×g for 15 minutes at 4°C. Whole-cell lysates (20-30μg protein) were subjected to SDS-PAGE electrophoresis on 12.5% gels and then transferred to an Immobilon-PSQmembrane (Millipore, SEQ85R). Membranes were blocked with 5% skimmed milk in TBST and then incubated with anti-MPO (1:3000 dilution, Dako) as loading control

(78) or anti-IL-33 (1:1000 dilution) specific antibodies (R&D, Nessy). For HL-60 protein extracts, mouse anti-human tubulin antibody was used as loading control (1:3000 dilution, ThermoFischer Scientific, A11126). Detection was performed using relevant HRP-linked antibodies (Millipore, USA) and enhanced chemiluminescent (ECL) detection reagents (Amersham Biosciences).

NETs protein precipitation for mass spectrometry

Neutrophils (4–7×106) where stimulated using PMA (100nM, Sigma-Aldrich) for 3 hours at 37°C. SLE neutrophils were stimulated using ICs (as described above) or left unstimulated (for 3 hours at 37°C) to release NETs spontaneously. Supernatants were carefully removed, cells were washed twice, and NETs were harvested using DNase (20U/ml, Roche, 4716728001) in HBSS (Thermofischer Scientific, 14025) for 20 minutes. Supernatant-containing NETs were isolated via centrifugation. NETs proteins were precipitated using 80% v/v acetone overnight at -20°C. Precipitated pellet was obtained via centrifugation at 10000g for 30 minutes. Then, precipitated proteins were washed twice using an acetone-based buffer (80% v/v acetone, 10mm Tris-HCl pH=8). Protein pellets were stored at -80°C until mass spectrometry analysis.

Mass spectrometry

Sample preparation

Samples were homogenized in lysis buffer consisting of 7M urea, 2M thiourea, 4% w/v CHAPS, 1% w/v DTE, and 2% v/v IPG ampholytes. Samples were sonicated for 10 minutes in a water bath sonicator followed by centrifugation at 16.000 rcf for 20 min at room temperature to collect supernatants. Protease inhibitors (3.6% v/v) were added to the extracts and the protein concentration was determined by the Bradford assay. Samples were processed with the GeLC-MS method as previously described (Makridakis M. et al., 2018). Briefly, 10μg of thesamples were loaded on SDS PAGE (5% stacking, 12% separating) and the electrophoresis wasstopped when the samples just entered the separating gel. Gels were fixed with 30% v/v methanol,10% v/v acetic acid for 30 min at room temperature, followed by wash with water (3 × 10 min washes). Gels were stained with coomassie colloidal blue stain overnight at room temperature. After washingthe gels with water, protein bands were excised and were

sliced into small pieces (1-2mm). Gel pieceswere destained with 40% acetonitrile, 50mM NH4HCO3, reduced with 10mM DTE in 100mM NH4HCO3 for 20 min at room temperature, and alkylated with 10mg/mL iodoacetamide in 100mM NH4HCO3 for 20 min at room temperature, in the dark. After alkylation, the samples were washed with 100mM NH4HCO3 followed by another wash with 40% acetonitrile, 50mM NH4HCO3 and a final wash with ultra-pure water was performed (20 min, at room temperature for each wash). Gel pieces were dried in a centrifugal vacuum concentrator (speed vac). Trypsinization was performed overnight at room temperature in the dark. Six hundred ng of trypsin was added per sample (10ng/μL tryspin stock solution in 10mM NH4HCO3, pH 8.5). Finally, the peptides were extracted after incubation with 50mM NH4HCO3 for 15min, room temperature, followed by two incubations with 10% formic acid, acetonitrile (1:1) for 15 min, room temperature. The peptide solution was filtered with PVDF filters(Merck Millipore) and was dried in a centrifugal vacuum concentrator. Samples were stored at -20°C until further use.

LC-MS/MS analysis

Samples were resuspended in 10μL mobile phase A (0.1% FA). A 5μL volume was injected into a Dionex Ultimate 3000 RSLS nano flow system (Dionex, Camberly, UK) configured with a Dionex 0.1 × 20 mm, 5 μm, 100 Å C18 nano trap column with a flow rate of 5 μL / min. The analytical column was an Acclaim PepMap C18 nano column 75 μm × 50 cm, 2 μm 100 Å with a flow rate of 300 nL/min. The trap and analytical column were maintained at 35°C. Mobile phase B was 100% ACN:0.1% formic acid. The column was washed and re-equilibrated prior to each sample injection. The eluent was ionized using a Proxeon nano spray ESI source operating in positive ion mode. For mass spectrometry analysis, a Q Exactive Orbitrap (Thermo Finnigan, Bremen, Germany) was operated in MS/MS mode. The peptides were eluted under a 60 minutes gradient from 2% (B) to 33% (B). Gaseous phase transition of the separated peptides was achieved with positive ion electrospray ionization applying a voltage of 2.5 kV. For every MS survey scan, the top 10 most abundant multiply charged precursor ions between m/z ratio 300 and 2200 and intensity threshold 500 counts were selected with FT mass resolution of 70,000 and subjected to HCD fragmentation. Tandem mass spectra

were acquired with FT resolution of 35,000. Normalized collision energy was set to 33 and already targeted precursors were dynamically excluded for further isolation and activation for 5 seconds with ppm mass tolerance.

MS data processing

Total proteome analysis

Raw files were analyzed with Proteome Discoverer 1.4 software package (Thermo Finnigan), using the Sequest search engine and the Uniprot human (Homo sapiens) reviewed database, downloaded on December 15, 2017, including 20,243 entries. The search was performed using carbamidomethylation of cysteine as static and oxidation of methionine as dynamic modifications. Two missed cleavage sites, a precursor mass tolerance of 10 ppm and fragment mass tolerance of 0.05 Da were allowed. False discovery rate (FDR) validation was based on q value: target FDR (strict): 0.01, target FDR (relaxed): 0.05. The intensity of the signal of MPO peptides was normalized for each sample by dividing with the total intensity of identified peptides and converted to ppm. The list of identified proteins is shown in Supplementary Tables.

Targeted proteomics analysis

Proteotypic peptides (peptides that uniquely represent the target protein) for IL-33 were selected based on available data from spectral libraries (http://www.nist.gov/) that were imported to the Skyline software for targeted proteomics analysis. Proteotypic peptides were also evaluated with the Protein Basic Local Alignment Search Tool (BLAST, http://blast.ncbi.nlm.nih.gov) and their proteotypicity was further validated. Skyline indicated the precursor ions that were utilized in the PRM (Parallel Reaction Monitoring) method. For each precursor ion, 2-5 transitions were used for the relative quantification. Data analysis was performed with the Skyline software and all chromatograms were manually inspected to ensure the good quality and accurate peak picking. The top signal producing transition was selected as the quantifier transition in all cases, while the remaining transitions

were used as qualifier transitions, for accurate peak profile and retention time confirmation. For pooled samples the IL-33 peptide intensity was normalized by dividing with the MPO intensity.

Flow cytometry

Cells were stained for extracellular markers for 20 minutes at 4°C in PBS/5% FBS. For phosphoprotein staining (PE-conjugated mouse anti-phosphorylated IRF-7 antibody, BD biosciences, K47-671), cells were permeabilized and stained using the Intracellular Fixation and Permeabilization Buffer Set kit (eBioscience, 88-8824-00). Conjugated antibodies against CD123, CD303, CD15, CD14, HLADR and CD10 were from Biolegend (catalogue numbers 306012, 354208, 301906, 325604, 307628, 312210, respectively). Ig isotype controls were used in all assays.

Quantitative real-time PCR

Total RNA from neutrophils or pDCs was collected using the TRIzol (Invitrogen, 15596026) extraction protocol followed by Turbo DNase (Ambion, AM2238) treatment according to the manufacturer instructions. cDNA was prepared using PrimeScript 1st strand cDNA Synthesis Kit (Takara, RR037A). Transcripts were quantified by incorporation of the KAPA SYBR FAST qPCR Kit Master Mix (2X) (Kapa Biosystem, KK4602) at a BIO-RAD CFX ConnectTM Real-Time System. Expression levels was normalized to GAPDH or HPRT1 and calculated by the change-in-threshold method [2ˆ(-ΔΔCT)]. Primer sequences are listed in Supplementary Table S5.

ELISA

NET-associated IL-33/dsDNA complexes were quantified by a modified capture ELISA. Specifically, 1μg/ml of mouse anti-human IL-33 (Nessy) antibody (Enzo) was coated overnight to 96-well microtiter plates. After blocking with 1% w/v BSA and 1% v/v donkey serum, human serum (1:6 dilution) was added together with a peroxidase-labeled anti-DNA monoclonal antibody of the Cell Death ELISAPLUS kit (1:25, Roche, 11774425001). The plate was incubated for 2 ½ hours, shaking at 300 rpm at room temperature. After 3 washes with PBS, peroxidase substrate (ABTS) was added to incubate at room temperature in the dark for 20 minutes. Absorbance at 405 nm wavelength was

measured (490nm used as reference filter). IL-33/MPO complexes were quantified using a goat antihuman IL-33 antibody (R&D) for coating (1:200 dilution) and a mouse anti-human MPO antibody (Hycult Biotech, HM1051) for detection (1:100 dilution). After 3 washes with PBS, anti-mouse HRP antibody (Millipore, AP308P, 1:10000 dilution) was added for 1 hour at room temperature. After 5 washes with PBS, TMB (Invitrogen, 002023) was added and light absorbance was measured at 450 nm (540nm used as reference filter). Detection of IFNα (PBL, Human IFN Alpha Multi-Subtype ELISA Kit, PBL41110-1) in culture supernatants was performed by pre-coated sandwich ELISA. Light absorbance at 450 nm was measured using the ELx800 Biotek. Background signal was subtracted. All samples were assessed in duplicates.

Statistical analysis

Data were analyzed using GraphPad Prism 8 software. Results are presented as the means ± SEM (standard error of the mean) and/or dot-plots. Data normality was assessed by the Shapiro-Wilk test to guide selection of parametric or non-parametric tests. In assays including multiple conditions/treatments, repeated measures ANOVA (analysis of variance) was used, followed by posthocvHolm-Sidak test to correct for multiple comparisons. The association between IL-33 serum complexes (IL-33/dsDNA, IL-33/MPO) and SLE disease activity (SLEDAI-2K) was assessed by the Spearman's rank correlation (rho) coefficient. Two-tailed p-value <0.05 was considered statistically significant.

6) Results

6.1 Inflammatory mediators enhance neutrophils IL-33 expression

It is well-established that IL-33 is mainly expressed by non-hematopoietic cells. Despite the fact that reports for neutrophil-expression of IL-33 are limited, we sought to determine if neutrophils could be a potential source of IL-33. For that purpose, we administrated recombinant IFN-α and TNF-α cytokines, mimicking thus SLE inflammatory milieu, to control neutrophils derived from healthy donors. Notably, combined IFN-α and TNF-α treatment led to a significant increase of *IL-33* mRNA levels **(Figure 1A)**. By employing immunostaining and confocal microscopy, we also monitored increased IL-33 protein expression in IFNa/TNFα-treated cells while there was no detectable IL-33 expression in untreated cells or in stimulated cells stained only with the appropriate negative control (anti-goat secondary Ab) **(Figure 1B)**. Next, we isolated neutrophils from healthy donors and active SLE patients and monitored *IL-33* mRNA levels. SLE patients displayed increased *IL-33* mRNA levels compared to healthy donors recapitulating the phenotype of inflammatory neutrophils of Fig1A **(Figure 1C)**. Additionally, cultured SLE neutrophils were captured to release spontaneously neutrophil extracellular traps, as previously reported (Garcia-Romo et al., 2011), which were decorated with IL-33 whereas healthy neutrophils display minimal/background-like IL-33 signal and no release of NETs **(Figure 1D)**. So, SLE-relevant inflammatory mediators promote neutrophil-specific IL-33 expression while SLE-neutrophils release spontaneously IL-33 decorated NETs when cultured *in vitro*.

6.2 SLE immune complexes induce IL-33 expression and IL-33-decoration of NETs

Soluble factors in the serum contribute to the immunogenicity and NETotic capacity of SLE neutrophils (Garcia-Romo G. et al., 2011, Frangou E. et al.,2019). By culturing healthy neutrophils in medium supplemented with SLE serum (derived from serologically active patients), we monitored upregulation of *IL33* mRNA levels and protein expression as well as the release of IL-33 decorated NETs **(Figure 2A-2B-2C)**. Within lupus serum, ICs induce NETs through activation of neutrophil Fcγ-receptors (FcR) and TLR-7.

To address this, neutrophils were pre-treated with both FcR blocking and TLR-7-antagonist (IRS661) reagents followed by incubation with lupus serum. Both inhibitory reagents led to reduced production of IL-33-containing NETs and *IL33* mRNA **(Figure 2A-2B-2C)**, consistent with the well-established previous finding that ICs mediate NETs-release in a FcR and TLR7- dependent manner (Garcia-Romo G. et al., 2011).

Figure 1

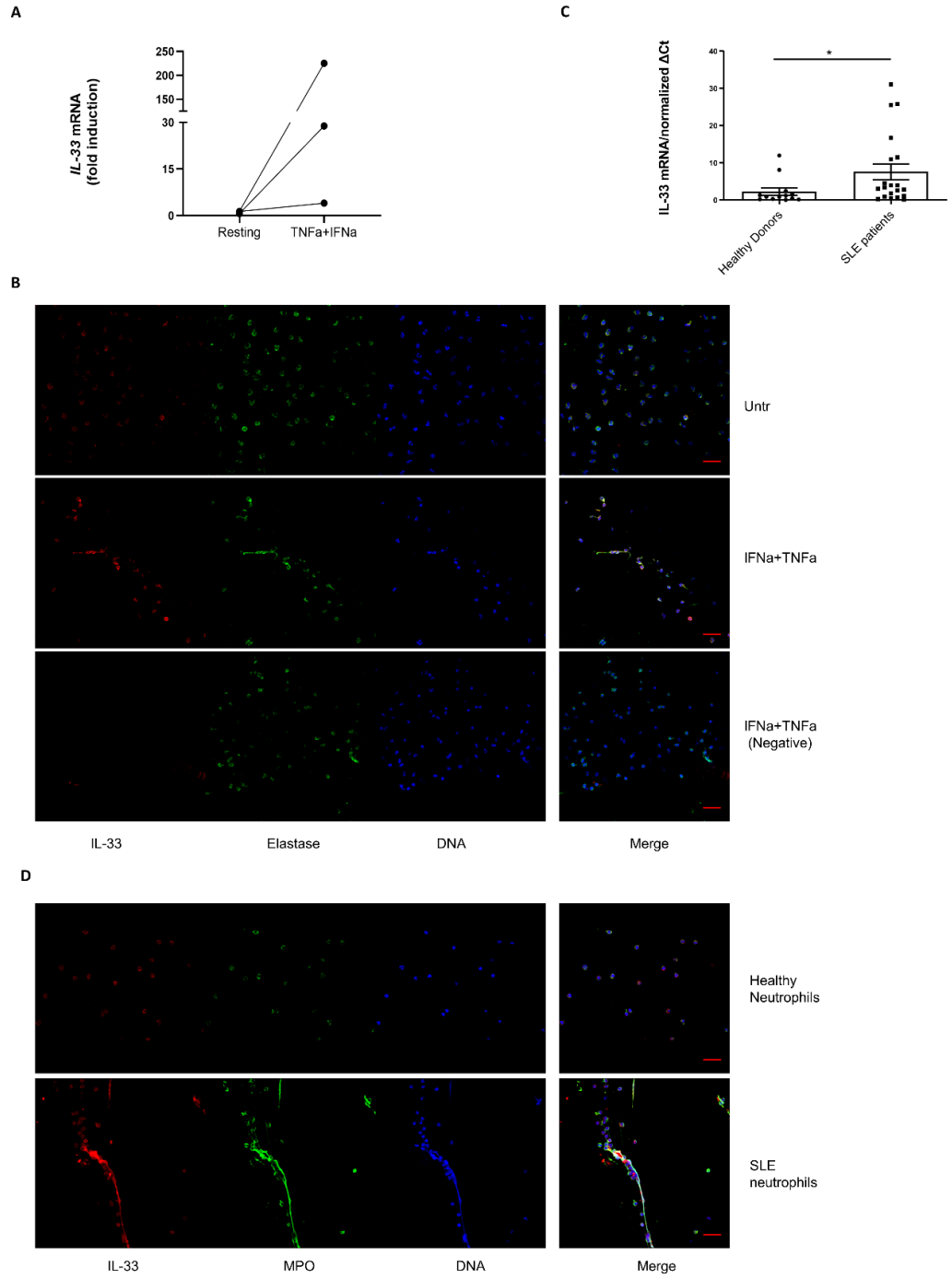

*Figure 1: (A) Isolated neutrophils derived from healthy donors were teated with IFN-α+TNF-α or left untreated and Real-time PCR was performed to confirm differential gene expression of IL33 (n=3). Data were normalized using the ΔCτ method (IL33 Cτ minus GAPDH Cτ). (B) Real-time PCR was performed to assay differential expression of IL33 mRNA in freshly isolated blood neutrophils from healthy (n=13) versus SLE (n=20) individuals. Data were normalized using the average of healthy donors ΔCτ (IL-33 Cτ minus GAPDH Cτ) values. Each dot represents a different donor and bar plots show the mean ± SEM expression. *p-value <0.05 (two-tailed, Mann-Whitney test). (C) (D) Blood neutrophils were purified from healthy donors and SLE patients, seeded onto coverslips coated with poly-l-lysine and cultured using TNF-α+IFN-α (C) or left untreated for 3 hours (followed by staining with anti-elastase(C), anti-MPO (D) and anti-IL-33 antibodies. DAPI was used for DNA staining. Representative confocal images (scale bar, 30μm) are shown*

Next, we sought to examine the effect of ICs directly on SLE neutrophils. The immune complexes that we used were consisted of SLE IgGs (from seropositive patients) combined with necrotic material from U937 cell line. Notably, SLE neutrophils exposed to ICs exhibited increased intracellular *IL-33* mRNA and protein levels **(Figure 2D-2E)**. Accordingly, both confocal microscopy of SLE neutrophils and immunoblotting of precipitated NET proteins revealed elevated IL-33 protein in IC versus spontaneously-released SLE NETs **(Figure 2F-2G)**. Contrary to SLE neutrophils, healthy neutrophils produced IL-33 NETs only after priming with exogenous IFN-α followed by administration of ICs **(Figure 2H)**, which reiterates the role of SLE milieu in determining the neutrophil NETotic potential. Conclusively, SLE-relevant nucleic acid-containing ICs stimulate neutrophils promoting thus increased IL-33 expression and the release of IL-33 decorated extracellular traps.

6.3 SLE IC-induced NETs exhibit distinct immunogenic properties

Neutrophil extracellular traps exhibit stimulus-dependent distinct properties. To begin with, we monitored increased levels of extracellular DNA concentration of IC-treated SLE- compared to resting SLE neutrophils which, as we already mentioned, are also prone to release NETs **(Figure 3A)**. Moreover, by treating control pDCs with NET-containing supernatants, we observed that IC-induced NETs exhibited increased interferogenic capacity compared to spontaneously-formed SLE NETs **(Figure 3B)**. As it is already reported, NETs immunogenicity is tightly correlated with the oxidation status of NET-DNA and its mitochondrial origin (Caielli S. et al.,2016). In confirmation of our experimental set-up, IC-induced NETs stained positive for 8-Oxo-2'-deoxyguanosine (a marker of oxidized DNA),

TOMM20 (an outer membrane mitochondrial protein) while both NET-structures and nuclei of NETotic cells are characterized by phosphorylated γH2Ax signal which is an additional sign of DNA oxidation (DNA damage) **(Figure 3C-3D)**.

Figure 2

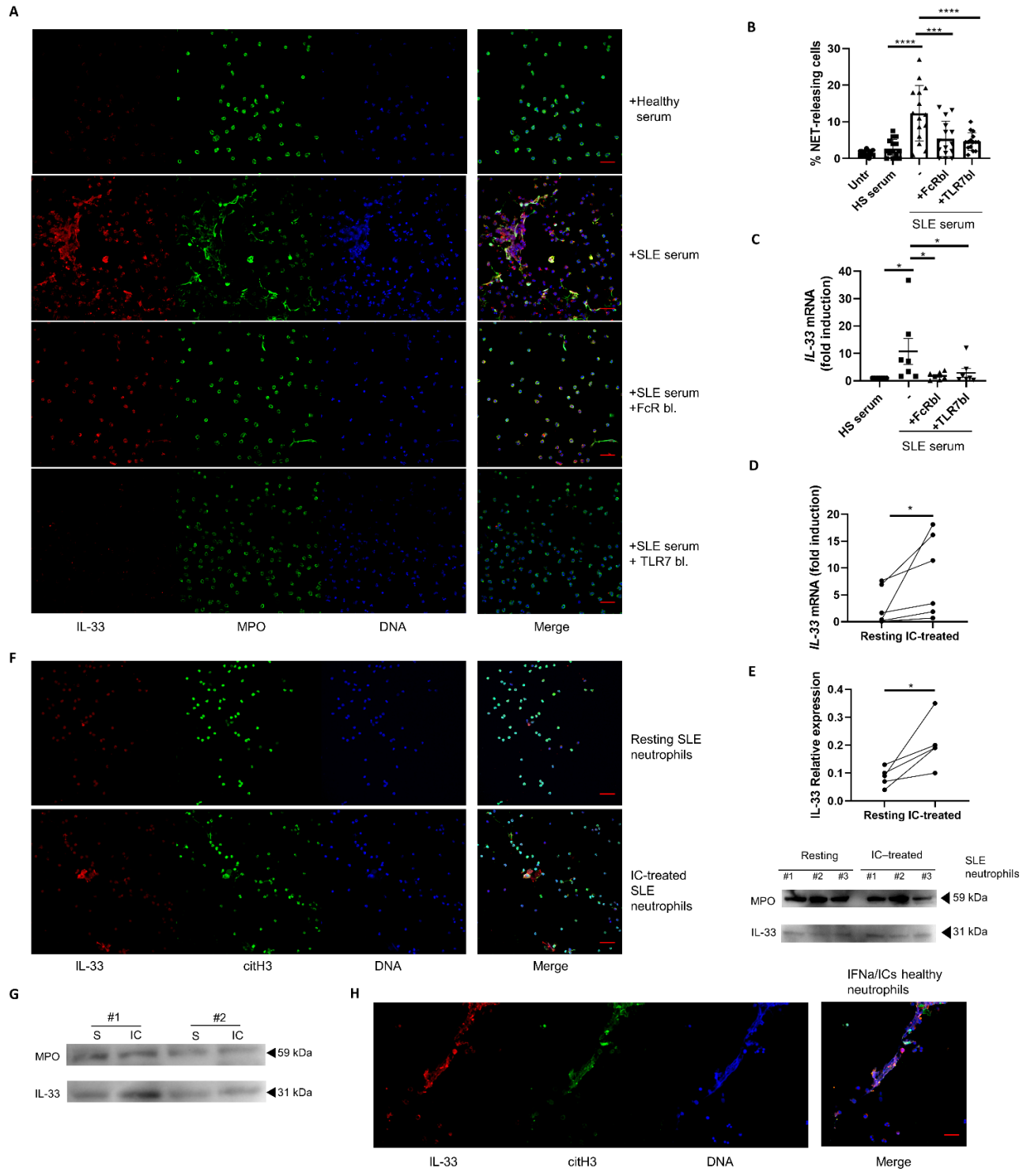

*Figure 2: (A) Healthy blood neutrophils were cultured in serum (10% v/v) obtained from two SLE patients who were positive for anti-dsDNA and anti-RNP autoantibodies for 3 hours, with or without pretreatment with FcR blocking agent or TLR-7 inhibitor (1μM, IRS661) for 45 minutes. Staining was performed with anti-IL-33 (IL-33), anti-myeloperoxidase (MPO) antibodies and DAPI for DNA. Representative confocal images (scale bar, 30μm) show induction of IL-33-containing NETs by SLE serum, which is reversed upon FcR or TLR-7 blockade (n=3 experiments were performed all exhibiting the same pattern). (B) Quantification of NETotic cells was conducted using the FIJI software as previously described (2). Each dot represents the percentage of NETotic cells measured in a randomly selected coverslip field (n=15) and bar plots show the mean ± standard error of the mean (SEM). **p<0.01 (two-tailed, repeated measures ANOVA with Holm-Sidak correction). (C) Real-time PCR was used to assess IL33 mRNA in healthy neutrophils cultured in presence of healthy serum or serum from two SLE patients who were positive for anti-dsDNA and anti-RNP autoantibodies, with/without FcR or TLR-7 blocking agent as described above. Quantification was performed using the double delta Ct method (2-ΔΔCT where ΔCτ=IL33 Cτ minus HPRT1 Cτ). Each dot represents a different neutrophil donor (n=7) and bar plots show the mean ± SEM. *p<0.05 (two-tailed, repeated measures ANOVA with Holm-Sidak correction). (D) Real-time PCR was performed to confirm differential gene expression of IL33 in resting versus IC-treated neutrophils from the peripheral blood of SLE patients (n=6). Data were normalized using the average value of resting neutrophils ΔCτ (IL33 Cτ minus GAPDH Cτ) values. Each dot represents a different donor and bar plots show the mean ± SEM expression. *p-value <0.05 (two-tailed, paired t-test). (E) Western immunoblotting was performed to examine intracellular IL-33 protein in unstimulated and IC-treated neutrophils from SLE patients (n=5). Results were normalized and quantified via densitometry by monitoring the relative expression of IL-33 over MPO (loading control) (left panel). *p-value <0.05 (two tailed, paired t-test). Representative blots from unstimulated and IC-treated neutrophils obtained from n=3 patients (right panel). (F) Unstimulated or IC-treated SLE neutrophils were cultured for 3 hours and then stained with anti-citrullinated histone-3 (citH3), anti-IL-33 (IL-33) antibodies, and DAPI for DNA. Representative confocal images (scale bar, 30μm) demonstrate that IC-treated SLE neutrophils generate abundant amounts of IL-33-decorated NETs. (G) Western immunoblotting for IL-33 protein in spontaneously-released versus IC-mediated NETs precipitates derived from SLE neutrophils (n=2). (H) Neutrophils from healthy donors were primed with recombinant IFN-a (2000IU/mL, 1 hour) followed by addition of SLE ICs. At 3 hours, cells were stained with anti-IL-33, anti-MPO antibodies and DAPI for DNA. Under these lupus-inducing conditions, neutrophils produced IL-33-decorated NETs. Representative confocal image from n=5 experimentss (scale bar, 30μm) isare shown.*

The profound oxidation status of NET-DNA was reported to be associated with defective mitophagy mechanisms which result in elevated mitochondrial ROS in IC-treated SLE neutrophils. Considering that SLE-NETs were observed to occur in a NOX-independent manner (Pieterse E. et al., 2018), we tried to address if IC-SLE NETs of our experimental set up exhibit similar properties.

For that purpose, we blocked NADPH oxidase using Diphenyleneiodonium chloride (DPI) to inhibit NOX-dependent NETosis of activated neutrophils. Notably, DPI administration did not affect extracellular DNA release of IC-treated SLE NETs while it reduced extracellular NET-DNA levels of PMA-treated cells **(Figure 3E)**. Furthermore, IC-SLE NETs exhibited enhanced citrullinated histone-3 expression (a marker indicative of NOX-independent pathway ofNETosis) while by comparing NOX-dependent (PMA-treated heathy neutrophils) versus NOX-independent (MSU-treated healthy neutrophils, IC-treated SLE neutrophils) NETs, we observed that only the latter exhibited significant IL-33 decoration **(Figure 3F)**, thus suggesting a mechanistic link between NOX-independent pathway of NETosis and IL-33-NET decoration. Conclusively, nucleic acid-containing ICs stimulation of SLE neutrophils recapitulates typical lupus NETosis while it is also associated with increased IL-33 expression and potent NETs' interferogenic potential.

6.4 IL-33 modulates TLR-responses of pDCs

Until now, we have monitored characteristic IL-33 decoration and increased interferogenicity of IC-SLE NETs. So, considering that alarmins were proposed to be potent mediators of NETs immunogenic potential, we sought to determine if IL-33 exert interferogenic effects combined with NET-chromatin. First, we monitored a relatively low but significant expression of ST2L of pDCs in steady state compared to an isotype control. Moreover, by using medium supplemented with SLE sera from active SLE patients, mimicking thus SLE milieu in vitro, we observed upregulated levels of ST2L expression **(Figure 4A)**. Notably, ST2L expression was more profound in CD303int pDCs which were previously reported as the IFN-producing subset because of BDCA-2's capacity to block IFN-α production (Rock J. et al., 2007). As shown in **Fig4B**, SLE pDCs display down-regulated levels of ST2L expression which may be an indication of pDCs' effort to regulate IL-33 excessive signaling in the periphery or infiltration of immunogenic ST2L+ pDCs in tissues. Taking into consideration, that NET-chromatin stimulate pDCs in a TLR-dependent fashion combined with the responsiveness of our cell subset of interest to IL-33, we performed an IFN-depedent screening using TLR7 and TLR9 ligands combined with recombinant full-length and cytokine- IL-33. Surprisingly, full length IL-33 reduced interferon stimulated gene (ISGs) mRNA levels both in TLR-9 or TLR7-stimulated pDCs while fl-IL-33 also down-regulates *IFNA* mRNA levels of R848-treated pDCs **(Figure 4C)**. However, cytokine-isoform of IL-33 increased *IFNA* mRNA levels of TLR7-treated pDCs while it

reduced *IFNA* transcription of TLR-9 stimulated cells. Additionally, treatment of pDCs with exogenous cytokine-isoform of IL-33 alone failed to induce significant *IFNA* transcription **(Figure 4C)**.

To prove that TLR7-mediated signaling is of significance regarding NET-mediated stimulation, we pre-treated pDCs using a TLR7-specific inhibitor (IRS661) prior to NET-stimulation and we monitored a clear reduction of *IFNA* mRNA levels **(Figure 4D)**.

Figure 3

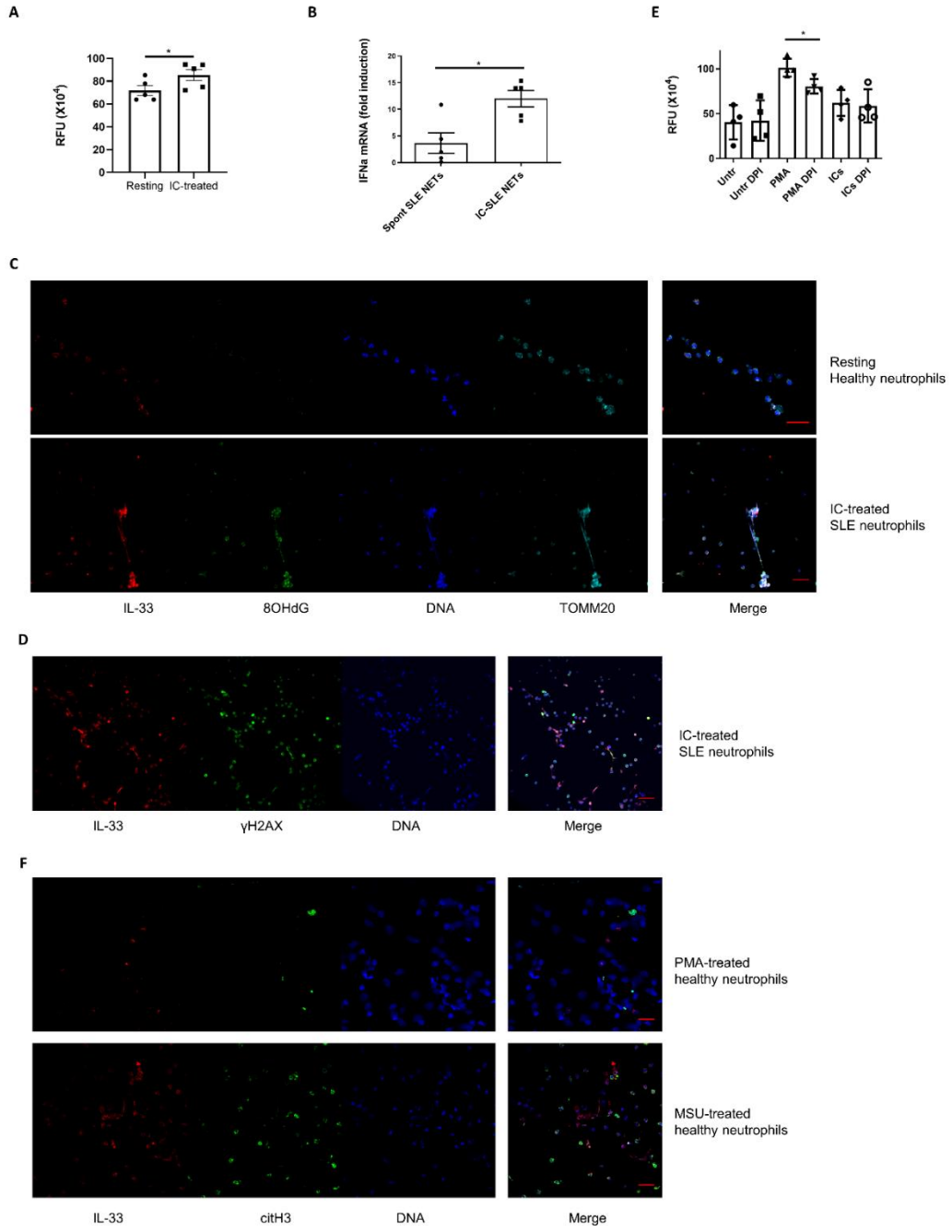

*Figure 3: (A) Unstimulated (resting) and immunocomplexes (ICs)-treated neutrophils from SLE patients were assessed for NETs production assayed by the extracellular DNA dye SYTOX Green. Each dot represents the relative fluorescence intensity in neutrophils derived from n=5 SLE patients. *p<0.05 (two tailed, paired t-test). (B) Real-time PCR was performed to determine* IFNA *mRNA levels, respectively, by healthy pDCs treated overnight with spontaneously-released SLE NETs and IC-induced SLE NET-containing supernatants (IC NETs) (25% v/v). *p<0.05; (paired t test). (C) Resting healthy neutrophils and IC-treated SLE neutrophils were cultured for 3 hours and then stained using anti-8-Oxo-2'-deoxyguanosine (8-OH-dG), anti-TOMM20 (TOMM20, Translocase Of Outer Mitochondrial Membrane 20), and anti-IL-33 (IL-33) antibodies. DAPI was used for DNA staining. Representative confocal images from n=3 experiments (scale bar, 30μm) are shown (D) IC-treated SLE NETs were cultured for 3 hours and stained with anti-pH2Ax and anti-IL-33 (IL-33) antibodies. DAPI was used for DNA staining. Representative confocal images from n=2 experiments (scale bar, 30μm) are shown (E) Control neutrophils pretreated or not with DPI (NOX inhibitor, 30 min) were cultured for 3 hours in medium supplemented with PMA or ICs. Supernatants were assessed for NETs production assayed by the extracellular DNA dye SYTOX Green. Each dot represents the relative fluorescence intensity in neutrophils derived from n=4 donors (two-tailed, repeated measures ANOVA with Holm-Sidak correction) (F) Healthy neutrophils were activated with PMA (phorbol myristate acetate, 100nM) or MSU (monosodium urate, 100μg/mL). At 3 hours, cells were stained with anti-IL-33 (IL-33) and anti-citrullinated histone-3 (citH3) antibodies. DAPI was used for DNA staining. Representative confocal images (scale bar, 30μm) from n=3 experiments indicate enhanced production of IL-33-decorated NETs by MSU-treated cells.*

So, IL-33/ST2L axis seems to enhance pDCs TLR7-mediated IFNα-responses suggesting that it could also promote TRL7-dependent activation by SLE NETs.

6.5 SLE NETs activate pDCs to produce type I IFN in an ST2L-dependent manner

We previously showed that IC-treated SLE neutrophils externalize NETs that trigger pDCs to produce type I IFN confirming thus the preexisting literature (Garcia Romo G. et al, 2011, Lande R. et al., 2016, Caielli S. et al., 2016). Besides the nucleic acid content, NETs interferogenic capacity is also regulated by the protein cargo, thus NET complex is a potent mediator of the lupus characteristic dysregulated immune response. Considering that IL-33 modulates TLR-mediated response we sought to investigate if IL-33, that decorates IC-SLE NETs, augments their interferogenic potential. We administered NETs derived from IC-treated SLE neutrophils to healthy pDCs which were pre-treated with a monoclonal inhibitory anti-ST2L antibody (aST2L) to block IL-33 signaling. pDCs were pre-treated with FcR blocker to minimize any ICs carry-over or non-specific aST2L effects.

In agreement with the aforementioned reports, SLE IC NETs induced robust *IFNA* mRNA and protein expression, which was significantly reduced upon ST2L blockade **(Figure 5A)**.

A similar effect was noted with the mRNA levels of *IRF7* (IFN regulatory factor 7), a characteristic interferon-stimulated gene **(Figure 5B)**. Additionally, neither NET- nor NET combined with ST2L blockade-stimulation affected pDCs viability **(Figure 5C)**. To gain insights into the intracellular events linking IL-33-complexed NETs with IFN-α production by pDCs, we examined the levels of phosphorylated (p-)IRF7, which is essential for the expression of type I IFN genes downstream to TLR signaling. Treatment of pDCs with SLE IC NETs caused upregulation of p-IRF7, which was reversed following ST2L blockade **(Figure 5D)**, therefore reiterating the role of IL-33/ST2L axis in SLE NETs interferogenic effect. Likewise, SLE IC NETs-containing supernatants pre-treated with anti-IL-33 blocking antibody displayed significantly reduced inteferogenic capacity (**Figure 5E**), thus further supporting the role of IL-33/ST2L axis on NETs–mediated IFN-α production by pDCs. Of note, PMA-induced NETs released from healthy neutrophils induced a less profound type I IFN response (*IFNA* and *IRF7* mRNA expression) by pDCs, which was not significantly altered by ST2L blockade (**Figure 5F**). Interestingly, ST2L blockade did not alter the effect of IC-NETs regarding antigen presentation (MHC-II expression) and maturation (CD83 expression) **(Figure 5G).** To discern the relative effects of NETs-associated DNA and IL-33, we cultured pDCs using cytochalasin D (blocks endocytosis of NETs) or chloroquine (disrupts endosomal TLR trafficking). By using either CytoD or chloroquine, IFN-α response by pDCs was diminished **(Figure 5H)**, suggesting that NET DNA scaffold is essential for the immunostimulatory effects of IL-33. That result comes in agreement with the disability of IL-33 to promote IFN-α responses of pDCs when used as a single stimulus **(Fig 4C)**. These results indicate that IL-33 associated with SLE NET DNA may interact with ST2L on pDCs to augment IFN-α responses in an IRF7-dependent fashion.

6.6 Loss of IL-33 impairs the interferogenic potential of SLE-like NETs

To provide direct evidence for the implication of IL-33 in the interferogenic capacity of SLE NETs, we pursued gene-silencing experiments. Due to the short lifespan and general sensitivity of primary neutrophils, we differentiated the HL60 myeloid cell line into neutrophil-like cells using a retinoic acid-basedprotocol (Nordenfelt P. et al., 2009).

Differentiated HL60 cells exhibited increased granularity, expressed characteristic neutrophil-specific markers **(Figure 6A)** and produced IL-33-decorated NETs following priming with IFN-α and treatment with SLE ICs **(Figure 6B)**. Next, we performed IL33 gene silencing in neutrophil-like HL60 cells, which resulted in efficient knock down of IL-33 protein **(Figure 6C)** without affecting the release and DNA content of IC-induced NETs **(Figure 6D)**. Notably, NETs derived from HL60 cells transfected with scramble siRNA induced significant amounts of *IFNA* mRNA and protein by healthy pDCs in an ST2L-dependent manner, thus recapitulating the effects of SLE NETs **(Figure 6E)**. In contrast, NETs from *IL33*-silenced neutrophil-like cells lost their interferogenic capacity and ST2L blockade had no effect **(Figure 6E)**. These data support that the IL-33/ST2L axis is critical for the interferogenic potential of SLE IC NETs.

6.7 SLE immune complexes-induced NETs are enriched in IL-33 isoforms with putative enhanced bioactivity

Our findings suggest that NETs-complexed IL-33 from IC-treated lupus neutrophils drives IFN-α production by pDCs. IL-33 exists in chromatin-associated, full-length nuclear form that can be cleaved by neutrophil serine proteases into highly bioactive forms (Lefrancais E. et al.,2012). We asked whether IC SLE NETs contain cleaved IL-33 isoforms not detectable by immunoblotting due to their low abundance. We performed Parallel Reaction Monitoring-Mass Spectrometry in NETs-precipitated proteins from untreated and IC-treated SLE neutrophils, as well as from healthy neutrophils undergoing PMA-induced NETosis (n=6–8 individuals in each group) **(Table 1-3)**. In line with the immunofluorescence data, IC-treated SLE NETs demonstrated the highest intensity of the IL-33 proteotypic peptide -VDSSENLCTENILFK[aa251-265] **(Figure 7A)**. We next designed a focused proteomic analysis using pooled NETs proteins to obtain a richer proteomic profile and gain additional insights on possible NETs protease-mediated IL-33 cleavage/activation. We collected NET-associated proteins from a new cohort of the same three groups of neutrophils followed by targeted IL-33 peptide quantification (normalized over MPO intensity to allow for comparative analyses). Through this approach, we identified two additional IL-33 proteotypic peptides, namely -MLMVTLSPTK[aa180-189] and -DNHLALIK[aa243-250], which displayed increased levels in IC-induced versus untreated SLE NETs and PMA-treated healthy NETs **(Figure 7B)**.

Importantly, all three IL-33 peptides found to be upregulated in SLE IC NETs are localized near the C-terminus, which exists in the bioactive isoforms of IL-33 and accounts for their signaling potential and not in the N-terminus, which is found only in the full-length protein **(Figure 7C)**. Together, these results suggest that IC-induced SLE NETs may be enriched in cleaved IL-33 isoforms with putative enhanced bioactivity.

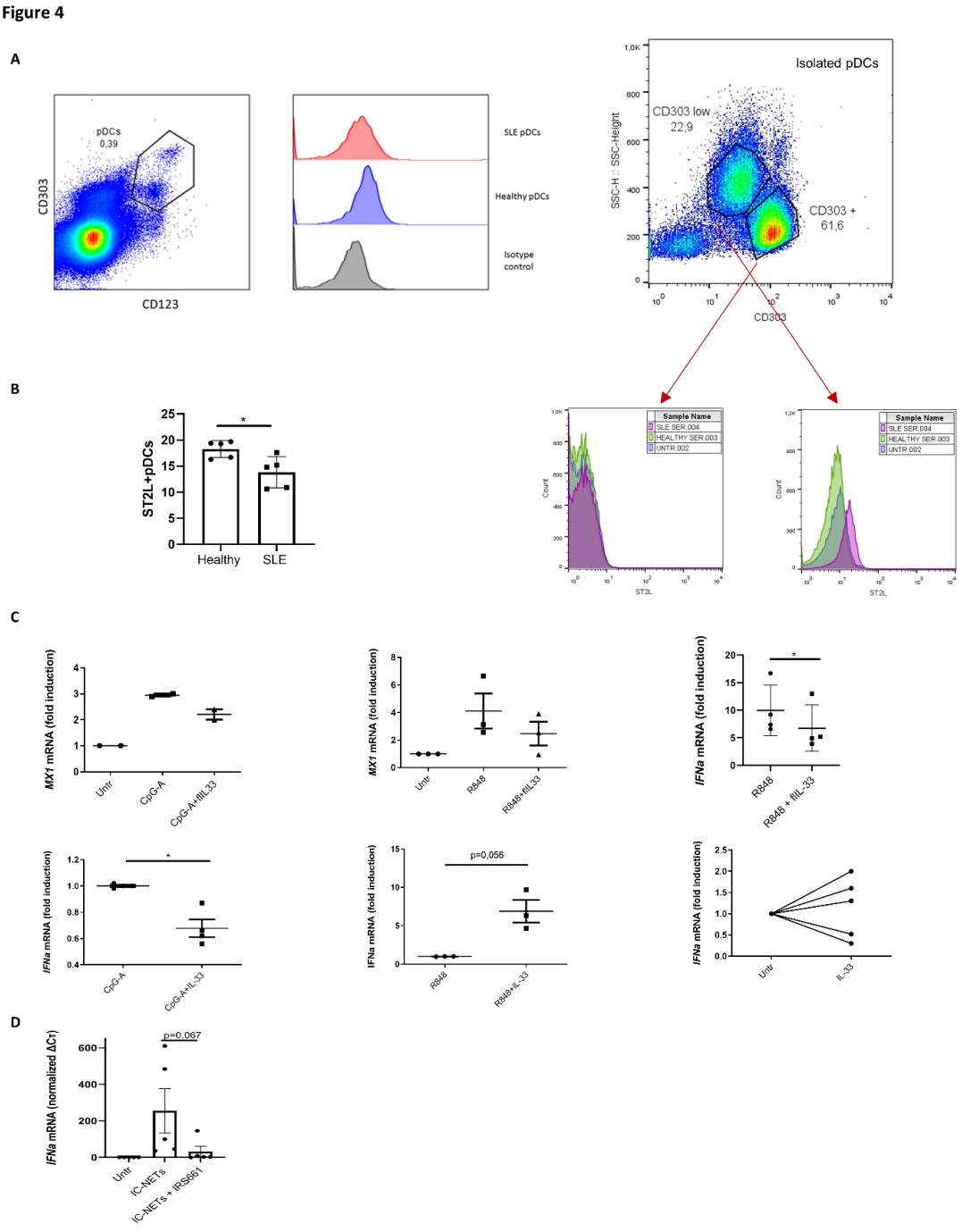

Figure 4: (A) pDCs were identified as CD123+ CD303+ peripheral blood mononuclear cells. A representative graph of the gating strategy in a patient with SLE is shown (left panel). Membrane ST2L within CD123+ CD303+ pDCs was measured by flow

*cytometry. At the right panel, ST2L expression of SLE sera treated pDCs (4hr) is illustrated (B) Following the procedure outlined in (A), the proportion of ST2L+ pDCs was determined in the peripheral blood of healthy individuals (n=5) and SLE patients (n=5). *p<0.05 (two-tailed, independent samples t-test). (C) Isolated pDCs were cultured with CpG-A(0,5μM) or R848 (5 μg/ml) combined with rfIIL-33 (100ng/m) or rIL-33(100ng/ml) for 17 hours. Real-time PCR was performed to monitor* IFNA *and* MX1 mRNA levels **p<0.05 (paired test). (D) Isolated pDCs pretreated or not with TLR7 antagonist IRS661 (0,1μM) were treated with IC-SLE NETs containing supernatants for 17 hours. IFNA mRNA levels were monitored using qPCR (p=0,067, paired t-test).*

Figure 5

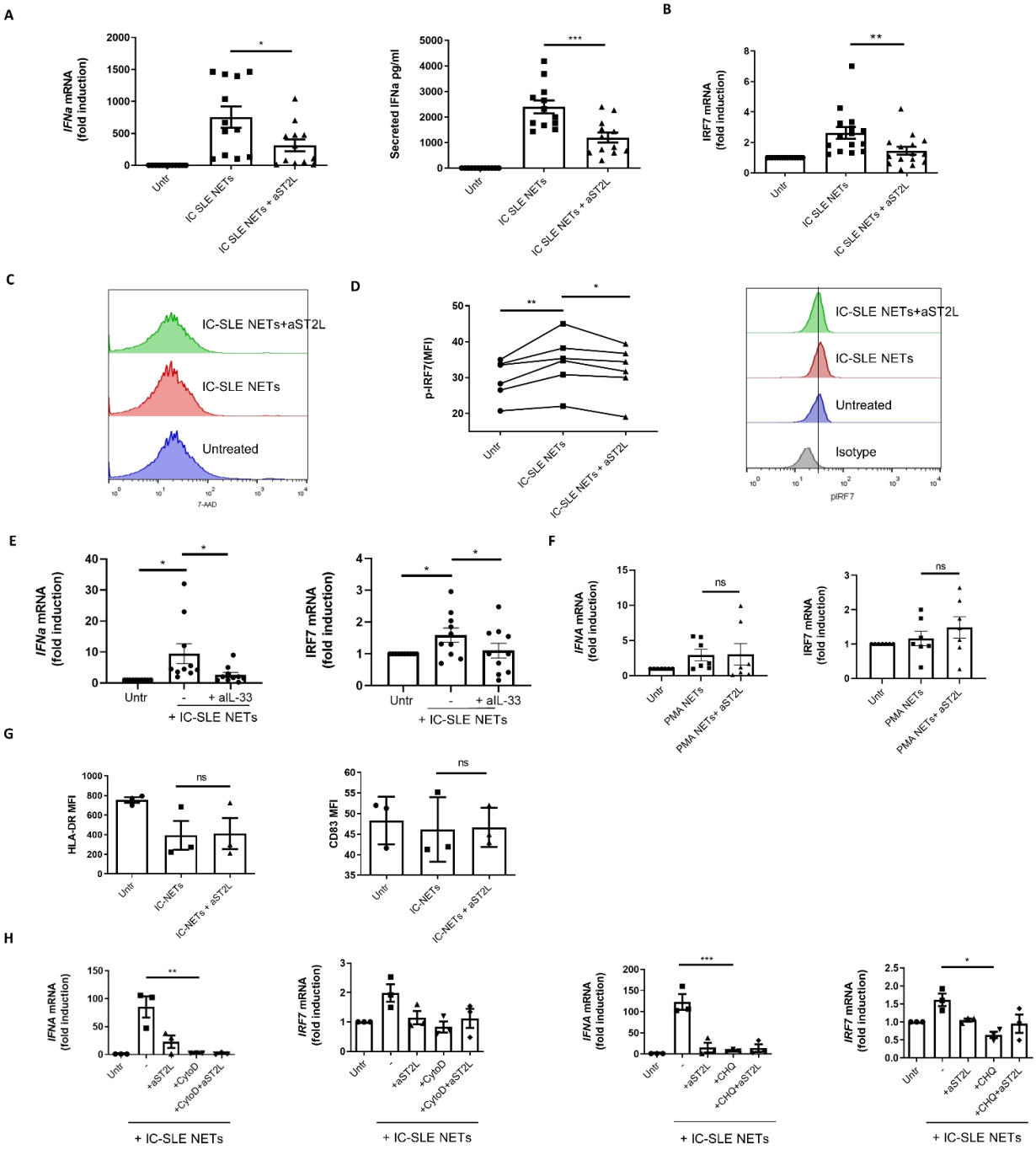

*Figure 5: (A) Real-time PCR (left panel) and ELISA (right panel) was performed to determine mRNA and protein expression/secretion of IFNα, respectively, by healthy pDCs treated overnight with IC-induced SLE NET-containing supernatants (IC NETs) (25% v/v). The contribution of IL-33/ST2L axis on IFNα response was assessed by pretreating pDCs with an antibody against ST2L (a-ST2L, 3 µg/ml). FcR blocking reagent was used to avoid any IC-carry over effect or non-specific a-ST2L binding. Each dot represents a different pDC donor (n=12) and bar plots show the mean ± SEM expression. *p<0.05; ***p<0.001 (two-tailed, repeated measured ANOVA with Holm-Sidak correction). (B) Real-time PCR for IRF7 mRNA expression in pDCs (n=12 healthy donors) stimulated with IC NETs (25% v/v), with or without pre-treatment with FcR blocking agent and a-ST2L as described above. Quantification was performed using the double delta Ct method (2-ΔΔCT where ΔCτ=IRF7 Cτ minus GAPDH Cτ) **p<0.01 (two-tailed, repeated measured ANOVA with Holm-Sidak correction). (C) pDCs viability was assessed using 7-AAD staining and flow cytometry in the aforementioned conditions (D) Intracellular phospho-IRF7 staining was performed 4 hours after stimulation of purified pDCs with IC NETs (25% v/v), with or without pre-treatment with FcR blocking agent and a-ST2L as described above. Each dot (open circle, full circle, triangle) corresponds to the kinetics of phospho-IRF7 (MFI: mean fluorescence intensity) in n=9 independent donors. *p<0.05 (two-tailed, repeated measured ANOVA with Holm-Sidak correction). Right panel illustrates a representative flow cytometry histogram of intracellular p-IRF7 levels in pDCs treated as described above. (E) Real-time PCR to quantify IRF7 and IFNA mRNA in healthy pDCs treated overnight with IC-induced NETs-containing supernatants (IC NETs) (25% v/v). The contribution of IL-33/ST2L axis was assessed by pretreating supernatants for 45 min with an antibody against IL-33 (a-IL33, 4µg/ml). FcR blocking reagent was used to avoid any IC-carry over effect or non-specific a-IL33 binding. Each dot represents a different pDC donor (n=10) and bar plots show the mean ± standard error of the mean (SEM). *p<0.05 (two-tailed, repeated measures(RM-) ANOVA with Holm-Sidak correction). (F) Real-time PCR to determine IRF7 and IFNA mRNA levels in healthy pDCs treated with PMA-induced NETs-containing supernatants (PMA-NETs) (25% v/v) from healthy neutrophils. The contribution of IL-33/ST2L axis was assessed by pretreating pDCs with a monoclonal antibody against ST2L (a-ST2L, 3µg/ml). FcR blocking reagent was used to avoid any non-specific a-ST2L binding. Each dot represents a different pDC donor (n=7). Two-tailed p-values are shown (RM-ANOVA with Holm-Sidak correction). (G) Flow cytometry was conducted to monitor HLA-DR and CD83 MFI in healthy pDCs treated overnight with IC-induced NETs-containing supernatants (IC NETs) (25% v/v). The contribution of IL-33/ST2L axis was assessed by pretreating supernatants for 45 min with an antibody against IL-33 (a-IL33, 4µg/ml). FcR blocking reagent was used to avoid any IC-carry over effect or non-specific a-IL33 binding. Each dot represents a different pDC donor (n=3). p>0,05 (RM-ANOVA with Holm-Sidak correction). (H) Real-time PCR to monitor IFNA and IRF7 mRNA in purified pDCs treated with IC-induced SLE NETs (25% v/v). Endocytosis and TLR trafficking were blocked by pre-treating pDCs for 30 min with cytochalasin D (5µg/ml) or chloroquine (4µM), respectively. The contribution of IL-33/ST2L was determined by pretreating pDCs with a-ST2L and FcR blocking reagent was also added. Each dot represents a different donor (n=4 for IFNA; n=3–5 for IRF7). **p<0.01; ***p<0.001 (two-tailed, RM-ANOVA with Holm-Sidak correction).*

Figure 6

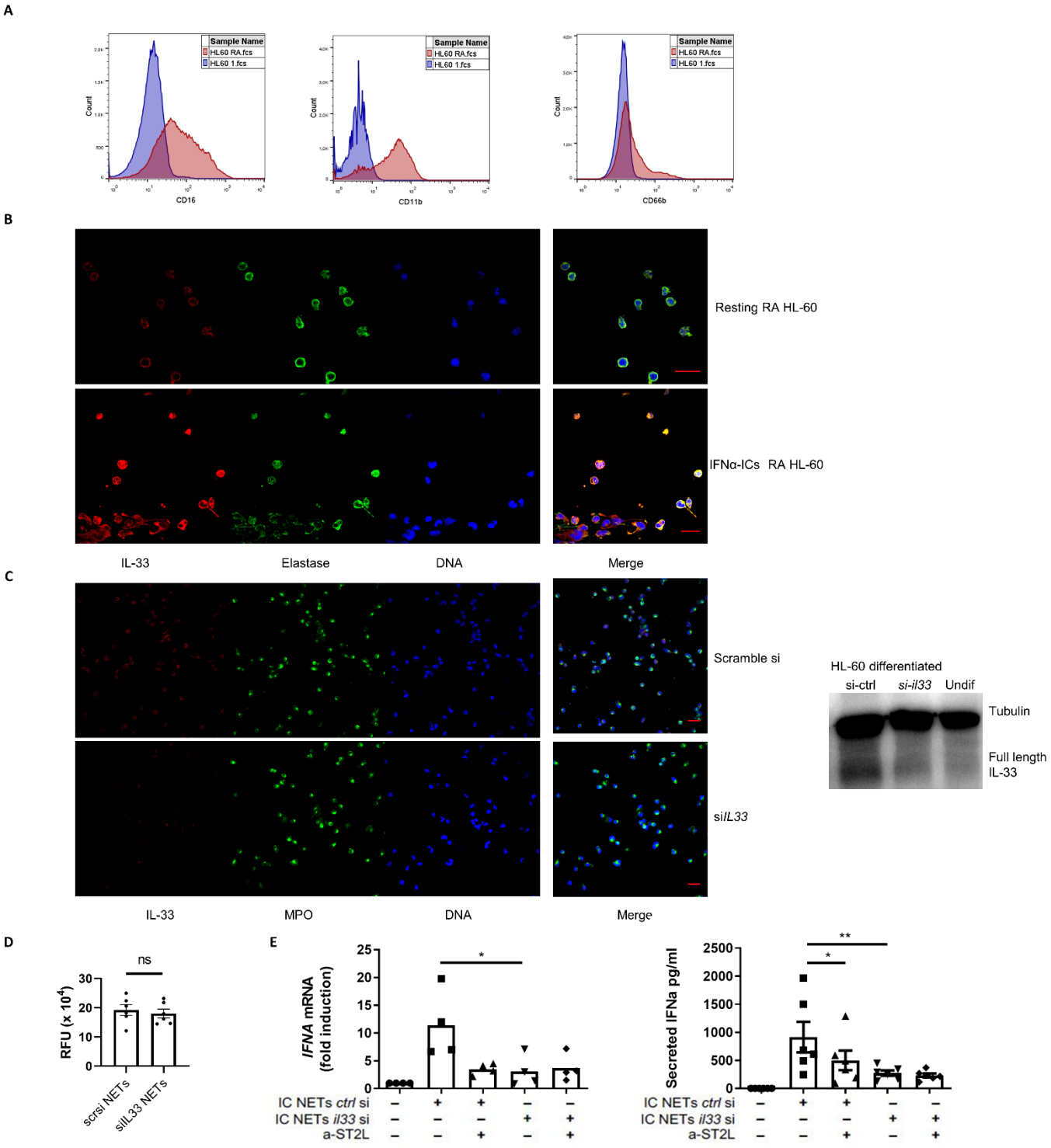

Figure 6: Surface expression of the neutrophil markers CD11b, CD16 and CD66b was assayed by flow cytometry on retinoic acid-differentiated versus control (undifferentiated) HL-60 cells. A total n=3 replicates were performed and representative histograms from a single experiment are shown. (B) Retinoic acid-differentiated, neutrophil-like HL-60 cells were primed with recombinant IFNα (2000U/ml, 1-hour) and treated with SLE ICs for 3 hours or left untreated, followed by staining with anti-IL-33 (IL-33), anti-elastase

*(Elastase) antibodies, and DAPI for DNA. HL-60 cells produced IL-33-decorated NETs as illustrated in the representative confocal image (n=3 experiments, scale bar, 30μm). (C) Control (scramble) and il33-silenced retinoic acid-differentiated HL-60 cells were stimulated using PMA (100nM) for 1 hour followed by staining using anti-IL-33 (IL-33), anti-myeloperoxidase (MPO) specific antibodies and DAPI for DNA. A representative confocal image from n=3 experiments (scale bar, 30μm) is shown. Protein extracts from the same cells were obtained and western blot analysis for IL-33 was performed to validate silencing efficiency. A representative blot from n=2 experiments is shown (D) NETs-containing supernatants from control (scramble) and IL33-silenced retinoic acid-differentiated HL-60 cells were primed with recombinant IFNα (2000U/ml, 1 hour), treated with SLE ICs for 3 hours and then stained with the extracellular DNA dye SYTOX Green. Relative fluorescence intensities were measured from n=6 independent replicates (two tailed p-value = 0.573, paired t-test). (E) Real-time PCR (left panel) and ELISA (right panel) to monitor IFNA mRNA and IFNα protein expression/secretion, respectively, by pDCs cultured with IC NETs (25% v/v) derived from control- (scramble) or IL33-silenced differentiated HL-60 cells. The contribution of IL-33/ST2L axis on IFNα response was assessed by pretreating pDCs with a monoclonal antibody against ST2L (a-ST2L, 3 μg/ml) for 45 minutes. FcR blocking reagent was used to avoid any IC-carry over effect or non-specific a-ST2L binding. Each dot represents an independent replicate (n=4 and n=5, respectively) and bar plots show the mean ± SEM expression. *p<0.05; **p<0.001 (two-tailed, repeated measures ANOVA with Holm-Sidak correction).*

6.8 NET-decorated proteases cleave IL-33 enhancing thus its bioactivity

IC SLE NETs are enriched in serine proteases including elastase and cathepsin G, which are potent IL-33 activators (Garcia Romo G. et al., 2011, Lefrancais E. et al., 2012). Driven by our proteomic data, we hypothesized that NETs may act as a platform for neutrophil proteases to target NETs-bound IL-33, thus generating bioactive isoforms that augment the interferogenic potential of SLE NETs. To evaluate this possibility, and due to the low endogenous IL-33, we administered recombinant full-length (fl)IL-33 in cultures of IC-treated NETotic neutrophils from SLE patients. As control, we used spontaneously NETotic SLE neutrophils and PMA- or MSU-induced NETotic neutrophils from healthy donors, all supplemented with the same amount of flIL-33. Immunoblotting in the supernatants revealed a ≃19 kd protein band present only in the supernatants from IC-treated SLE netting neutrophils, which might correspond to protease-generated IL-33 isoforms **(Figure 8A)**. To address more directly the implication of neutrophil proteases in the interferogenic properties of NET-bound IL-33, we blocked neutrophil elastase using the selective inhibitor sivelestat optimizing the inhibitor concentration and timing of administration to minimize any interference with the NETotic process **(Figure 8B)**.

We repeated the flIL-33/NETs mixture assay using IC-treated SLE netting neutrophils which were pre-treated with sivelestat. Immunoblotting of the sivelestat-treated supernatants showed reduced abundance of the ≃19-kd protein band of putative bioactive IL-33 isoforms **(Figure 8C)**, thus suggesting diminished elastase-mediated cleavage of flIL-33. Following treatment with sivelestat, IC-treated SLE NETs abolished their capacity to induce IFNα response by pDCs **(Figure 8D)**, implying that NETs-bound IL-33 signaling is abrogated due to lack of protease-mediated activation. A similar effect was observed using an inhibitor of cathepsin G **(Figure 8E)**, another NETs-associated neutrophil protease that mediates IL-33 cleavage. Additionally, we also wanted to assess the significance of NET-DNA scaffold as a platform for IL-33 cleavage. By treating IC-SLE NETs with rDNAse before adding them to pDCs, we monitored a slight decrease of their interferogenicity but a complete abrogation of ST2L blockade effect on IFN-α production that may be a result of disturbed protease-IL-33 interaction on NETs **(Figure 8F).**

Finally, to assess IL-33 bioactivity, we administered SLE NETs-cleaved or unprocessed flIL-33 to cultures of pDCs which were stimulated with the TLR-9 ligand CpG-A. Supernatants derived from the incubation of IC-treated SLE netting neutrophils with flIL-33 caused a significant, ST2L-dependent increase in phospho-IRF7 levels of pDCs, suggesting enrichment in bioactive IL-33, whereas an equivalent dosage of uncleaved flIL-33 had the opposite effect **(Figure 8G)**. Furthermore, SLE NETs-processed IL-33-containing supernatants promoted *IFNA* and *IRF7* mRNA expression by CpG-A-activated pDCs **(Figure 8H)**.

Finally, in order to recapitulate in vitro the elastase/IL-33 interaction presumed to occur on SLE NETs, we incubated (fl)IL-33 with recombinant elastase to obtain supernatants enriched in bioactive IL-33. Notably, CpG-A–treated pDCs supplemented with bioactive(elastase-treated) IL-33–containing supernatants showed significant upregulation of *IFNA* and *IRF7*mRNA expression, as compared to the effect of unprocessed recombinant **(Figure 8I)**. These results suggest that neutrophil proteases play a critical role in augmenting IC SLE NETs interferogenic capacity through cleavage-mediated IL-33 activation that uses NET-DNA as a scaffold.

Figure 7

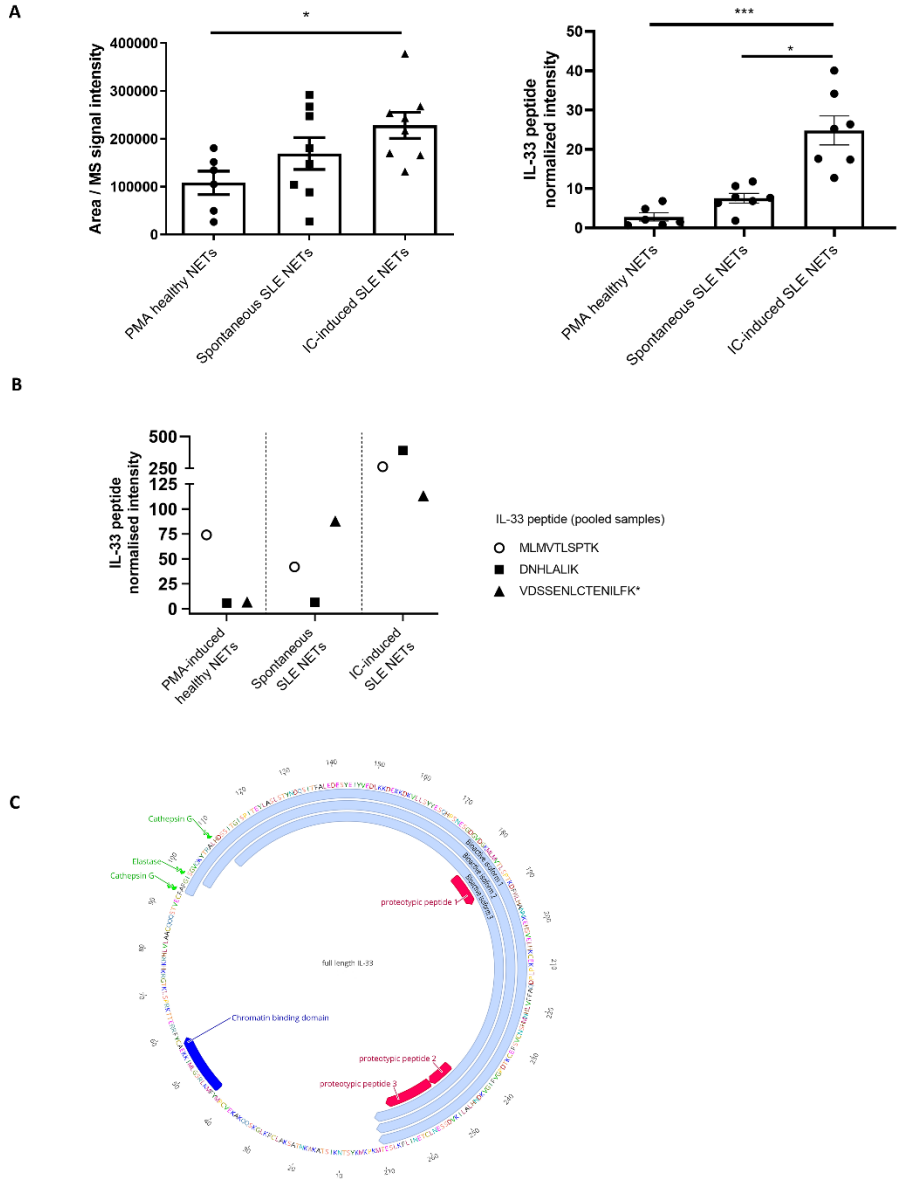

Figure 7: IL-33-targeted proteomic analysis (Parallel Reaction Monitoring, PRM) in NETs protein precipitates from PMA-treated healthy neutrophils (PMA-induced healthy NETs), unstimulated SLE (spontaneously-related SLE NETs) and IC-treated SLE (IC-induced SLE NETs) neutrophils. The signal intensity of the IL-33 proteotypic peptide -VDSSENLCTENILFK[aa251-265] is higher in C-induced SLE NETs. Signal quantification was performed based on the area of the corresponding peptide peaks in the ion chromatograms. At the right panel, we provide with normalized peptide values using the respective MPO ppm values. Each dot

*represents the quantification values from different donors (n=6-8 in each group) and bar plots show the mean ± SEM expression. *p<0.05 (two-tailed, one-way ANOVA). (B) Proteomic analysis was repeated in pooled NETs from an independent cohort of PMA-treated healthy (n=6), resting SLE (n=8) and IC-treated SLE (n=8) neutrophils. Quantification was performed as described above, and data were normalized by dividing the IL-33 peptide signal intensity with the normalized signal intensity (parts per million, ppm) of MPO (derived from whole proteome and used as an indicator of NETosis) in each sample. On the left panel, intensities of the -MLMVTLSPTK[aa180-189] (open circle) and -DNHLALIK[aa243-250] (full square) IL-33-proteotypic peptides are shown. (C) Amino-acid sequence of full-length IL-33 depicted using Geneious Prime software. Nuclear localization domain, NET protease cleavage sites, previously detected bioactive isoforms and proteotypic peptides derived from our proteomic analysis are annotated.*

6.9 IL-33 decorated NETs are accumulated on both SLE periphery and inflamed tissues

Based on previous work linking blood neutrophil activation and NETosis in active severe SLE (Hakkim A. et al., 2010), we screened for IL-33 NETs in the serum of SLE patients. For this, we developed two sandwich ELISA systems based on an anti-IL-33 coating antibody and a detection antibody specific for either double-stranded (ds)DNA, the most prevalent nucleic acid in SLE ICs, or neutrophil myeloperoxidase (MPO). Using both assays in independent patient cohorts, serum samples from SLE individuals exhibited increased levels of IL-33-complexed NETs as compared to healthy counterparts **(Figure 9A and B)**. Serum IL-33 NETs concentration correlated significantly with patient disease activity assessed by the validated SLE Disease Activity Index (SLEDAI) **(Figure 9A and B)**, and longitudinal reduction in serum IL-33/MPO complexes was noted in patients with good clinical response to belimumab treatment (**Figure 9C).** To validate our technique and in agreement with previous reports (Frangou E. et al., 2019), we also detected increased NETs containing neutrophil myeloperoxidase (MPO/dsDNA complexes) in SLE versus healthy sera **(Figure 9D).** NETs were also detected in inflamed tissues of SLE patients like kidney and skin (Frangou E. et al., 2019). Notably, we identified extracellular structures especially at the tubulointerstitium, where IL-33 and NET markers were co-localized, indicative of IL-33-containing NETs **(Figure 9E)**. IL-33-decorated chromatin structures were also detected in lupus-affected dermis contrary to healthy skin which exhibited no inflammation or IL-33-decorated NETs **(Figure 9F)**.

NET-stimulation was also reported to induce IL-33 expression in human fibroblasts (Carmona-Rivera C. et al.,2020). Hypothesizing that NET-stimulation could have similar effects on epithelial and endothelial cells of inflamed tissues we sought to examine if NET-stimulated-non-hematopoietic cell-derived- IL-33 could have any paracrine effect on SLE neutrophils. It is already established that IL-33 acts as a chemoattractant for neutrophils (Liang M. et al.,2019, Lefrancais E. et al., 2012) but we also proved that IL-33 can promote NET-generation of control neutrophils creating thus a vicious feedback loop **(Figure 9G)**. Of note, by pretreating neutrophils with aST2L monoclonal antibody, neutrophils did not manage to release NETotic structures after IL-33 stimulation **(Figure 9G)**.

Low density granulocytes (LDGs) are already introduced as a pathogenic neutrophil subset that orchestrates lupus pathogenesis by acting both in the periphery and in inflamed tissues (Mistry P. et al.,2019). For that purpose, we sorted out LDGs from an active SLE patient and stimulate them in vitro. We observed that LDGs can also release IL-33 decorated NETs **(Figure 9H)**. To sum up, IL-33 decorated NETs are present both in the periphery, in inflamed tissues of SLE patients and they can also be released from highly inflammatory neutrophil subsets, like LDGs, which govern SLE pathogenesis. Additionally, IL-33 has the ability to attract neutrophils and trigger them to produce NETs leading thus to pathogenic feedback loops.

Figure 8

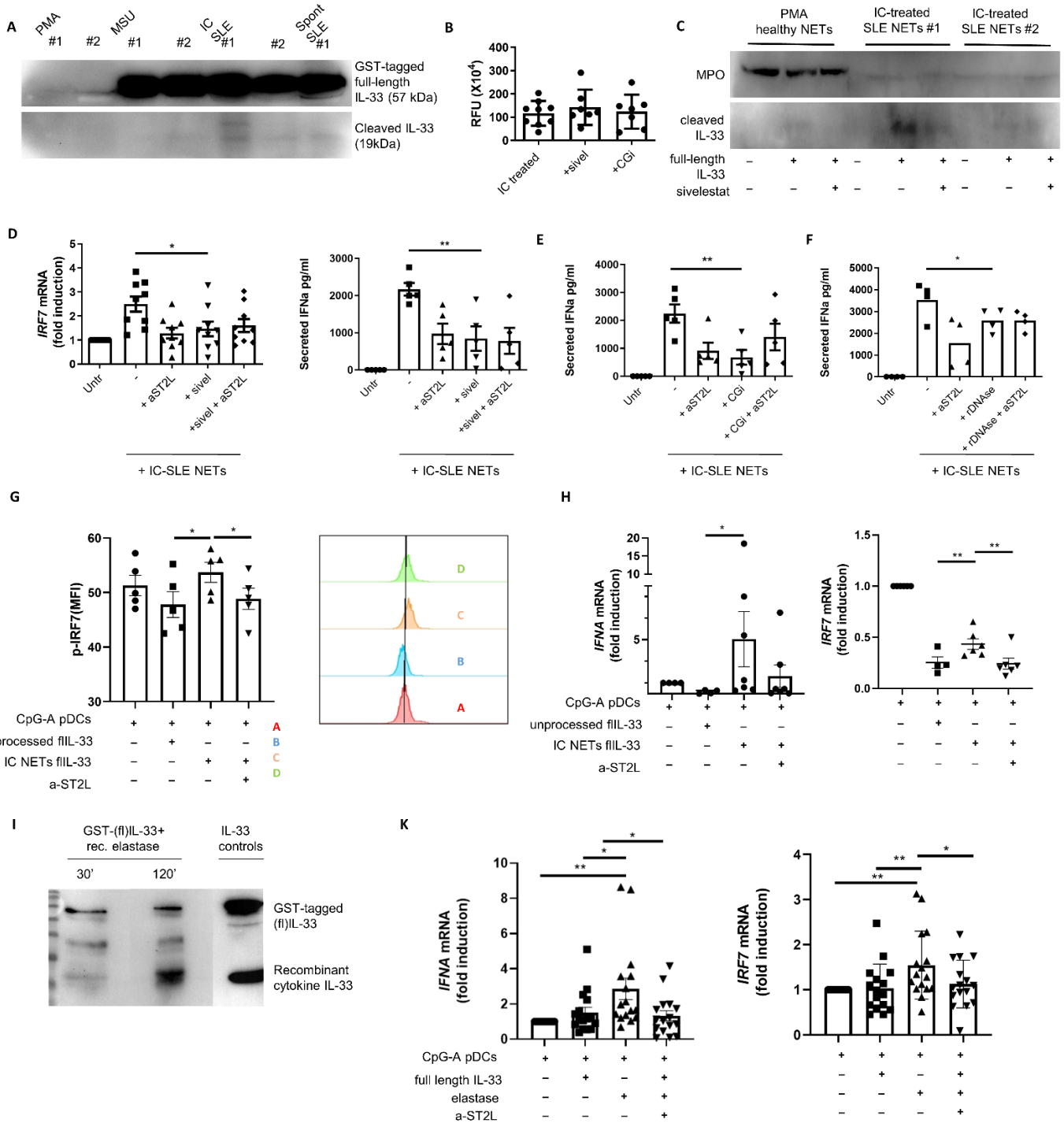

Figure 8: (A) Recombinant full-length (fl)IL-33 was added to cultures of PMA-, MSU-treated healthy, unstimulated or IC-treated SLE neutrophils. After 3 hours, DNase (200U/ml, 30 minutes, 37°C) was added and NET-proteins were harvested. Immunoblotting revealed band of ≃19 kd corresponding to protease-generated IL-33 isoform in the supernatants from IC-treated SLE neutrophils. (B) SLE patient-derived neutrophils were stimulated with ICs for 75 minutes, followed by addition of the elastase inhibitor sivelestat

*(2μM) or the cathepsin G inhibitor CGi (20μM). At 3 hours, NETs-containing supernatants were collected and stained using the extracellular DNA dye SYTOX Green. Each dot represents the relative fluorescence intensities from independent blood donors (n = 7 to 9 in each condition) and bar plots show the mean ± SEM (standard error of the mean) fluorescence intensity values (p=0.840; two-tailed, repeated measures mixed model to account for missing data). (C) The same assay as in (A) was repeated using cultures of IC-treated SLE neutrophils pretreated (or not) with sivelestat (2μM). Immunoblotting of NETs from sivelestat-treated neutrophils showed reduced intensity of the ≃19-kd band. A representative blot from n=2 experiments is shown. (D) SLE neutrophils were stimulated with ICs followed by addition of sivelestat. NETs were collected and administered to pDCs. After overnight culture, supernatants were assayed by PCR for IRF7 mRNA levels and by ELISA for IFNα. Each dot represents a different donor (n=6) and bar plots show the mean ± SEM expression. **p<0.01 (two-tailed, repeated measures (RM-)ANOVA with Holm-Sidak correction). (E) The same experiment, as in (D) was conducted using Cathepsin-G inhibitor (20mM).(F) ELISA was performed to determine protein secretion of IFNα, respectively, by healthy pDCs treated overnight with IC-induced SLE NET-containing supernatants (IC NETs) (25% v/v). The contribution of IL-33/ST2L axis on IFNα response was assessed by pretreating pDCs with an antibody against ST2L (a-ST2L, 3 μg/ml). FcR blocking reagent was used to avoid any IC-carry over effect or non-specific a-ST2L binding. NET-supernatants were treated or not wth 100IU/ml rDNAse for 1hr to assess NET-DNA contribution. Each dot represents a different pDC donor (n=4) and bar plots show the mean ± SEM expression. *p<0.05;(two-tailed, repeated measured ANOVA with Holm-Sidak correction) (G-H) pDCs were cultured with CpG-A (0.1μM) and either (fl)IL-33 (100nM) or supernatants from the incubation of IC-treated SLE neutrophils with (fl)IL-33 for 4 hours. IL-33 NETs-cleaved supernatants were treated with DNAse. The contribution of IL-33/ST2L was determined by pretreating pDCs with a-ST2L. pDCs were assayed by flow cytometry for intracellular phospho-IRF7 (p-IRF7) (G)mean fluorescence intensity (MFI) and by qPCR for IRF7 and IFNA mRNA levels (n=6) (H). Left panel summarizes the results from n=5 donors represented by different dots, and right panel illustrates a representative flow cytometry histogram. *p<0.05 **p<0.001 (two-tailed, RM-ANOVA with Holm-Sidak correction).(I) Immunoblotting was employed to verify that in vitro co-incubation (30 min, 2 hours) of recombinant elastase and (fl)IL-33 leads to the generation of a ≃19-kd band resembling the previously described bioactive IL-33 isoform. IL-33 controls (recombinant (fl)IL-33 and recombinant cytokine-isoform IL-33) were loaded (3rd lane) to assess specificity. A representative blot from n=3 experiments is shown. (K) pDCs were cultured with CpG-A and supernatants (2.5% v/v) derived from the in vitro reaction of (fl)IL-33 (1.8μg/ml) with/without elastase (50ng/ml). pDCs were assayed for IFNA (left panel) and IRF7 (right panel) mRNA by real-time PCR (n=16 donors). *p<0.05; **p<0.01 (two-tailed, RM-ANOVA with Holm-Sidak correction).*

Figure 9

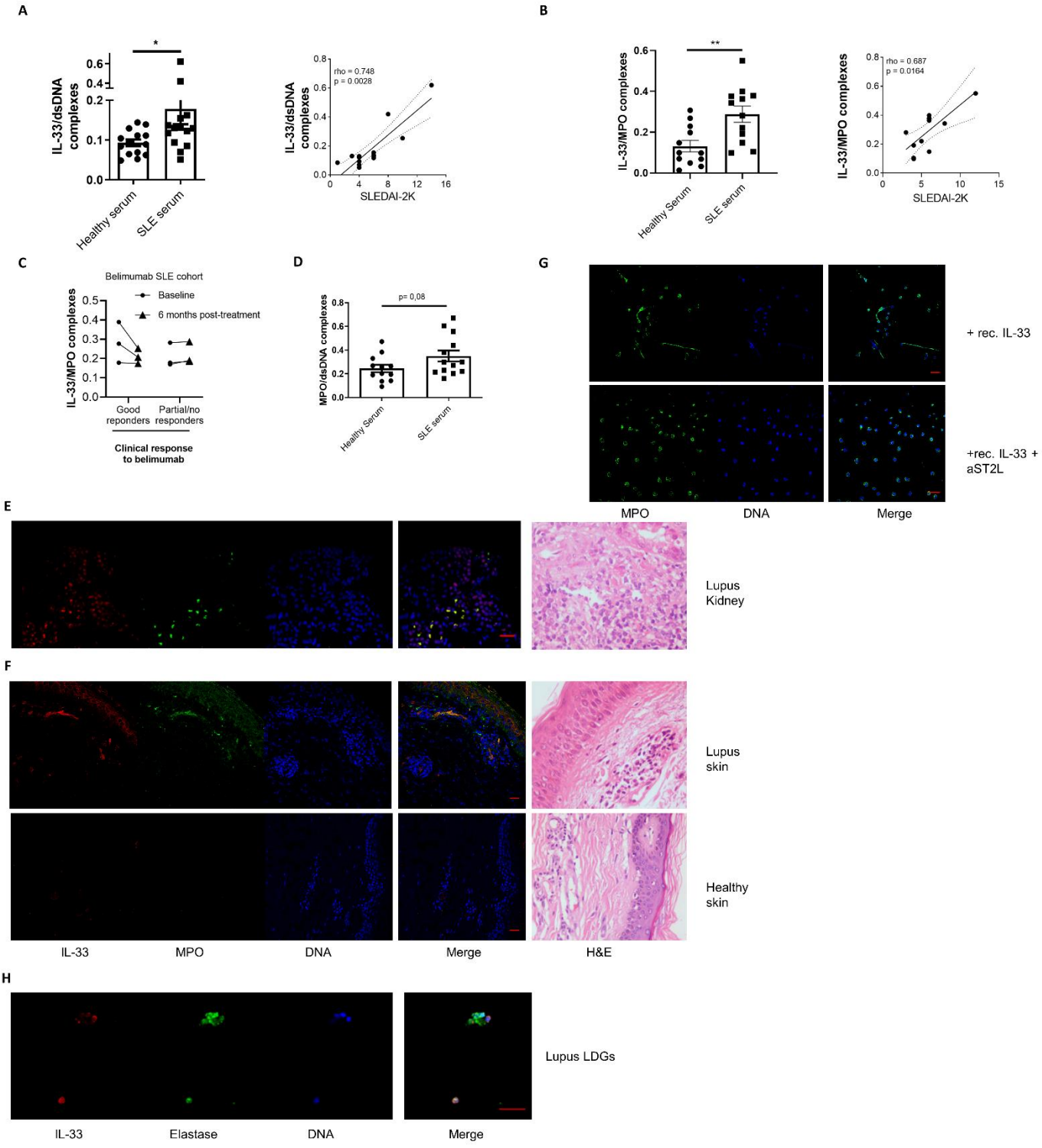

*Figure 9: (A-B) IL-33/double stranded(ds)DNA and IL-33/MPO complexes were quantified by sandwich ELISA in serum samples from healthy (n=14 and n=12, respectively) and SLE (n=15 and n=12, respectively) individuals. Each dot represents a different donor and bar plots show the mean ± standard error of the mean (SEM) absorbance (405/490nm and 450/540 nm, respectively). *p-value <0.05 and **p<0.01 respectively (two-tailed, Mann-Whitney test). Serum IL-33/dsDNA and IL-33/MPO complexes are*

positively correlated with disease activity (assessed by the SLEDAI-2K) in SLE patients (spearman's rho 0.748 and 0.687, respectively). Dashed lines demonstrate the 95% boundaries of the regression line. (C) IL-33/MPO complexes were quantified by sandwich ELISA in paired longitudinal serum samples collected from n=6 SLE patients at the time of treatment initiation (t=0) and after 6 months (t=6) of treatment with belimumab. Clinical response to treatment was evaluated according to the validated SLE Responder Index-4 (SRI-4). Each dot represents a different donor tested at the aforementioned time points. Mean ± SEM (standard error of the mean) change (6 months minus baseline) in serum IL-33/MPO concentration was -20.8 ± 9.7% in responders as compared to 5.8 ± 3.0% in non-responders (two-tailed p-value = 0.058, unpaired t-test). (D) MPO/double stranded(ds)DNA complexes were detected and quantified by sandwich ELISA in serum samples from healthy donors (n=12) and SLE patients (n=13). Each dot represents a different donor and bar plots show the mean ± SEM absorbance (450/540nm) of MPO/dsDNA complexes (two-tailed p-value = 0.087, Mann-Whitney test). (E-F) IL-33-complexed NETs visualized by confocal microscopy on kidney and skin sections from patients with active proliferative lupus nephritis and cutaneous lupus, respectively. Skin sections from healthy donors were used as controls. IL-33 NETs are identified through immunostaining with anti-myeloperoxidase (MPO) and anti-IL-33 (IL-33) antibodies (green: MPO, red: IL-33, blue: 4',6-diamidino-2-phenylindole (DAPI)/DNA). Representative confocal image (scale bar, 30μm) from one patient (n=4 patients were evaluated). The same tissue sections were also stained with hematoxylin & eosin (H&E, 400X magnification). (G) Isolated neutrophils from healthy donors were pretreated or not with a-ST2L and then cultured with rIL-33 (100ng/ml) for 3 hours. NETs are identified through immunostaining with anti-myeloperoxidase (MPO) and DAPI (green: MPO, red: IL-33, blue: 4',6-diamidino-2-phenylindole (DAPI)/DNA). Representative confocal image (scale bar, 30μm) from one donor (n=2 experiments). (H) Low-density granulocytes (LDGs) were sorted as CD15+ CD14lo HLA-DRint CD10+ cells from the peripheral blood of patients with SLE and cultured in standard medium. At 3 hours, cells were stained with anti-IL-33 (IL-33), anti-elastase (Elastase) specific antibodies and DAPI for DNA staining. Representative confocal image (scale bar, 30μm) from a single patient is shown.

7) Discussion

A poorly explained feature of SLE is unabated type I IFN signaling that spurs autoreactive responses and persists even during clinical remission (Panousis N. et al., 2019, Ronnblom L. et al., 2019). pDCs are a major source of IFN-α and lupus-prone mice with defective pDC-mediated IFN response show reduced autoantibody formation, reduced lymphadenopathy and prolonged survival (Baccala R. et al.,2013). Perpetual production of IFN-α in SLE is triggered by self-derived nucleic acids complexed with autoantibodies or immunostimulatory proteins such as in the form of NETs (Garcia Romo G. et al, 2011, Lande R. et al., 2016, Caielli S. et al., 2016). We focused on IL-33, a chromatin-bound alarmin with context-specific immunomodulatory effects, and evaluated its role in human SLE. Driven by our observation that neutrophils infiltrate and release IL-33-bearing NETs in the blood and other inflamed tissues of SLE patients, we herein demonstrate that lupus neutrophils are prone to producing IL-33 NETs which induce robust IFNα response by pDCs through the ST2L receptor. Importantly, our NETs proteome data coupled with ex vivo inhibition assays implicate NETs proteases in the generation of bioactive IL-33 of high interferogenicity, thus offering novel mechanistic insights linking neutrophil activation and NETosis with IFNα and end-organ injury in human SLE.

Extracellular IL-33 augments immune responses during tissue inflammation and injury, however, its precise role in autoimmunity remains elusive. We showed that IL-33 is externalized on SLE NETs and contributes to their intereferogenic capacity through ST2L on pDCs. This is in line with a previous study suggesting that chromatin binding regulates ST2-mediated bioactivity of IL-33 (Travers J. et al., 2018). Possibl explanations for the adjuvant effect of NETs-complexed IL-33 include protecting the NET-structure from degradation (Lande R. et al., 2011) or facilitating NET uptake through the ST2L (Tian J. et al.,2007). IL-33/ST2L can both enhance (Espinassous Q. et al., 2009) and inhibit (Brink E. et al, 2004) TLR signaling in a context-specific fashion, and IL-33 induces IRF7 expression in innate lymphoid cells (He J. et al., 2019), which might represent a mechanism by which NET IL-33 renders pDCs more responsive to immunostimulatory DNA. IL-36, another IL-1 family cytokine, induces IFNα production by facilitating endosomal TLR trafficking in pDCs (Catapano M. et al.,2020).

Notably, the in vitro studies that we conducted, indicated that neither full length nor recombinant cytokine isoform IL-33 enhances TRL9-mediated IFN-α response. On the contrary, cytokine isoform IL-33 increased TLR-7 mediated IFN-α response. NETs were found to stimulate both TLR-9 and cytoplasmic DNA receptors (Garcia-Romo G. et al.,2011, Apel F. et al., 2021) whereas NET-associated RNA can also trigger immune responses (Herster F. et al., 2020). The inability of IL-33 to induce TLR-9 mediated responses in vitro might be explained by the nature of TLR-9 ligand (synthetic oligonucleotides rather than complex chromatin structures like NETs) or by the magnitude of ST2L signaling, considering that neutrophil proteases-cleaved IL-33 (19KDa) is much more bioactive than the cytokine isoform (18KDa)). Additionally, TLR-7 recently reported to be able to sense modified DNA-nucleosides like deoxyguanosine (Davenne T. et al., 2020) so it is possible that oxidized-DNA (like in the form of NETs) could be sensed by also other non-DNA-related receptors of which IL-33 is able to potentiate their IFN-α responses.

Of interest, previous studies have indicated a crosstalk between cGAS-STING, known to be triggered by NET DNA (Apel F. et al., 2021), and IL-33/ST2L in the context of allergic airway inflammation (Han Y. et al., 2020, She L. et al., 2021), therefore raising the hypothesis that NETs–associated IL-33 might also amplify non-TLR cytoplasmic nucleic acid-sensing signaling pathways. Of note, our and other proteomic studies (Chapman E. et al., 2019) indicated that histones are some of the most characteristic components of SLE NETs. At the same time, Tsourouktsoglou et al., described that the inflammatory potential of NETs can be also exerted histones in a TLR-4 dependent manner while NET-DNA has an auxiliary role. Thus, considering that IL-33 was reported to enhance histone-mediated immune responses (Travers J. et al.,2018), it would be worth investigating the interplay between NET-histones and IL-33 and its effect on SLE pathogenesis.

IL-33 complexed with or processed by SLE NETs -but not the recombinant cytokine form- was capable of inducing robust IFN-α production by pDCs. This raised the possibility that IL-33 may be modified by NETs to gain biological activity. Indeed, IL-1 family cytokines require proteolytic processing for activation and IL-33 can be cleaved into highly bioactive isoforms by neutrophil proteases (Lefrancais E. et al.,2012, Clancy D. et al., 2018). However, the topology of this process in the setting of autoimmunity has not been demonstrated.

To this end, our proteomic analysis in SLE IC NETs revealed upregulation of threedistinct IL-33 peptides exclusively localized near the C-terminal cytokine
domain, which exists in mature IL-33 isoforms (Liew F. et al., 2016) In this regard, SLE neutrophils and their NETs exhibit a potent serine protease signature (Garcia Romo G. et al.,2011)); moreover, our proteomic analysis revealed the absence of a major endogenous inhibitor of elastase (SerpinB1) from IC SLE NETs (Tables S2-4). Additionally, PR-3, a NET-decorating protein that was described to reduce significantly IL-33's bioactivity (Clancy D. et al., 2018) was absent from our IC-mediated SLE NETs proteome list.

In this study we did not address whether IL-33's cleavage occurs intracellularly or extracellularly. Elastase is enzymatically active during the initiation of NETotic process leading thus to DNA condensation by cleaving histones (Papayannopoulos V. et al., 2010). Additionally, nuclear IL-33 resides in acidic patches in close proximity to histones (Roussel L. et al., 2008) so its cleavage could have been taking place intracellularly during the first steps of NETosis. Alternatively, it is well established that NET-bound elastase retains its enzymatic potential (Kolaczkowska E. et al., 2015) so IL-33 could be also cleaved extracellularly using the ''loose'' NET-DNA as a scaffold. Despite the fact the hypothesis of extracellular IL-33 cleavage is more likely further investigation of the exact mechanism is required.

Accordingly, inhibition of elastase and cathepsin G in netting SLE neutrophils abrogated the IL-33-mediated interferogenic effect of NETs. Our data are in line with findings implicating NETs proteases-processed IL-1β in gout attacks (Guma M. et al., 2009) and of neutrophil protease-generated IL-33 in acute lung injury (Lefrancais E. et al., 2012), pointing to neutrophil proteases generating NETs-associated IL-33 with high interferogenic activity in the context of lupus. Limited studies have detected proteolytically processed forms of IL-33 in biological samples since characterization of human extracellular IL-33 has been challenging due to its low abundance. Geneticevidence supports that even small changes in IL-33 expression are implicated in disease susceptibility (Cayrol C. et al., 2018). Under inflammatory conditions, neutrophils are rapidly recruited into afflicted tissues and the expression level of alarmins may increase significantly reaching locally high concentrations. Intriguingly, under high neutrophil densities, NETs may accumulate (Schauer C. et al.,2014) and presumably,

act as platforms for the extracellular scavenging and processing of IL-33 released by neighboring damaged epithelial and endothelial cells (Lefrancais E. et al., 2012, Clancy D. et al.,2018). Thus, considering that immune complexes are accumulated on SLE inflamed tissues and can trigger infiltrating neutrophils in an FcR-dependent manner, IC-mediated NETs could also serve as activating platforms for non-hematopoietic-derived full length IL-33 which will probably lead to deleterious immune responses that subsequently exacerbate inflammation and tissue damage.

Previous work has suggested that oxidation of IL-33 limits its bioactivity due to formation of disulfide bridges which impede the IL-33/ST2L interaction (Cohen E. et al.,2015). Since neutrophil activation and NETosis in SLE occur under oxidative stress driven by mitochondrial reactive oxygen species (Lood C. et al., 2016, Caielli S. et al., 2016), it is of interest to discern how NETs-associated IL-33 may retain its bioactivity. Notably, oxidized isoforms have not been detected in nuclear (DNA-bound) IL-33 (Cohen E. et al.,2015), which could indicate that NET-DNA scaffold or histones are protective against oxidation. Also, according to published data (Bruschi M. et al., 2019) and our proteomics analysis, SLE NETs are decorated with molecules that display reducing capacity, including thioredoxin reductase, peroxiredoxin-2 and glutathione S-transferase, which might counteract IL-33 oxidation. Finally, if IL-33 abolishes NET-protection extracellularly, it is possible that it exerts its biological effects acutely before its oxidation, pertinent to the close proximity of NETting neutrophils and pDCs in lupus inflamed tissues (Fiore N. et al., 2008, Skopelja-Gardner S. et al., 2016).

Our group (Panousis N. et al., 2019, Frangou E. et al., 2019) and others (Villanueva E. et al., 2011, Hakkim A. et al., 2010, Knight J.S et al., 2015) have associated neutrophils and aberrant NETs formation with lupus nephritis but the implication of specific alarmins externalized on SLE NETs to the kidney disease is not well understood. Additionally, sST2 was described to correlate with SLE-related renal involvement implying indirectly that regulation of IL-33 levels is of interest regarding LN pathogenesis. (Moreau et al., 2021). Our ex vivo functional assays coupled with evidence that pDCs infiltrate the inflamed kidneys in SLE (Fiore N. et al., 2008), raise the possibility that IL-33-decorated NETs trigger intra-renal type I IFN production in lupus nephritis as recently suggested by single-cell transcriptomic studies (Der E. et al., 2019). Interestingly, we found that IL-33 NETs were predominantly localized within the tubulointerstitium and tubulointerstitial inflammation has been correlated with pDCs infiltrates (Cheng M. et al., 2016) and poor prognosis in lupus

nephritis (Wilson P. et al., 2018). IL-33 exhibits myeloid cell chemoattractant properties (Ferhat M. et al.,2018), thus it might also attract neutrophils within the lupus inflamed kidneys. Moreover, we and other groups (Wang X. et al., 2021, Yazdani H et al. 2017), described that IL-33 can also trigger the release of NETs orchestrating thus a perpetuating vicious feedback loop.

Considering that IL-33-decorates NETs were also detected in SLE cutaneous lesions, it is possible that these structures can be sensed by skin-infiltrating pDCs, thus contributing to the profound type I IFN signature observed in lupus skin (Stannard J. et al., 2017). Notably, both of damaged or activated keratinocytes and fibroblasts are able to release IL-33 which could presumably increase its bioactivity in a NET-dependent manner (Balato A et al., 2012, Carmona-Rivera C. et al., 2020). These findings corroborate previous studies showing that the kidney and skin tissue in SLE patients share common genomic perturbations including upregulated type I IFN-inducible genes (Der E. et al., 2019).

Although we focused on the role of IL-33 in regulating the interferogenic capacity of NETs, it is possible that IL-33 might contribute to SLE through other mechanisms. Thus, IL-33-bearing NETs might interact with other ST2L-expressing immune cell types such as Th2, regulatory T-cells or NKcells (Liew F. et al.,2016, Hatzioannou et al., 2020). In addition, the IL-33/ST2L axis has been shown to promote fibrosis under inflammatory conditions (Gao Q. et al., 2015) while fibrosis is one of the main causes of SLE-related renal failure (Yung S. et al. ,2017).

Our results have potential implications for the design of novel therapeutics to counteract aberrant IFN-α production in SLE and other relevant pathologies such as infection-induced autoinflammatory pneumonitis (Zizzo G. et al., 2020). Since IL-33 is released by activated neutrophils undergoing NETosis, targeting IL-33/ST2L might be beneficial in selectively neutralizing excessive IFNα response without inducing generalized immunosuppression. Anti-IL-33 and/or anti-ST2L antibodies are currently under clinical development (Chen Y. et al., 2019); in a preliminary report, administration of anti-IL-33 antibody in MRL/*lpr* lupus prone mice reduced anti-dsDNA and ICs levels, kidney inflammation and proteinuria (Li P. et al., 2014). Additionally, NET proteases like elastase and Cathepsin-G that potentiate IL-33's and other IL-1-related cytokines' bioactivity could also be potential pharmaceutical targets.In conclusion, we provide evidence that SLE NETs-derived IL-33 processed by neutrophil proteases may contribute to disease pathogenesis by augmenting IFN-α production by pDCs.

IL-33-bearing NETs infiltrating lupus end-organs such as the kidneys and skin, suggest an important role in regulating local autoimmune inflammation and tissue injury. Accordingly, IL-33 and/or its maturation process represent drugable targets towards ameliorating excessive IFN-α production and SLE pathology.

A more abstract conclusion of this study is that in biology, dogmatic thinking has to be avoided. Most of the cells have the potential to secrete several cytokines or other protein factors in a context-dependent manner and discrimination of cytokines as hematopoietic cell- or non-hematopoietic cell- derived might be misleading. Additionally, even in negligible amounts, cytokines can be profoundly bioactive leading to immune response-related potent effects. An efficient immune response is a matter of quality of the enmeshed factors and not a matter of quantity.

Proposed model

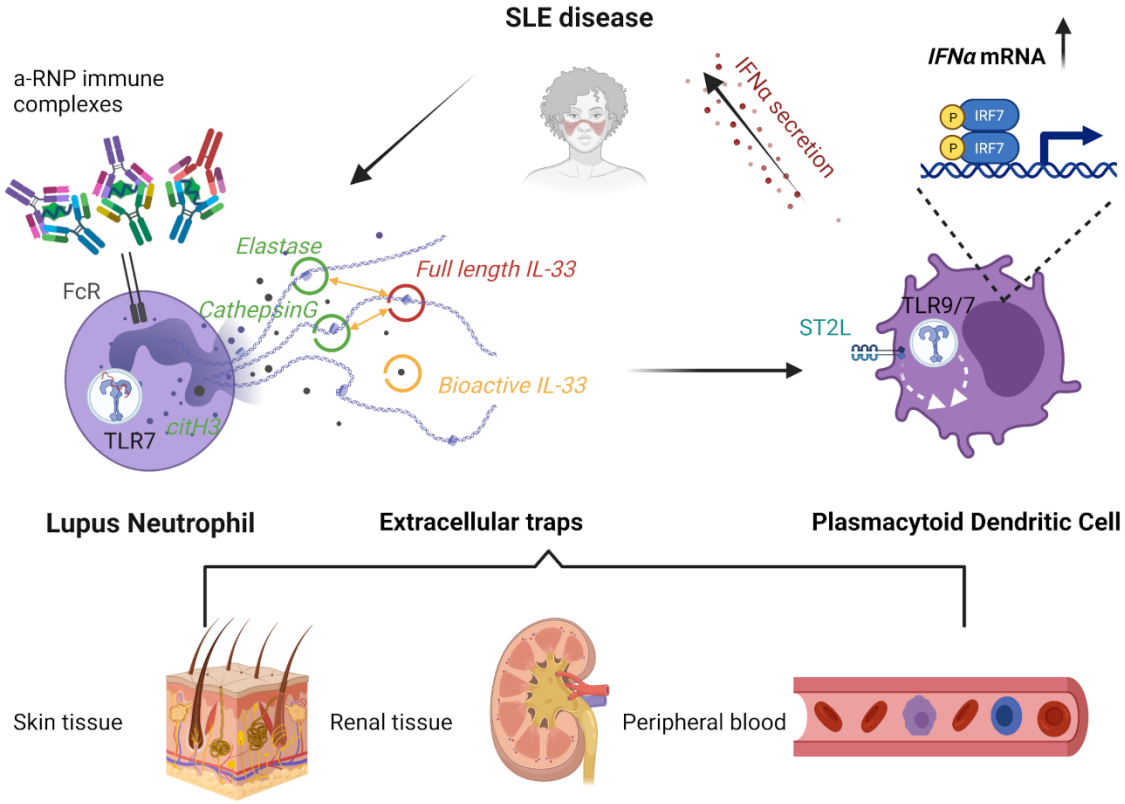

Figure 6; Our proposed model of how NET-derived IL-33 contributes to SLE pathogenesis. In brief, immune complexes stimulate SLE neutrophils to release IL-33 decorated NETs. NET-derived IL-33 is cleaved by neutrophil proteases like elastase and Cathepsin-G using DNA as a scaffold leading to generation of bioactive isoforms. Bioactive IL-33 combined with NET-chromatin stimulate pDCs to release IFN-α in an IRF-7-dependent manner leading thus to SLE exacerbation

8) Future directions

In this study, we discovered a new mediator of NETs' interferogenic capacity. In particular, SLE-relevant immune complexes promote IL-33 decorated-NETs generation. NET proteases seem to cleave IL-33 into highly bioactive isoforms which, in combination with NET-chromatin, enhance pDCs' IFN-α response. Notably, IL-33 decorated NETs were detected also in inflamed blood and non-blood tissues of SLE patients. Based on our data several questions have been raised that could be further investigated:

1) Do IL-33/ST2L signaling pathway or IL-33's maturation process represent drugable targets towards SLE amelioration?
2) Which is the exact mechanism of how IL-33 potentiates IFN-α responses?
3) Describing the exact process of IL-33's cleavage by neutrophil proteases
4) Does non-hematopoietic cells – derived IL-33 exhibit similar properties with NET-derived IL-33? Do IL-33 decorated NETs stimulate other leukocytes except pDCs?
5) Investigating the effect of IL-33 decorate NETs in autoimmune or other comorbidities

Those research questions are further elaborated below

8.1 Investigating the potential therapeutic efficacy of targeting IL-33/ST2L signaling pathway or IL-33's maturation process towards SLE amelioration

For this research project lupus-prone mice will be used. Interestingly, IL-33 blockade had controversial effects regarding murine SLE progression (Mok et al., 2010?). Considering that IL-33 circulates in negligible amounts we strongly believe that ST2L blocking might be a more suitable targer for our purpose. First of all, an appropriate SLE mouse model will be selected based on its capacity to generate NET-dependent autoimmune responses. MRL/*lpr* spontaneous lupus murine model was reported to exhibit NET-dependent pathology (Knight J et al.,2015).

To begin with, BM neutrophils will be isolated from control and mice exhibiting established disease (14 weeks old) and will be treated with autologous serum (control or MRL/*lpr*) for 3-4 hours.

Their ability to release IL-33 decorated NETs will be assessed using both NET-dependent ELISA and immunostaining. If we establish that murine SLE neutrophils release IL-33 decorated NETs then MRL/*lpr* mice will be treated with anti-ST2L (10 mg/kg/day) or vehicle by daily subcutaneous injection, beginning at 8 weeks of age until euthanasia at 16 weeks. Then, typical manifestations of murine lupus will be compared between anti-ST2L-treated and vehicle-treated mice. More specifically, spleen weight and autoantibody levels will be assessed (anti-dsDNA, ANA etc) via ELISA. Moreover, transcriptomic analysis of blood and non-blood inflamed tissues will be employed to investigate if ST2L blockade interferes with the characteristic IFN- signature of lupus prone mice. It would be also of interest to address if ST2L blockade can ameliorate renal or skin SLE inflammation. To assess renal involvement, immune cell infiltration in the interstitial area and C3, IgG deposition on glomeruli will be monitored using immunohistochemistry and immunofluorescence of renal tissue isolated from euthanized a-ST2L or vehicle-treated lupus prone mice. Additionally, renal tissues from a-ST2L- and vehicle-treated mice will be stained to monitor fibrotic manifestations. To monitor renal failure caused by nephritis, proteinuria will be also measured in our groups of interest (a-ST2L, vehicle-treated). Regarding skin inflammation, infiltration of immune cells in the skin and skin lesions will be observed via immunohistochemistry in the aforementioned groups.

The same experimental approach could be employed to assess the effect of neutrophil proteases blockade towards SLE amelioration. Antibodies against elastase and Cathpesin G could be used as therapeutic reagents to ameliorate SLE in lupus prone mice. The effect of proteases inhibition will be assessed by measuring systemic inflammation, type I IFN signature, autoantibody secretion, renal and skin involvement as previously mentioned. To unravel if our effects are IL-33-dependent, a focused proteomic analysis (Parallel Reaction Monitoring) will be used to detect proteotypic peptides of cleaved-IL-33 in our lupus-prone mice groups of interest (a-elastase or a-CathG and vehicle-treated). Potential amelioration of SLE symptoms along with decrease in bioactive IL-33 levels in the a-elastase or a-CathG group will be a strong sign of IL-33-dependent SLE inflammation.

8.2 Unravelling the exact mechanism of how IL-33 potentiates IFN-α responses

Alarmins were described enhancing the inflammatory capacity of extracellular chromatin using distinct mechanisms like protecting chromatin from degradation (15) or by facilitating chromatin uptake through

their receptors (48). Both hypotheses will be tested using human-derived primary cells from SLE and healthy donors. Full length IL-33 (recombinant or derived from necrotic endothelial cells) will be co-incubated with SLE NETs or recombinant elastase to generate bioactive IL-33 isoforms. Cleaved-IL-33 isoforms will be isolated and concentrated using an a-IL-33 based-pull down assay. Then, cleaved IL-33 isoforms will be co-incubated with purified chromatin either in the form of SLE NETs or as plain nucleosome-particles. Notably, bioactive IL-33 isoforms lack the chromatin binding domain of full length isoform (Lefrancais et al., 2014) but they can also form complexes with chromatin via their basic aminoacid residues. To assess the potential binding of bioactive IL-33 to NET or chromatin structures gel electrophoresis mobility shift assay (EMSA) will be employed.

To test the first hypothesis, our IL-33/chromatin complexes will be co-incubated with rDNAseI or rDNAse1L3 using different time points (15 min-1 hour – 2 hours). The differences in chromatin degradation of cleaved IL-33-bound or control chromatin will be monitored using both Picogreen- DNA fluorescent DNA dye and classic DNA electrophoresis. For the second hypothesis, immunostaining and imaging will be employed. More specifically, we will stain chromatin structures (both cleaved IL-33 complexed and control) with sytox green, an extracellular DNA fluorescent dye. Then, their ability to co-localize with ST2L and to be endocytosed from pDCs or other immune cells will be examined and quantitated using confocal imaging. Additionally, ST2L will be blocked before chromatin complexes' treatment to investigate if IL-33 complexed chromatin structures could be engulfed properly using confocal imaging and quantitation scripts.

8.3 Investigating the exact mechanism of neutrophil proteases-dependent IL-33 cleavage

As we already mentioned, it would be of interest to delineate whether IL-33 cleavage occurs intracellularly or extracellularly. In our project, we proved that SLE neutrophil-released NET structures are able to cleave exogenously administrated recombinant full length IL-33 but taking into consideration the specific features of NETosis initiation (elastase translocation into the nucleus to cleave histones and promote decondensation of chromatin) and full length IL-33 localization (chromatin bound, in histone-mediated acidic patches) we would like to address if the described process could also be taking place intracellularly. To begin with, we will isolate peripheral blood SLE neutrophils and we will stimulate them ex vivo using SLE-relevant immune complexes. To assess pre- NETosis or post-NETosis elastase bioactivity, we will use

neutrophil serine proteases probes to label the proteolytically active form (Kasperkiewicz P. et al., 2020) in distinct time points (30 min, 1hr, 2hr, 4hr). To validate our results, we will also use elastase-centered fluorimetric assays in SLE neutrophil extracts (employing nuclear/cytoplasmic fractionation) using the same time points. Therefore, by employing immunostaining/imaging techniques, we will validate if elastase retains its bioactivity during the initial steps of NETosis. Additionally, we will test for potential co-localization of proteolytically active elastase and IL-33 to examine their potential intracellular interaction. Then, we will co-incubate full length IL-33-containing purified nucleosomes with recombinant elastase to verify by western blot that histone-bound IL-33 can be a potential elastase- substrate. To obtain IL-33-containing nucleosomes, we will combine acid-based histone extraction protocols with IL-33-dependent immunoprecipitation assays. Lastly, we will compare elastase-treated or control nucleosome inflammatory potential by measuring NFkb phosphorylation in IL-33 responsive HMC-1 mast cell line and assess IL-33 contribution by pre-treating them with an a-ST2L blocking antibody. By describing an intracellular elastase-mediated IL-33 cleavage mechanism we will provide with a novel mechanism of how oxidation-sensitive proteins can be activated prior to their release into oxidative milieus.

8.4 Delineating the role of SLE NETs as cleavage platforms of non-hematopoietic cell-derived IL-33.

In our study, we described the inflammatory potential of NET-derived IL-33. Moreover, we detected IL-33 decorated NETs in SLE-relevant-inflamed tissues (kidney, skin). Considering that damaged / necrotic / activated non-hematopoietic cells express relatively increased levels of IL-33 compared to immune cells and that NETotic neutrophils are in close proximity to non-hematopoietic cells in SLE inflamed tissues, it would be of interest to investigate if an IL-33-centered interaction of non-hematopoietic cells and NETotic neutrophils could lead to SLE exacerbation. In our study, we managed to detect IL-33-decorated NETs in the tubulointerstitial area of LN renal sections and in the dermis of CLE patients. For that purpose, we will use primary human cell lines of Renal Proximal Tubule Epithelial Cells (RPTEC, ATCC) and Dermal Fibroblasts (HDFA, ATCC) which are cells located to tubulointerstitium and dermis respectively. Then, we will screen for potential SLE-relevant stimuli (type I IFNs, immune complexes, NETs etc) that are able induce IL-33 secretion. Notably, recent findings propose that elevated IFN-signaling in systemic lupus erythematosus (SLE) augments necroptosis, a hallmark feature of which is IL-33 secretion (Sarhan J. et.,

2019). In this assay, necrotic tubule epithelial cells and dermal fibroblasts will be used as positive controls regarding IL-33 expression. After establishing the IL-33-expressing stimulus, we will use full length IL-33-containing supernatants from the aforementioned primary cell lines and co-incubate them with SLE NETotic neutrophils. Then, we will test if non-hematopoietic cell derived IL-33 can be cleaved from SLE NETotic structures by detecting IL-33 cleaved isoforms via immunoblotting. After establishing the NET-mediated SLE cleavage of IL-33, cleaved-IL-33 containing supernatants will be used alone or in combination with extracellular chromatin (NETs or other SLE-relevant extracellular DNA-containing complexes) to address their inflammatory potential. For that purpose, immune cells will be isolated from healthy donors' peripheral blood. To carefully select the immune cell-target that we will use to obtain information about site-specific inflammatory potential of NET-cleaved IL-33 we will employ multiplex imaging (Allam M et al, 2020) of SLE renal and skin biopsies. By using this novel imaging technique, we will be able to obtain information about the spatial interaction of damaged non-hematopoietic cells, NETs and infiltrating immune cells. Infiltrating immune cells that are in close proximity with NETs in renal or skin tissues will be used as targets to test the inflammatory potential (by employing transcriptomic analysis [RNAseq]) of cleaved IL-33-containing supernatants along or in combination with extracellular SLE-relevant chromatin. The goal of this study will be to completely characterize the NET-mediated SLE inflamed tissue-specific IL-33 inflammatory potential.

8.5 Investigating the pro-fibrotic potential of NET-derived IL-33

Renal fibrosis is a main feature of late stage LN a. Considering that IL-33 was reported to exert potent pro-fibrogenic capacity (Kotsiou OS. et al., 2018), we would like to examine if bioactive–IL-33 -bearing SLE NETs can promote fibrosis directly or indirectly through trans-differentiating or through stimulating renal resident macrophages. To begin with, SLE renal tissues will be immunostained with the relevant markers to observe if IL-33 decorated NETs (IL-33, MPO) are in close proximity with tissue resident-macrophages (F4/80). Then, naïve human peripheral blood monocytes (CD14+) will be isolated and differentiated into M0 macrophages using M-CSF, then they will be treated ex vivo with IC-mediated SLE NETs with or without concomitant ST2L blockade and transcriptomic analysis will be employed (RNA sequencing) in order to delineate if SLE NETs promote fibrogenic factors expression or the transdifferentiation of macrophages into myofibroblast-like cells. NET-IL-33 contribution will be addressed by comparing a-ST2L treated with control

cells both treated with SLE NETs. To address the in vivo significance of IL-33 decorated NETs towards tubulointerstitial fibrosis of LN we will also employ a novel accelerated mouse model of lupus, using pristane treatment in SNF1 (SWR X NZB F1) lupus prone mice (Gardet A et al., 2016). This mouse model exhibits human Lupus Nephritis-like fibrosis starting from week 12. Those mice will be genetically modified to knock-out conditionally *ILRL1* gene only in renal resident macrophages (Cre-*SIGLEC1/IL1RL1*-LoxP). After 14-weeks, both conditional knock out and control lupus prone mice will be euthanized and renal fibrosis (immuhistochemistry) and other aspects of LN will be monitored.

8.6 Unraveling the role of IL-33-decorated NETs regarding rheumatoid arthritis pathogenesis

In this study, we investigated the role of IC-mediated IL-33 decorated NETs in SLE pathogenesis. Considering that IL-33 is upregulated in RA sera and reflects clinical activity (Xiangyang Z., et al., 2012) and that NETs promote RA pathogenesis. First, we could monitor IL-33 decorated NETs both in serum and synovial fluid derived from RA patients and healthy donors (and correlated with RA-specific manifestations) by using the sandwich ELISA that we designed. Then, we could establish an RA-relevant stimulus (immune complexes [anti-RF, anti-CCP, anti-collagenII) that promotes NETosis of RA neutrophils. By employing immunostaining of RA-neutrophils, we could verify IL-33 decoration of both spontaneously released and IC-mediated RA NETs. After triggering of IC-mediated RA NETosis, we will isolate NET-containing supernatant and we will use them to treat control macrophages isolated from healthy donors' peripheral blood. We will assess IC-mediated NETs inflammatory potential by monitoring both mRNA and protein levels of TNF-α and IL-6. IL-33's contribution will be addressed by pretreating control macrophages with a-ST2L blocking antibody. Additionally, a focused proteomic analysis (PRM) will be conducted in control heathy NETs, spontaneous RA NETs and IC-mediated NETs to check for proteotypic petides of bioactive IL-33 like those that we managed to detect exhibiting upregulated levels in IC-SLE NETs. Lastly, we will perform immunostaining of RA and healthy synovial tissue to screen for IL-33 decorated NETs.

9) References

1. Apel F, Andreeva L, Knackstedt LS, et al. The cytosolic DNA sensor cGAS recognizes neutrophil extracellular traps. Sci Signal. 2021;14(673). doi:10.1126/scisignal.aax7942

2. Arazi A, Rao DA, Berthier CC, et al. The immune cell landscape in kidneys of patients with lupus nephritis. Nat Immunol. 2019;20(7):902-914. doi:10.1038/s41590-019-0398-x

3. Baccala R, Gonzalez-Quintial R, Blasius AL, et al. Essential requirement for IRF8 and SLC15A4 implicates plasmacytoid dendritic cells in the pathogenesis of lupus. Proc Natl Acad Sci U S A. 2013;110(8):2940-2945. doi:10.1073/pnas.1222798110

4. Balato A, Lembo S, Mattii M, et al. IL-33 is secreted by psoriatic keratinocytes and induces pro-inflammatory cytokines via keratinocyte and mast cell activation. Exp Dermatol. 2012;21(11):892-894. doi:10.1111/exd.12027

5. Banchereau J, Pascual V. Type I Interferon in Systemic Lupus Erythematosus and Other Autoimmune Diseases. Immunity. 2006;25(3):383-392. doi:10.1016/j.immuni.2006.08.010

6. Barbhaiya M, Costenbader KH. Environmental exposures and the development of systemic lupus erythematosus. Curr Opin Rheumatol. 2016;28(5):497-505. doi:10.1097/BOR.0000000000000318

7. Baumann C, Bonilla W V., Fröhlich A, et al. T-bet- And STAT4-dependent IL-33 receptor expression directly promotes antiviral Th1 cell responses. Proc Natl Acad Sci U S A. 2015;112(13):4056-4061. doi:10.1073/pnas.1418549112

8. Bennett L, Palucka AK, Arce E, et al. Interferon and granulopoiesis signatures in systemic lupus erythematosus blood. J Exp Med. 2003;197(6):711-723. doi:10.1084/jem.20021553

9. Besnard AG, Togbe D, Couillin I, et al. InflammasomeIL-1Th17 response in allergic lung inflammation. J Mol Cell Biol. 2012;4(1):3-10. doi:10.1093/jmcb/mjr042

10. Bessa J, Meyer CA, de Vera Mudry MC, et al. Altered subcellular localization of IL-33 leads to non-resolving lethal inflammation. J Autoimmun. 2014;55(1):33-41. doi:10.1016/j.jaut.2014.02.012

11. Blanco P, Palucka AK, Gill M, Pascual V, Banchereau J. Induction of dendritic cell differentiation by IFN-α in systemic lupus erythematosus. Science (80-). 2001;294(5546):1540-1543. doi:10.1126/science.1064890

12. Bonilla W V., Fröhlich A, Senn K, et al. The alarmin interleukin-33 drives protective antiviral CD8+ T cell responses. Science (80-). 2012;335(6071):984-989. doi:10.1126/science.1215418

13. Brinkmann V, Reichard U, Goosmann C, et al. Neutrophil Extracellular Traps Kill Bacteria. Science (80-). 2004;303(5663):1532-1535. doi:10.1126/science.1092385

14. Brint EK, Xu D, Liu H, et al. ST2 is an inhibitor of interleukin 1 receptor and Toll-like receptor 4 signaling and maintains endotoxin tolerance. Nat Immunol. 2004;5(4):373-379. doi:10.1038/ni1050

15. Bruschi M, Petretto A, Santucci L, et al. Neutrophil Extracellular Traps protein composition is specific for patients with Lupus nephritis and includes methyl-oxidized α enolase (methionine sulfoxide 93). Sci Rep. 2019;9(1). doi:10.1038/s41598-019-44379-w

16. Burn GL, Foti A, Marsman G, Patel DF, Zychlinsky A. The Neutrophil. Immunity. 2021;54(7):1377-1391. doi:10.1016/j.immuni.2021.06.006

17. Caielli S, Athale S, Domic B, et al. Oxidized mitochondrial nucleoids released by neutrophils drive type I interferon production in human lupus. J Exp Med. 2016;213(5):697-713. doi:10.1084/jem.20151876

18. Caielli S, Veiga DT, Balasubramanian P, et al. A CD4+ T cell population expanded in lupus blood provides B cell help through interleukin-10 and succinate. Nat Med. 2019;25(1):75-81. doi:10.1038/s41591-018-0254-9

19. Caielli S, Veiga DT, Balasubramanian P, et al. A CD4+ T cell population expanded in lupus blood provides B cell help through interleukin-10 and succinate. Nat Med. 2019;25(1):75-81. doi:10.1038/s41591-018-0254-9

20. Carmona-Rivera C, Carlucci PM, Goel RR, et al. Neutrophil extracellular traps mediate articular cartilage damage and enhance cartilage component immunogenicity in rheumatoid arthritis. JCI Insight. 2020;5(13). doi:10.1172/jci.insight.139388

21. Carmona-Rivera C, Carlucci PM, Moore E, et al. Synovial fibroblast-neutrophil interactions promote pathogenic adaptive immunity in rheumatoid arthritis. Sci Immunol. 2017;2(10). doi:10.1126/sciimmunol.aag3358

22. Carrasco TG, Morales RA, Pérez F, et al. Alarmin' immunologists: IL-33 as a putative target for modulating T cell-dependent responses. Front Immunol. 2015;6(JUN). doi:10.3389/fimmu.2015.00232
23. Carriere V, Roussel L, Ortega N, et al. IL-33, the IL-1-like Cytokine Ligand for ST2 Receptor, Is a Chromatin-Associated Nuclear Factor in Vivo. Vol 104.; 2007. doi:10.1073/pnas.0606854104
24. Catapano M, Vergnano M, Romano M, et al. IL-36 Promotes Systemic IFN-I Responses in Severe Forms of Psoriasis. J Invest Dermatol. 2020;140(4):816-826.e3. doi:10.1016/j.jid.2019.08.444
25. Cayrol C, Duval A, Schmitt P, et al. Environmental allergens induce allergic inflammation through proteolytic maturation of IL-33. Nat Immunol. 2018;19(4):375-385. doi:10.1038/s41590-018-0067-5
26. Cayrol C, Girard JP. Interleukin-33 (IL-33): A nuclear cytokine from the IL-1 family. Immunol Rev. 2018;281(1):154-168. doi:10.1111/imr.12619
27. Cayrol C, Girard JP. IL-33: An alarmin cytokine with crucial roles in innate immunity, inflammation and allergy. Curr Opin Immunol. 2014;31:31-37. doi:10.1016/j.coi.2014.09.004
28. Chapman EA, Lyon M, Simpson D, et al. Caught in a trap? Proteomic analysis of neutrophil extracellular traps in rheumatoid arthritis and systemic lupus erythematosus. Front Immunol. 2019;10(MAR). doi:10.3389/fimmu.2019.00423
29. Chapman EA, Lyon M, Simpson D, et al. Caught in a trap? Proteomic analysis of neutrophil extracellular traps in rheumatoid arthritis and systemic lupus erythematosus. Front Immunol. 2019;10(MAR). doi:10.3389/fimmu.2019.00423
30. Charles N, Hardwick D, Daugas E, Illei GG, Rivera J. Basophils and the T helper 2 environment can promote the development of lupus nephritis. Nat Med. 2010;16(6):701-707. doi:10.1038/nm.2159
31. Chen YL, Gutowska-Owsiak D, Hardman CS, et al. Proof-of-concept clinical trial of etokimab shows a key role for IL-33 in atopic dermatitis pathogenesis. Sci Transl Med. 2019;11(515). doi:10.1126/scitranslmed.aax2945
32. Cheng M, Gu X, Herrera GA. Dendritic cells in renal biopsies of patients with acute tubulointerstitial nephritis. Hum Pathol. 2016;54:113-120. doi:10.1016/j.humpath.2016.03.020
33. Clancy DM, Sullivan GP, Moran HBT, et al. Extracellular Neutrophil Proteases Are Efficient Regulators of IL-1, IL-33, and IL-36 Cytokine Activity but Poor Effectors of Microbial Killing. Cell Rep. 2018;22(11):2937-2950. doi:10.1016/j.celrep.2018.02.062

34. Cohen ES, Scott IC, Majithiya JB, et al. Oxidation of the alarmin IL-33 regulates ST2-dependent inflammation. Nat Commun. 2015;6(1). doi:10.1038/ncomms9327

35. Craft JE. Follicular helper T cells in immunity and systemic autoimmunity. Nat Rev Rheumatol. 2012;8(6):337-347. doi:10.1038/nrrheum.2012.58

36. Davenne T, Bridgeman A, Rigby RE, Rehwinkel J. Deoxyguanosine is a TLR7 agonist. Eur J Immunol. 2020;50(1):56-62. doi:10.1002/eji.201948151

37. Der E, Suryawanshi H, Morozov P, et al. Tubular cell and keratinocyte single-cell transcriptomics applied to lupus nephritis reveal type I IFN and fibrosis relevant pathways. Nat Immunol. 2019;20(7). doi:10.1038/s41590-019-0386-1

38. Douda DN, Khan MA, Grasemann H, Palaniyar N. SK3 channel and mitochondrial ROS mediate NADPH oxidase-independent NETosis induced by calcium influx. Proc Natl Acad Sci U S A. 2015;112(9):2817-2822. doi:10.1073/pnas.1414055112

39. Eloranta ML, Lövgren T, Finke D, et al. Regulation of the interferon-α production induced by RNA-containing immune complexes in plasmacytoid dendritic cells. Arthritis Rheum. 2009;60(8):2418-2427. doi:10.1002/art.24686

40. Espinassous Q, Garcia-de-Paco E, Garcia-Verdugo I, et al. IL-33 Enhances Lipopolysaccharide-Induced Inflammatory Cytokine Production from Mouse Macrophages by Regulating Lipopolysaccharide Receptor Complex. J Immunol. 2009;183(2):1446-1455. doi:10.4049/jimmunol.0803067

41. Farrera C, Fadeel B. Macrophage Clearance of Neutrophil Extracellular Traps Is a Silent Process. J Immunol. 2013;191(5):2647-2656. doi:10.4049/jimmunol.1300436

42. Ferhat M, Robin A, Giraud S, et al. Endogenous IL-33 contributes to kidney ischemia-reperfusion injury as an alarmin. J Am Soc Nephrol. 2018;29(4):1272-1288. doi:10.1681/ASN.2017060650

43. Fiore N, Castellano G, Blasi A, et al. Immature myeloid and plasmacytoid dendritic cells infiltrate renal tubulointerstitium in patients with lupus nephritis. Mol Immunol. 2008;45(1):259-265. doi:10.1016/j.molimm.2007.04.029

44. Frangou E, Chrysanthopoulou A, Mitsios A, et al. REDD1/autophagy pathway promotes thromboinflammation and fibrosis in human systemic lupus erythematosus (SLE) through NETs decorated with tissue factor (TF) and interleukin-17A (IL-17A). Ann Rheum Dis. 2019;78(2):238-248. doi:10.1136/annrheumdis-2018-213181

45. Furie R, Werth VP, Merola JF, et al. Monoclonal antibody targeting BDCA2 ameliorates skin lesions in systemic lupus erythematosus. J Clin Invest. 2019;129(3):1359-1371. doi:10.1172/JCI124466

46. Fürnrohr BG, Wach S, Kelly JA, et al. Polymorphisms in the Hsp70 gene locus are genetically associated with systemic lupus erythematosus. Ann Rheum Dis. 2010;69(11):1983-1989. doi:10.1136/ard.2009.122630

47. Gao Q, Li Y, Li M. The potential role of IL-33/ST2 signaling in fibrotic diseases. J Leukoc Biol. 2015;98(1):15-22. doi:10.1189/jlb.3ru0115-012r

48. Garcia-Romo GS, Caielli S, Vega B, et al. Netting Neutrophils Are Major Inducers of Type I IFN Production in Pediatric Systemic Lupus Erythematosus. Vol 3.; 2011. doi:10.1126/scitranslmed.3001201

49. Gehrke N, Mertens C, Zillinger T, et al. Oxidative damage of dna confers resistance to cytosolic nuclease trex1 degradation and potentiates STING-dependent immune sensing. Immunity. 2013;39(3):482-495. doi:10.1016/j.immuni.2013.08.004

50. Gestermann N, Di Domizio J, Lande R, et al. Netting Neutrophils Activate Autoreactive B Cells in Lupus. J Immunol. 2018;200(10):3364-3371. doi:10.4049/jimmunol.1700778

51. Goel RR, Wang X, O'Neil LJ, et al. Interferon lambda promotes immune dysregulation and tissue inflammation in TLR7-induced lupus. Proc Natl Acad Sci U S A. 2020;117(10):5409-5419. doi:10.1073/pnas.1916897117

52. Guma M, Ronacher L, Liu-Bryan R, Takai S, Karin M, Corr M. Caspase 1-independent activation of interleukin-1β in neutrophil-predominant inflammation. Arthritis Rheum. 2009;60(12):3642-3650. doi:10.1002/art.24959

53. Guo J, Xiang Y, Peng YF, Huang HT, Lan Y, Wei YS. The association of novel IL-33 polymorphisms with sIL-33 and risk of systemic lupus erythematosus. Mol Immunol. 2016;77:1-7. doi:10.1016/j.molimm.2016.07.001

54. Gupta S, Kaplan MJ. The role of neutrophils and NETosis in autoimmune and renal diseases. Nat Rev Nephrol. 2016;12(7):402-413. doi:10.1038/nrneph.2016.7

55. Hakkim A, Fürnrohr BG, Amann K, et al. Impairment of neutrophil extracellular trap degradation is associated with lupus nephritis. Proc Natl Acad Sci U S A. 2010;107(21):9813-9818. doi:10.1073/pnas.0909927107

56. Han Y, Chen L, Liu H, et al. Airway Epithelial cGAS Is Critical for Induction of Experimental Allergic Airway Inflammation. J Immunol. 2020;204(6):1437-1447. doi:10.4049/jimmunol.1900869

57. Harigai M, Kawamoto M, Hara M, Kubota T, Kamatani N, Miyasaka N. Excessive Production of IFN-γ in Patients with Systemic Lupus Erythematosus and Its Contribution to Induction of B Lymphocyte Stimulator/B Cell-Activating Factor/TNF Ligand Superfamily-13B. J Immunol. 2008;181(3):2211-2219. doi:10.4049/jimmunol.181.3.2211

58. Hatzioannou A, Banos A, Sakelaropoulos T, et al. An intrinsic role of IL-33 in Treg cell–mediated tumor immunoevasion. Nat Immunol. 2020;21(1):75-85. doi:10.1038/s41590-019-0555-2

59. He J, Yang Q, Xiao Q, et al. IRF-7 Is a Critical Regulator of Type 2 Innate Lymphoid Cells in Allergic Airway Inflammation. Cell Rep. 2019;29(9):2718-2730.e6. doi:10.1016/j.celrep.2019.10.077

60. Herster F, Bittner Z, Archer NK, et al. Neutrophil extracellular trap-associated RNA and LL37 enable self-amplifying inflammation in psoriasis. Nat Commun. 2020;11(1). doi:10.1038/s41467-019-13756-4

61. Hochberg MC. Updating the American College of Rheumatology revised criteria for the classification of systemic lupus erythematosus. Arthritis Rheum. 1997;40(9):1725. doi:10.1002/art.1780400928

62. Hu SCS, Yu HS, Yen FL, Lin CL, Chen GS, Lan CCE. Neutrophil extracellular trap formation is increased in psoriasis and induces human β-defensin-2 production in epidermal keratinocytes. Sci Rep. 2016;6(1). doi:10.1038/srep31119

63. Hung LY, Tanaka Y, Herbine K, et al. Cellular context of IL-33 expression dictates impact on anti-helminth immunity. Sci Immunol. 2020;5(53). doi:10.1126/sciimmunol.abc6259

64. Ittah M, Miceli-Richard C, Gottenberg JE, et al. B cell-activating factor of the tumor necrosis factor family (BAFF) is expressed under stimulation by interferon in salivary gland epithelial cells in primary Sjögren's syndrome. Arthritis Res Ther. 2006;8(2). doi:10.1186/ar1912

65. Jacquemin C, Schmitt N, Contin-Bordes C, et al. OX40 Ligand Contributes to Human Lupus Pathogenesis by Promoting T Follicular Helper Response. Immunity. 2015;42(6):1159-1170. doi:10.1016/j.immuni.2015.05.01

66. Jenks SA, Cashman KS, Zumaquero E, et al. Distinct Effector B Cells Induced by Unregulated Toll-like Receptor 7 Contribute to Pathogenic Responses in Systemic Lupus Erythematosus. Immunity. 2018;49(4):725-739.e6. doi:10.1016/j.immuni.2018.08.015

67. Jiang HR, Milovanović M, Allan D, et al. IL-33 attenuates EAE by suppressing IL-17 and IFN-γ production and inducing alternatively activated macrophages. Eur J Immunol. 2012;42(7):1804-1814. doi:10.1002/eji.201141947

68. Jorch SK, Kubes P. An emerging role for neutrophil extracellular traps in noninfectious disease. Nat Med. 2017;23(3):279-287. doi:10.1038/nm.4294

69. Kahlenberg JM, Carmona-Rivera C, Smith CK, Kaplan MJ. Neutrophil Extracellular Trap–Associated Protein Activation of the NLRP3 Inflammasome Is Enhanced in Lupus Macrophages. J Immunol. 2013;190(3):1217-1226. doi:10.4049/jimmunol.1202388

70. Kansal R, Richardson N, Neeli I, et al. Sustained B cell depletion by CD19-targeted CAR T cells is a highly effective treatment for murine lupus. Sci Transl Med. 2019;11(482). doi:10.1126/scitranslmed.aav1648

71. Kaplan MJ. Neutrophils in the pathogenesis and manifestations of SLE. Nat Rev Rheumatol. 2011;7(12):691-699. doi:10.1038/nrrheum.2011.132

72. Katsuyama E, Suarez-Fueyo A, Bradley SJ, et al. The CD38/NAD/SIRTUIN1/EZH2 Axis Mitigates Cytotoxic CD8 T Cell Function and Identifies Patients with SLE Prone to Infections. Cell Rep. 2020;30(1):112-123.e4. doi:10.1016/j.celrep.2019.12.014

73. Knight JS, Subramanian V, O'Dell AA, et al. Peptidylarginine deiminase inhibition disrupts NET formation and protects against kidney, skin and vascular disease in lupus-prone MRL/lpr mice. Ann Rheum Dis. 2015;74(12):2199-2206. doi:10.1136/annrheumdis-2014-205365

74. Kolaczkowska E, Jenne CN, Surewaard BGJ, et al. Molecular mechanisms of NET formation and degradation revealed by intravital imaging in the liver vasculature. Nat Commun. 2015;6(1). doi:10.1038/ncomms7673

75. Komai-Koma M, Gilchrist DS, McKenzie ANJ, Goodyear CS, Xu D, Liew FY. IL-33 Activates B1 Cells and Exacerbates Contact Sensitivity. J Immunol. 2011;186(4):2584-2591. doi:10.4049/jimmunol.1002103
76. Kurowska-Stolarska M, Stolarski B, Kewin P, et al. IL-33 Amplifies the Polarization of Alternatively Activated Macrophages That Contribute to Airway Inflammation. J Immunol. 2009;183(10):6469-6477. doi:10.4049/jimmunol.0901575
77. Labonte AC, Kegerreis B, Geraci NS, et al. Identification of alterations in macrophage activation associated with disease activity in systemic lupus erythematosus. PLoS One. 2018;13(12). doi:10.1371/journal.pone.0208132
78. Lanata CM, Paranjpe I, Nititham J, et al. A phenotypic and genomics approach in a multi-ethnic cohort to subtype systemic lupus erythematosus. Nat Commun. 2019;10(1). doi:10.1038/s41467-019-11845-y
79. Lande R, Palazzo R, Gestermann N, et al. Native/citrullinated LL37-specific T-cells help autoantibody production in Systemic Lupus Erythematosus. Sci Rep. 2020;10(1). doi:10.1038/s41598-020-62480-3
80. Lande R, Ganguly D, Facchinetti V, et al. Neutrophils activate plasmacytoid dendritic cells by releasing self-DNA-peptide complexes in systemic lupus erythematosus. Sci Transl Med. 2011;3(73). doi:10.1126/scitranslmed.3001180
81. Lande R, Gregorio J, Facchinetti V, et al. Plasmacytoid dendritic cells sense self-DNA coupled with antimicrobial peptide. Nature. 2007;449(7162):564-569. doi:10.1038/nature06116
82. Lang PA, Merkler D, Funkner P, et al. Oxidized ATP inhibits T-cell-mediated autoimmunity. Eur J Immunol. 2010;40(9):2401-2408. doi:10.1002/eji.200939838
83. Leffler J, Martin M, Gullstrand B, et al. Neutrophil Extracellular Traps That Are Not Degraded in Systemic Lupus Erythematosus Activate Complement Exacerbating the Disease. J Immunol. 2012;188(7):3522-3531. doi:10.4049/jimmunol.1102404
84. Lefrançais E, Roga S, Gautier V, et al. IL-33 is processed into mature bioactive forms by neutrophil elastase and cathepsin G. Proc Natl Acad Sci U S A. 2012;109(5):1673-1678. doi:10.1073/pnas.1115884109
85. Li H, Fu YX, Wu Q, et al. Interferon-induced mechanosensing defects impede apoptotic cell clearance in lupus. J Clin Invest. 2015;125(7):2877-2890. doi:10.1172/JCI81059

86. Li P, Lin W, Zheng X. IL-33 neutralization suppresses lupus disease in lupus-prone mice. Inflammation. 2014;37(3):824-832. doi:10.1007/s10753-013-9802-0

87. Li P, Lin W, Zheng X. IL-33 neutralization suppresses lupus disease in lupus-prone mice. Inflammation. 2014;37(3):824-832. doi:10.1007/s10753-013-9802-0

88. Liang Y, Yi P, Yuan DMK, et al. IL-33 induces immunosuppressive neutrophils via a type 2 innate lymphoid cell/IL-13/STAT6 axis and protects the liver against injury in LCMV infection-induced viral hepatitis. Cell Mol Immunol. 2019;16(2):126-137. doi:10.1038/cmi.2017.147

89. Liew FY, Girard JP, Turnquist HR. Interleukin-33 in health and disease. Nat Rev Immunol. 2016;16(11):676-689. doi:10.1038/nri.2016.95

90. Liu B, Dai J, Zheng H, Stoilova D, Sun S, Li Z. Cell surface expression of an endoplasmic reticulum resident heat shock protein gp96 triggers MyD88-dependent systemic autoimmune diseases. Proc Natl Acad Sci U S A. 2003;100(26):15824-15829. doi:10.1073/pnas.2635458100

91. Lood C, Blanco LP, Purmalek MM, et al. Neutrophil extracellular traps enriched in oxidized mitochondrial DNA are interferogenic and contribute to lupus-like disease. Nat Med. 2016;22(2):146-153. doi:10.1038/nm.4027

92. Lövgren T, Eloranta ML, Båve U, Alm G V., Rönnblom L. Induction of interferon-α production in plasmacytoid dendritic cells by immune complexes containing nucleic acid released by necrotic or late apoptotic cells and lupus IgG. Arthritis Rheum. 2004;50(6):1861-1872. doi:10.1002/art.20254

93. Lövgren T, Eloranta ML, Båve U, Alm G V., Rönnblom L. Induction of interferon-α production in plasmacytoid dendritic cells by immune complexes containing nucleic acid released by necrotic or late apoptotic cells and lupus IgG. Arthritis Rheum. 2004;50(6):1861-1872. doi:10.1002/art.20254

94. Lu J, Kang J, Zhang C, Zhang X. The role of IL-33/ST2L signals in the immune cells. Immunol Lett. 2015;164(1):11-17. doi:10.1016/j.imlet.2015.01.008

95. Luo Q, Huang Z, Ye J, et al. PD-L1-expressing neutrophils as a novel indicator to assess disease activity and severity of systemic lupus erythematosus. Arthritis Res Ther. 2016;18(1). doi:10.1186/s13075-016-0942-0

96. Lüthi AU, Cullen SP, McNeela EA, et al. Suppression of Interleukin-33 Bioactivity through Proteolysis by Apoptotic Caspases. Immunity. 2009;31(1):84-98. doi:10.1016/j.immuni.2009.05.007

97. Makridakis M, Vlahou A. GeLC-MS: A Sample Preparation Method for Proteomics Analysis of Minimal Amount of Tissue. In: Methods in Molecular Biology. Vol 1788. ; 2018:165-175. doi:10.1007/7651_2017_76

98. Martin SJ. Cell death and inflammation: the case for IL-1 family cytokines as the canonical DAMPs of the immune system. FEBS J. 2016;283(14):2599-2615. doi:10.1111/febs.13775

99. Menon M, Blair PA, Isenberg DA, Mauri C. A Regulatory Feedback between Plasmacytoid Dendritic Cells and Regulatory B Cells Is Aberrant in Systemic Lupus Erythematosus. Immunity. 2016;44(3):683-697. doi:10.1016/j.immuni.2016.02.012

100. Migliorini A, Angelotti ML, Mulay SR, et al. The antiviral cytokines IFN-α and IFN-β modulate parietal epithelial cells and promote podocyte loss: Implications for IFN toxicity, viral glomerulonephritis, and glomerular regeneration. Am J Pathol. 2013;183(2):431-440. doi:10.1016/j.ajpath.2013.04.017

101. Minns D, Smith KJ, Findlay EG. Orchestration of Adaptive T Cell Responses by Neutrophil Granule Contents. Mediators Inflamm. 2019;2019. doi:10.1155/2019/8968943

102. Mistry P, Nakabo S, O'Neil L, et al. Transcriptomic, epigenetic, and functional analyses implicate neutrophil diversity in the pathogenesis of systemic lupus erythematosus. Proc Natl Acad Sci U S A. 2019;116(50):25222-25228. doi:10.1073/pnas.1908576116

103. Mizui M, Koga T, Lieberman LA, et al. IL-2 Protects Lupus-Prone Mice from Multiple End-Organ Damage by Limiting CD4 − CD8 − IL-17–Producing T Cells . J Immunol. 2014;193(5):2168-2177. doi:10.4049/jimmunol.1400977

104. Mohan C, Adams S, Stanik V, Datta SK. Nucleosome: A major immunogen for pathogenic autoantibody-inducing T cells of lupus. J Exp Med. 1993;177(5):1367-1381. doi:10.1084/jem.177.5.1367

105. Mok CC, Lau CS. Pathogenesis of systemic lupus erythematosus. J Clin Pathol. 2003;56(7):481-490. doi:10.1136/jcp.56.7.481

106. Mok MY, Huang FP, Ip WK, et al. Serum levels of IL-33 and soluble ST2 and their association with disease activity in systemic lupus erythematosus. Rheumatology. 2009;49(3):520-527. doi:10.1093/rheumatology/kep402

107. Molofsky AB, Savage AK, Locksley RM. Interleukin-33 in Tissue Homeostasis, Injury, and Inflammation. Immunity. 2015;42(6):1005-1019. doi:10.1016/j.immuni.2015.06.006

108. Moreau A, Nicaise C, Awada A, Soyfoo MS. Soluble ST2 is increased in systemic lupus erythematous and is a potential marker of lupus nephritis. Clin Exp Rheumatol. Published online June 8, 2021.

109. Mosca M, Bombardieri S. Assessing remission in systemic lupus erythematosus. Clin Exp Rheumatol. 24(6 Suppl 43).

110. Mukherjee R, Kanti Barman P, Kumar Thatoi P, Tripathy R, Kumar Das B, Ravindran B. Non-Classical monocytes display inflammatory features: Validation in Sepsis and Systemic Lupus Erythematous. Sci Rep. 2015;5(1). doi:10.1038/srep13886

111. Nakano M, Ayano M, Kushimoto K, et al. Increased Proportion of CD226+ B Cells Is Associated With the Disease Activity and Prognosis of Systemic Lupus Erythematosus. Front Immunol. 2021;12. doi:10.3389/fimmu.2021.713225

112. Neubert E, Meyer D, Rocca F, et al. Chromatin swelling drives neutrophil extracellular trap release. Nat Commun. 2018;9(1). doi:10.1038/s41467-018-06263-5

113. Nordenfelt P, Bauer S, Lönnbro P, Tapper H. Phagocytosis of Streptococcus pyogenes by All-Trans Retinoic Acid-Differentiated HL-60 Cells: Roles of Azurophilic Granules and NADPH Oxidase. PLoS One. 2009;4(10). doi:10.1371/journal.pone.0007363

114. Oboki K, Ohno T, Kajiwara N, et al. IL-33 is a crucial amplifier of innate rather than acquired immunity. Proc Natl Acad Sci. 2010;107(43). doi:10.1073/pnas.1003059107

115. Östberg T, Kawane K, Nagata S, et al. Protective targeting of high mobility group box chromosomal protein 1 in a spontaneous arthritis model. Arthritis Rheum. 2010;62(10). doi:10.1002/art.27590

116. Palmer G, Talabot-Ayer D, Lamacchia C, et al. Inhibition of interleukin-33 signaling attenuates the severity of experimental arthritis. Arthritis Rheum. 2009;60(3). doi:10.1002/art.24305

117. Panousis NI, Bertsias GK, Ongen H, et al. Combined genetic and transcriptome analysis of patients with SLE: distinct, targetable signatures for susceptibility and severity. Ann Rheum Dis. 2019;78(8). doi:10.1136/annrheumdis-2018-214379

118. Papadaki G, Kambas K, Choulaki C, et al. Neutrophil extracellular traps exacerbate Th1-mediated autoimmune responses in rheumatoid arthritis by promoting DC maturation. Eur J Immunol. 2016;46(11). doi:10.1002/eji.201646542

119. Papayannopoulos V, Metzler KD, Hakkim A, Zychlinsky A. Neutrophil elastase and myeloperoxidase regulate the formation of neutrophil extracellular traps. J Cell Biol. 2010;191(3). doi:10.1083/jcb.201006052

120. Park SH, Kang K, Giannopoulou E, et al. Type I interferons and the cytokine TNF cooperatively reprogram the macrophage epigenome to promote inflammatory activation. Nat Immunol. 2017;18(10). doi:10.1038/ni.3818

121. Parsa R, Lund H, Georgoudaki A-M, et al. BAFF-secreting neutrophils drive plasma cell responses during emergency granulopoiesis. J Exp Med. 2016;213(8). doi:10.1084/jem.20150577

122. Paulson JC. Innate Immune Response Triggers Lupus-like Autoimmune Disease. Cell. 2007;130(4). doi:10.1016/j.cell.2007.08.009

123. Pavlov KA, Chistiakov DA, Chekhonin VP. Genetic determinants of aggression and impulsivity in humans. J Appl Genet. 2012;53(1). doi:10.1007/s13353-011-0069-6

124. Pieterse E, Rother N, Yanginlar C, et al. Cleaved N-terminal histone tails distinguish between NADPH oxidase (NOX)-dependent and NOX-independent pathways of neutrophil extracellular trap formation. Ann Rheum Dis. 2018;77(12). doi:10.1136/annrheumdis-2018-213223

125. Psarras A, Alase A, Antanaviciute A, et al. Functionally impaired plasmacytoid dendritic cells and non-haematopoietic sources of type I interferon characterize human autoimmunity. Nat Commun. 2020;11(1). doi:10.1038/s41467-020-19918-z

126. Rank MA, Kobayashi T, Kozaki H, Bartemes KR, Squillace DL, Kita H. IL-33–activated dendritic cells induce an atypical TH2-type response. J Allergy Clin Immunol. 2009;123(5). doi:10.1016/j.jaci.2009.02.026

127. Röck J, Schneider E, Grün JR, et al. CD303 (BDCA-2) signals in plasmacytoid dendritic cellsvia a BCR-like signalosome involving Syk, Slp65 and PLCγ2. Eur J Immunol. 2007;37(12). doi:10.1002/eji.200737711

128. Rönnblom L, Leonard D. Interferon pathway in SLE: one key to unlocking the mystery of the disease. Lupus Sci Med. 2019;6(1). doi:10.1136/lupus-2018-000270

129. Rose T, Dörner T. Drivers of the immunopathogenesis in systemic lupus erythematosus. Best Pract Res Clin Rheumatol. 2017;31(3). doi:10.1016/j.berh.2017.09.007

130. Rose WA, Okragly AJ, Hu NN, et al. Interleukin-33 Contributes Toward Loss of Tolerance by Promoting B-Cell-Activating Factor of the Tumor-Necrosis-Factor Family (BAFF)-Dependent Autoantibody Production. Front Immunol. 2018;9. doi:10.3389/fimmu.2018.02871

131. Roussel L, Erard M, Cayrol C, Girard J. Molecular mimicry between IL-33 and KSHV for attachment to chromatin through the H2A–H2B acidic pocket. EMBO Rep. 2008;9(10). doi:10.1038/embor.2008.145

132. Rowland SL, Riggs JM, Gilfillan S, et al. Early, transient depletion of plasmacytoid dendritic cells ameliorates autoimmunity in a lupus model. J Exp Med. 2014;211(10). doi:10.1084/jem.20132620

133. Schauer C, Janko C, Munoz LE, et al. Aggregated neutrophil extracellular traps limit inflammation by degrading cytokines and chemokines. Nat Med. 2014;20(5). doi:10.1038/nm.3547

134. Schiering C, Krausgruber T, Chomka A, et al. The alarmin IL-33 promotes regulatory T-cell function in the intestine. Nature. 2014;513(7519). doi:10.1038/nature13577

135. Sharp AJ, Polak PE, Simonini V, et al. P2x7 deficiency suppresses development of experimental autoimmune encephalomyelitis. J Neuroinflammation. 2008;5(1). doi:10.1186/1742-2094-5-33

136. She L, Barrera GD, Yan L, et al. STING activation in alveolar macrophages and group 2 innate lymphoid cells suppresses IL-33–driven type 2 immunopathology. JCI Insight. 2021;6(3). doi:10.1172/jci.insight.143509

137. Singh RR, Yen EY. SLE mortality remains disproportionately high, despite improvements over the last decade. Lupus. 2018;27(10). doi:10.1177/0961203318786436

138. Silverman, G. J. (2019). The microbiome in SLE pathogenesis. Nature Reviews Rheumatology. https://doi.org/10.1038/s41584-018-0152-

139. Sisirak V, Ganguly D, Lewis KL, et al. Genetic evidence for the role of plasmacytoid dendritic cells in systemic lupus erythematosus. J Exp Med. 2014;211(10). doi:10.1084/jem.20132522

140. Skopelja-Gardner S, Tai J, Sun X, et al. Acute skin exposure to ultraviolet light triggers neutrophil-mediated kidney inflammation. Proc Natl Acad Sci. 2021;118(3). doi:10.1073/pnas.2019097118

141. Stannard JN, Reed TJ, Myers E, et al. Lupus Skin Is Primed for IL-6 Inflammatory Responses through a Keratinocyte-Mediated Autocrine Type I Interferon Loop. J Invest Dermatol. 2017;137(1). doi:10.1016/j.jid.2016.09.008

142. Stier MT, Mitra R, Nyhoff LE, et al. IL-33 Is a Cell-Intrinsic Regulator of Fitness during Early B Cell Development. J Immunol. 2019;203(6). doi:10.4049/jimmunol.1900408

143. Sutton CE, Lalor SJ, Sweeney CM, Brereton CF, Lavelle EC, Mills KHG. Interleukin-1 and IL-23 Induce Innate IL-17 Production from γδ T Cells, Amplifying Th17 Responses and Autoimmunity. Immunity. 2009;31(2). doi:10.1016/j.immuni.2009.08.001

144. Swiecki M, Colonna M. The multifaceted biology of plasmacytoid dendritic cells. Nat Rev Immunol. 2015;15(8). doi:10.1038/nri3865

145. Syrett CM, Paneru B, Sandoval-Heglund D, et al. Altered X-chromosome inactivation in T cells may promote sex-biased autoimmune diseases. JCI Insight. 2019;4(7). doi:10.1172/jci.insight.126751

146. Tian J, Avalos AM, Mao S-Y, et al. Toll-like receptor 9–dependent activation by DNA-containing immune complexes is mediated by HMGB1 and RAGE. Nat Immunol. 2007;8(5). doi:10.1038/ni1457

147. Tjota MY, Williams JW, Lu T, et al. IL-33–dependent induction of allergic lung inflammation by FcγRIII signaling. J Clin Invest. 2013;123(5). doi:10.1172/JCI63802

148. Travers J, Rochman M, Miracle CE, et al. Chromatin regulates IL-33 release and extracellular cytokine activity. Nat Commun. 2018;9(1). doi:10.1038/s41467-018-05485-x

149. Tsokos GC. Systemic Lupus Erythematosus. N Engl J Med. 2011;365(22). doi:10.1056/NEJMra1100359

150. Tsokos GC. Autoimmunity and organ damage in systemic lupus erythematosus. Nat Immunol. 2020;21(6). doi:10.1038/s41590-020-0677-6

151. Tsourouktsoglou T-D, Warnatsch A, Ioannou M, Hoving D, Wang Q, Papayannopoulos V. Histones, DNA, and Citrullination Promote Neutrophil Extracellular Trap Inflammation by Regulating the Localization and Activation of TLR4. Cell Rep. 2020;31(5). doi:10.1016/j.celrep.2020.107602

152. Tuncel J, Benoist C, Mathis D. T cell anergy in perinatal mice is promoted by T reg cells and prevented by IL-33. J Exp Med. 2019;216(6). doi:10.1084/jem.20182002

153. Tvinnereim AR, Hamilton SE, Harty JT. Neutrophil Involvement in Cross-Priming CD8 + T Cell Responses to Bacterial Antigens. J Immunol. 2004;173(3). doi:10.4049/jimmunol.173.3.1994

154. van Lent PLEM, Grevers L, Blom AB, et al. Myeloid-related proteins S100A8/S100A9 regulate joint inflammation and cartilage destruction during antigen-induced arthritis. Ann Rheum Dis. 2008;67(12). doi:10.1136/ard.2007.077800

155. Villanueva E, Yalavarthi S, Berthier CC, et al. Netting Neutrophils Induce Endothelial Damage, Infiltrate Tissues, and Expose Immunostimulatory Molecules in Systemic Lupus Erythematosus. J Immunol. 2011;187(1). doi:10.4049/jimmunol.1100450

156. Villanueva E, Yalavarthi S, Berthier CC, et al. Netting Neutrophils Induce Endothelial Damage, Infiltrate Tissues, and Expose Immunostimulatory Molecules in Systemic Lupus Erythematosus. J Immunol. 2011;187(1):538-552. doi:10.4049/jimmunol.1100450

157. Wald D, Qin J, Zhao Z, et al. SIGIRR, a negative regulator of Toll-like receptor–interleukin 1 receptor signaling. Nat Immunol. 2003;4(9). doi:10.1038/ni968

158. Warnatsch A, Ioannou M, Wang Q, Papayannopoulos V. Neutrophil extracellular traps license macrophages for cytokine production in atherosclerosis. Science (80-). 2015;349(6245). doi:10.1126/science.aaa8064

159. Watanabe T, Yamashita K, Arai Y, et al. Chronic Fibro-Inflammatory Responses in Autoimmune Pancreatitis Depend on IFN-α and IL-33 Produced by Plasmacytoid Dendritic Cells. J Immunol. 2017;198(10):3886-3896. doi:10.4049/jimmunol.1700060

160. Weiss H. A brief history of the super-ego with an introduction to three papers. Int J Psychoanal. 2020;101(4). doi:10.1080/00207578.2020.1796073

161. Wilson PC, Kashgarian M, Moeckel G. Interstitial inflammation and interstitial fibrosis and tubular atrophy predict renal survival in lupus nephritis. Clin Kidney J. 2018;11(2). doi:10.1093/ckj/sfx093

162. Wong SL, Demers M, Martinod K, et al. Diabetes primes neutrophils to undergo NETosis, which impairs wound healing. Nat Med. 2015;21(7). doi:10.1038/nm.3887

163. Yang, D., Chen, Q., Yang, H., Tracey, K. J., Bustin, M., Oppenheim, J. J. (2007). High mobility group box-1 protein induces the migration and activation of human dendritic cells and acts as an alarmin. Journal of Leukocyte Biology https://doi.org/10.1189/jlb.0306180

164. Yazdani HO, Chen H-W, Tohme S, et al. IL-33 exacerbates liver sterile inflammation by amplifying neutrophil extracellular trap formation. J Hepatol. 2018;68(1). doi:10.1016/j.jhep.2017.09.010

165. Yung S, Chan TM. Mechanisms of Kidney Injury in Lupus Nephritis – the Role of Anti-dsDNA Antibodies. Front Immunol. 2015;6. doi:10.3389/fimmu.2015.00475

166. Yurasov S, Wardemann H, Hammersen J, et al. Defective B cell tolerance checkpoints in systemic lupus erythematosus. J Exp Med. 2005;201(5). doi:10.1084/jem.20042251

167. Zhao Q, Chen G. Role of IL-33 and Its Receptor in T Cell-Mediated Autoimmune Diseases. Biomed Res Int. 2014;2014. doi:10.1155/2014/587376

168. Zizzo G, Cohen PL. Imperfect storm: is interleukin-33 the Achilles heel of COVID-19? Lancet Rheumatol. 2020;2(12). doi:10.1016/S2665-9913(20)30340-4

APPENDIX

Supplementary table 1

No.	Gender	Age	Autoantibodies	Medications	SLEDAI-2K
SLE1	F	31	ANA, anti-Sm, anti-RNP, anti-SSA	HCQ, prednisolone	8
SLE2	F	41	ANA, anti-dsDNA, anti-SSA	prednisolone	14
SLE3	M	32	ANA	-	6
SLE4	F	70	ANA, anti-CCP, anti-SSA	AZA	8
SLE5	F	39	ANA, anti-dsDNA	-	8
SLE6	F	64	ANA, anti-dsDNA	HCQ, MTX, prednisolone	8
SLE7	F	16	ANA, anti-dsDNA, anti-Sm, anti-RNP	HCQ, prednisolone	12
SLE8	F	47	ANA	HCQ, MTX	8
SLE9	F	38	ANA, anti-dsDNA, anti-SSA, anti-cardiolipin IgG	-	8
SLE10	F	35	ANA, anti-Sm, anti-dsDNA, anti-RNP	HCQ, AZA	10
SLE11	M	18	ANA, anti-dsDNA, anti-Sm, anti-RNP	HCQ, prednisolone	18
SLE12	F	73	ANA, anti-dsDNA, RF	MMF, prednisolone	12
SLE13	F	48	ANA, anti-dsDNA, anti-ENA	HCQ, MTX	2
SLE14	F	25	ANA, anti-RNP	HCQ	4
SLE15	F	54	ANA, anti-SSA/SSB, anti-dsDNA	HCQ	10
SLE16	F	57	ANA	HCQ, MTX	2
SLE17	F	19	ANA, anti-dsDNA, anti-Sm, anti-RNP	HCQ, prednisolone	10
SLE18	F	44	ANA, anti-dsDNA	HCQ, AZA	8
SLE19	M	24	ANA, anti-dsDNA, anti-RNP, lupus anticoagulant	HCQ, prednisolone	12
SLE20	F	36	ANA, anti-dsDNA, anti-SSA	HCQ, MTX, prednisolone	8
SLE21	F	19	ANA, anti-dsDNA, anti-SSA/SSB, lupus anticoagulant, anti-cardiolipin IgG/IgM, anti-β2GPI IgG/IgM	Prednisolone	6
SLE22	F	49	ANA	-	8
SLE23	F	56	ANA, anti-dsDNA, anti-SSA	-	6
SLE24	F	56	ANA	MTX, prednisolone	4
SLE25	F	54	ANA	belimumab, MTX, HCQ	6
SLE26	F	62	ANA, anti-dsDNA	AZA, prednisolone	2
SLE27	F	75	ANA, anti-dsDNA	prednisolone	12

SLE28	F	42	-	-	10
SLE29	M	44	ANA, anti-SSA/SSB, anti-Sm, anti-β2GPI IgG	-	8
SLE30	F	35	ANA, anti-dsDNA	HCQ, MTX	6
SLE31	F	38	ANA, anti-dsDNA	HCQ	3
SLE32	F	37	ANA, anti-SSA, anti-RNP, anti-dsDNA, anti-β2GPI IgG/IgM	HCQ	8

SLE33	F	52	ANA, anti-dsDNA	-	8
SLE34	M	51	ANA, anti-SSA, anti-CCP	MTX, thalidomide	6
SLE35	F	74	ANA, anti-dsDNA	-	6
SLE36	F	32	ANA, anti-Sm, anti-SSB	HCQ, prednisolone, CsA	6
SLE37	F	51	ANA, anti-dsDNA, anti-Sm, anti-RNP, anti-JO-1	HCQ, MMF	6
SLE38	F	43	ANA	HCQ, MMF	6
SLE39	F	40	ANA, anti-cardiolipin IgG	-	6
SLE40	F	69	ANA, anti-dsDNA, anti-Sm, anti-SSA, anti-RNP	AZA, prednisolone	5
SLE41	F	37	ANA	HCQ	8
SLE42	F	35	ANA	HCQ	10
SLE43	F	33	ANA, anti-cardiolipin IgG	MTX, HCQ	6
SLE44	F	42	ANA, lupus anticoagulant	MMF, HCQ, prednisolone	6
SLE45	F	47	ANA, anti-dsDNA, anti-Sm	prednisolone	6
SLE46	M	76	ANA, anti-dsDNA	AZA, HCQ, prednisolone	12
SLE47	F	48	ANA	MTX	9
SLE48	F	32	ANA, anti-dsDNA, anti-RNP	HCQ, AZA, prednizolone	16
SLE49	F	87	ANA, C3, C4,	MTX	6
SLE50	F	60	ANA, C4	Belimumab, MTX, HCQ, prednisolone	4
SLE51	F	62	ANA, anti-cardiolipinIgM	Belimumab, HCQ, AZA,	6
SLE52	F	59	C3, C4	MTX, HCQ	6
SLE53	F	57	ANA, anti-dsDNA	MTX, HCQ	10
SLE54	F	36	ANA, C3	Belimumab, MMF, HCQ, prednisolone	1
SLE55	M	16	ANA, anti-dsDNA, C3, C4 anti-SSA, anti-Sm, anti-RNP, άμεση coombs	Belimumab, AZA, HCQ	14
SLE56	F	52	ANA, anti-SSA	AZA, HCQ	10
SLE57	F	47	C3	AZA, HCQ, prednisolone	8
SLE58	F	51	ANA, C3, C4, anti-dsDNA, anti-cardiolipin IgM, antib2GPI IgM, LA	AZA, prednisolone	8
SLE59	F	65	ANA	AZA	12

F, female; M, male; ANA, anti-nuclear antibodies; anti-dsDNA, anti-double stranded(ds)DNA; anti-RNP, anti- ribonucleoprotein; anti-ENA, anti- extractable nuclear antigen antibodies; anti-β2GPI, anti-β2 glycoprotein I; HCQ, hydroxychloroquine; AZA, azathioprine; MTX, methotrexate; MMF, mycophenolate mofetil; CsA, cyclosporin A; SLEDAI-2K, SLE disease activity index-2000

Supplementary table 2

Accession	Description	Score	Coverage	# Proteins	# Uni
P02768	Serum albumin OS=Homo sapiens GN=ALB PE=1 SV=2 - [ALBU_HUMAN]	137,25	6,73	1	
P02788	Lactotransferrin OS=Homo sapiens GN=LTF PE=1 SV=6 - [TRFL_HUMAN]	130,20	47,61	1	
P05109	Protein S100-A8 OS=Homo sapiens GN=S100A8 PE=1 SV=1 - [S10A8_HUMAN]	105,49	41,94	1	
P62805	Histone H4 OS=Homo sapiens GN=HIST1H4A PE=1 SV=2 - [H4_HUMAN]	89,92	41,75	1	
P05164	Myeloperoxidase OS=Homo sapiens GN=MPO PE=1 SV=1 - [PERM_HUMAN]	89,89	38,79	2	
P60709	Actin, cytoplasmic 1 OS=Homo sapiens GN=ACTB PE=1 SV=1 - [ACTB_HUMAN]	83,45	52,53	10	
O60814	Histone H2B type 1-K OS=Homo sapiens GN=HIST1H2BK PE=1 SV=3 - [H2B1K_HUMAN]	75,48	26,98	10	
P06899	Histone H2B type 1-J OS=Homo sapiens GN=HIST1H2BJ PE=1 SV=3 - [H2B1J_HUMAN]	73,93	26,98	8	
P06702	Protein S100-A9 OS=Homo sapiens GN=S100A9 PE=1 SV=1 - [S10A9_HUMAN]	53,79	81,58	1	
P04406	Glyceraldehyde-3-phosphate dehydrogenase OS=Homo sapiens GN=GAPDH PE=1 SV=3 - [G3P_HUMAN]	48,43	47,46	1	
P13796	Plastin-2 OS=Homo sapiens GN=LCP1 PE=1 SV=6 - [PLSL_HUMAN]	44,85	25,04	3	
P0C0S5	Histone H2A.Z OS=Homo sapiens GN=H2AFZ PE=1 SV=2 - [H2AZ_HUMAN]	40,17	7,03	15	
P68871	Hemoglobin subunit beta OS=Homo sapiens GN=HBB PE=1 SV=2 - [HBB_HUMAN]	35,60	71,43	5	
P29401	Transketolase OS=Homo sapiens GN=TKT PE=1 SV=3 - [TKT_HUMAN]	34,97	22,31	1	
P08311	Cathepsin G OS=Homo sapiens GN=CTSG PE=1 SV=2 - [CATG_HUMAN]	31,30	31,76	1	
P68431	Histone H3.1 OS=Homo sapiens GN=HIST1H3A PE=1 SV=2 - [H31_HUMAN]	29,18	40,44	3	
P68032	Actin, alpha cardiac muscle 1 OS=Homo sapiens GN=ACTC1 PE=1 SV=1 - [ACTC_HUMAN]	28,57	25,73	7	
P69905	Hemoglobin subunit alpha OS=Homo sapiens GN=HBA1 PE=1 SV=2 - [HBA_HUMAN]	27,38	47,18	2	
P08246	Neutrophil elastase OS=Homo sapiens GN=ELANE PE=1 SV=1 - [ELNE_HUMAN]	27,07	30,71	1	
P12814	Alpha-actinin-1 OS=Homo sapiens GN=ACTN1 PE=1 SV=2 - [ACTN1_HUMAN]	27,06	11,21	4	
P04083	Annexin A1 OS=Homo sapiens GN=ANXA1 PE=1 SV=2 - [ANXA1_HUMAN]	25,70	27,17	1	
P12429	Annexin A3 OS=Homo sapiens GN=ANXA3 PE=1 SV=3 - [ANXA3_HUMAN]	24,62	27,55	1	
Q71DI3	Histone H3.2 OS=Homo sapiens GN=HIST2H3A PE=1 SV=3 - [H32_HUMAN]	22,48	40,44	3	
P04040	Catalase OS=Homo sapiens GN=CAT PE=1 SV=3 - [CATA_HUMAN]	21,84	16,70	1	
P84243	Histone H3.3 OS=Homo sapiens GN=H3F3A PE=1 SV=2 - [H33_HUMAN]	20,71	40,44	3	
P20160	Azurocidin OS=Homo sapiens GN=AZU1 PE=1 SV=3 - [CAP7_HUMAN]	19,64	20,32	1	
P35579	Myosin-9 OS=Homo sapiens GN=MYH9 PE=1 SV=4 - [MYH9_HUMAN]	19,50	4,34	4	
P06744	Glucose-6-phosphate isomerase OS=Homo sapiens GN=GPI PE=1 SV=4 - [G6PI_HUMAN]	18,37	16,31	1	
P00558	Phosphoglycerate kinase 1 OS=Homo sapiens GN=PGK1 PE=1 SV=3 - [PGK1_HUMAN]	17,76	11,27	1	
P30740	Leukocyte elastase inhibitor OS=Homo sapiens GN=SERPINB1 PE=1 SV=1 - [ILEU_HUMAN]	17,23	20,84	1	
P80188	Neutrophil gelatinase-associated lipocalin OS=Homo sapiens GN=LCN2 PE=1 SV=2 - [NGAL_HUMAN]	17,18	40,40	1	
P61626	Lysozyme C OS=Homo sapiens GN=LYZ PE=1 SV=1 - [LYSC_HUMAN]	15,90	35,81	1	
P14618	Pyruvate kinase PKM OS=Homo sapiens GN=PKM PE=1 SV=4 - [KPYM_HUMAN]	15,43	12,05	1	
P52209	6-phosphogluconate dehydrogenase, decarboxylating OS=Homo sapiens GN=PGD PE=1 SV=3 - [6PGD_HUMAN]	15,03	13,87	1	
P06396	Gelsolin OS=Homo sapiens GN=GSN PE=1 SV=1 - [GELS_HUMAN]	13,70	5,50	1	
P04075	Fructose-bisphosphate aldolase A OS=Homo sapiens GN=ALDOA PE=1 SV=2 - [ALDOA_HUMAN]	11,22	14,29	1	
P07737	Profilin-1 OS=Homo sapiens GN=PFN1 PE=1 SV=2 - [PROF1_HUMAN]	11,21	45,71	1	
P50395	Rab GDP dissociation inhibitor beta OS=Homo sapiens GN=GDI2 PE=1 SV=2 - [GDIB_HUMAN]	11,13	8,54	2	
P09211	Glutathione S-transferase P OS=Homo sapiens GN=GSTP1 PE=1 SV=2 - [GSTP1_HUMAN]	11,04	27,14	1	
P08670	Vimentin OS=Homo sapiens GN=VIM PE=1 SV=4 - [VIME_HUMAN]	10,27	10,73	1	
P41218	Myeloid cell nuclear differentiation antigen OS=Homo sapiens GN=MNDA PE=1 SV=1 - [MNDA_HUMAN]	10,26	11,79	1	
Q01518	Adenylyl cyclase-associated protein 1 OS=Homo sapiens GN=CAP1 PE=1 SV=5 - [CAP1_HUMAN]	9,54	9,89	1	

P63104	14-3-3 protein zeta/delta OS=Homo sapiens GN=YWHAZ PE=1 SV=1 - [1433Z_HUMAN]	9,43	21,63	6	
P80511	Protein S100-A12 OS=Homo sapiens GN=S100A12 PE=1 SV=2 - [S10AC_HUMAN]	9,06	19,57	1	
P12724	Eosinophil cationic protein OS=Homo sapiens GN=RNASE3 PE=1 SV=2 - [ECP_HUMAN]	8,56	22,50	1	
P00338	L-lactate dehydrogenase A chain OS=Homo sapiens GN=LDHA PE=1 SV=2 - [LDHA_HUMAN]	8,55	11,14	4	
P52790	Hexokinase-3 OS=Homo sapiens GN=HK3 PE=1 SV=2 - [HXK3_HUMAN]	8,41	2,06	1	
P31946	14-3-3 protein beta/alpha OS=Homo sapiens GN=YWHAB PE=1 SV=3 - [1433B_HUMAN]	8,02	8,94	6	
P59998	Actin-related protein 2/3 complex subunit 4 OS=Homo sapiens GN=ARPC4 PE=1 SV=3 - [ARPC4_HUMAN]	8,02	11,31	1	
P06733	Alpha-enolase OS=Homo sapiens GN=ENO1 PE=1 SV=2 - [ENOA_HUMAN]	7,34	7,37	2	
P24158	Myeloblastin OS=Homo sapiens GN=PRTN3 PE=1 SV=3 - [PRTN3_HUMAN]	7,13	11,33	1	
O75594	Peptidoglycan recognition protein 1 OS=Homo sapiens GN=PGLYRP1 PE=1 SV=1 - [PGRP1_HUMAN]	6,93	15,82	1	
P61158	Actin-related protein 3 OS=Homo sapiens GN=ACTR3 PE=1 SV=3 - [ARP3_HUMAN]	6,01	5,50	3	
P60660	Myosin light polypeptide 6 OS=Homo sapiens GN=MYL6 PE=1 SV=2 - [MYL6_HUMAN]	5,93	19,21	2	
P49913	Cathelicidin antimicrobial peptide OS=Homo sapiens GN=CAMP PE=1 SV=1 - [CAMP_HUMAN]	5,43	7,65	1	
Q00610	Clathrin heavy chain 1 OS=Homo sapiens GN=CLTC PE=1 SV=5 - [CLH1_HUMAN]	5,18	1,25	2	
P08758	Annexin A5 OS=Homo sapiens GN=ANXA5 PE=1 SV=2 - [ANXA5_HUMAN]	5,15	5,00	1	
P15259	Phosphoglycerate mutase 2 OS=Homo sapiens GN=PGAM2 PE=1 SV=3 - [PGAM2_HUMAN]	5,03	9,88	3	
P04264	Keratin, type II cytoskeletal 1 OS=Homo sapiens GN=KRT1 PE=1 SV=6 - [K2C1_HUMAN]	4,98	3,42	8	
P01023	Alpha-2-macroglobulin OS=Homo sapiens GN=A2M PE=1 SV=3 - [A2MG_HUMAN]	4,78	2,92	1	
P0DMV9	Heat shock 70 kDa protein 1B OS=Homo sapiens GN=HSPA1B PE=1 SV=1 - [HS71B_HUMAN]	4,75	3,12	7	
P08133	Annexin A6 OS=Homo sapiens GN=ANXA6 PE=1 SV=3 - [ANXA6_HUMAN]	4,33	2,97	1	
P11413	Glucose-6-phosphate 1-dehydrogenase OS=Homo sapiens GN=G6PD PE=1 SV=4 - [G6PD_HUMAN]	4,28	4,47	1	
P28676	Grancalcin OS=Homo sapiens GN=GCA PE=1 SV=2 - [GRAN_HUMAN]	4,09	12,90	1	
P60174	Triosephosphate isomerase OS=Homo sapiens GN=TPI1 PE=1 SV=3 - [TPIS_HUMAN]	3,86	4,20	1	
P31146	Coronin-1A OS=Homo sapiens GN=CORO1A PE=1 SV=4 - [COR1A_HUMAN]	3,71	3,47	1	
P02765	Alpha-2-HS-glycoprotein OS=Homo sapiens GN=AHSG PE=1 SV=1 - [FETUA_HUMAN]	3,64	3,27	1	
Q9Y536	Peptidyl-prolyl cis-trans isomerase A-like 4A OS=Homo sapiens GN=PPIAL4A PE=2 SV=1 - [PAL4A_HUMAN]	3,42	8,54	2	
Q8WVE0	EEF1A lysine methyltransferase 1 OS=Homo sapiens GN=EEF1AKMT1 PE=1 SV=1 - [EFMT1_HUMAN]	3,33	5,61	1	
P05089	Arginase-1 OS=Homo sapiens GN=ARG1 PE=1 SV=2 - [ARGI1_HUMAN]	3,32	3,73	1	
P25815	Protein S100-P OS=Homo sapiens GN=S100P PE=1 SV=2 - [S100P_HUMAN]	3,31	13,68	1	
P22894	Neutrophil collagenase OS=Homo sapiens GN=MMP8 PE=1 SV=1 - [MMP8_HUMAN]	3,25	3,85	1	
P23528	Cofilin-1 OS=Homo sapiens GN=CFL1 PE=1 SV=3 - [COF1_HUMAN]	3,20	10,24	2	1
P37837	Transaldolase OS=Homo sapiens GN=TALDO1 PE=1 SV=2 - [TALDO_HUMAN]	3,07	3,86	1	1
O15511	Actin-related protein 2/3 complex subunit 5 OS=Homo sapiens GN=ARPC5 PE=1 SV=3 - [ARPC5_HUMAN]	2,86	7,95	1	1
P31949	Protein S100-A11 OS=Homo sapiens GN=S100A11 PE=1 SV=2 - [S10AB_HUMAN]	2,85	15,24	1	1
P59665	Neutrophil defensin 1 OS=Homo sapiens GN=DEFA1 PE=1 SV=1 - [DEF1_HUMAN]	2,77	9,57	2	1
P46976	Glycogenin-1 OS=Homo sapiens GN=GYG1 PE=1 SV=4 - [GLYG_HUMAN]	2,57	2,86	1	1
O15143	Actin-related protein 2/3 complex subunit 1B OS=Homo sapiens GN=ARPC1B PE=1 SV=3 - [ARC1B_HUMAN]	2,52	2,69	1	1
P20742	Pregnancy zone protein OS=Homo sapiens GN=PZP PE=1 SV=4 - [PZP_HUMAN]	2,31	2,29	1	1
P00491	Purine nucleoside phosphorylase OS=Homo sapiens GN=PNP PE=1 SV=2 - [PNPH_HUMAN]	2,29	3,46	1	1
P14780	Matrix metalloproteinase-9 OS=Homo sapiens GN=MMP9 PE=1 SV=3 - [MMP9_HUMAN]	2,21	2,55	1	2
O75367	Core histone macro-H2A.1 OS=Homo sapiens GN=H2AFY PE=1 SV=4 - [H2AY_HUMAN]	2,20	2,42	2	1
P26038	Moesin OS=Homo sapiens GN=MSN PE=1 SV=3 - [MOES_HUMAN]	2,16	1,56	3	1
P52566	Rho GDP-dissociation inhibitor 2 OS=Homo sapiens GN=ARHGDIB PE=1 SV=3 - [GDIR2_HUMAN]	2,14	12,94	1	1
P06703	Protein S100-A6 OS=Homo sapiens GN=S100A6 PE=1 SV=1 - [S10A6_HUMAN]	2,04	8,89	1	1
P11217	Glycogen phosphorylase, muscle form OS=Homo sapiens GN=PYGM PE=1 SV=6 - [PYGM_HUMAN]	2,02	0,95	3	1
P01008	Antithrombin-III OS=Homo sapiens GN=SERPINC1 PE=1 SV=1 - [ANT3_HUMAN]	1,86	3,45	1	2
O75131	Copine-3 OS=Homo sapiens GN=CPNE3 PE=1 SV=1 - [CPNE3_HUMAN]	1,78	1,68	8	1
Q8NG11	Tetraspanin-14 OS=Homo sapiens GN=TSPAN14 PE=1 SV=1 - [TSN14_HUMAN]	1,77	2,96	1	1
P05543	Thyroxine-binding globulin OS=Homo sapiens GN=SERPINA7 PE=1 SV=2 - [THBG_HUMAN]	1,75	2,41	1	1
P01024	Complement C3 OS=Homo sapiens GN=C3 PE=1 SV=2 - [CO3_HUMAN]	1,71	0,42	1	1
Q9P225	Dynein heavy chain 2, axonemal OS=Homo sapiens GN=DNAH2 PE=2 SV=3 - [DYH2_HUMAN]	1,63	0,20	1	1
Q6ZRS2	Helicase SRCAP OS=Homo sapiens GN=SRCAP PE=1 SV=3 - [SRCAP_HUMAN]	1,62	0,25	1	1
Q9UKU7	Isobutyryl-CoA dehydrogenase, mitochondrial OS=Homo sapiens GN=ACAD8 PE=1 SV=1 - [ACAD8_HUMAN]	0,00	2,17	1	1
Q92667	A-kinase anchor protein 1, mitochondrial OS=Homo sapiens GN=AKAP1 PE=1 SV=1 - [AKAP1_HUMAN]	0,00	1,00	1	1
Q86WK7	Amphoterin-induced protein 3 OS=Homo sapiens GN=AMIGO3 PE=2 SV=1 - [AMGO3_HUMAN]	0,00	2,38	1	1
A6NKF2	AT-rich interactive domain-containing protein 3C OS=Homo sapiens GN=ARID3C PE=3 SV=1 - [ARI3C_HUMAN]	0,00	1,46	1	1
Q2TB18	Protein asteroid homolog 1 OS=Homo sapiens GN=ASTE1 PE=1 SV=1 - [ASTE1_HUMAN]	0,00	1,33	1	1

P51861	Cerebellar degeneration-related antigen 1 OS=Homo sapiens GN=CDR1 PE=1 SV=2 - [CDR1_HUMAN]	0,00	2,67	1	1
P29973	cGMP-gated cation channel alpha-1 OS=Homo sapiens GN=CNGA1 PE=1 SV=3 - [CNGA1_HUMAN]	0,00	3,33	1	1
P12109	Collagen alpha-1(VI) chain OS=Homo sapiens GN=COL6A1 PE=1 SV=3 - [CO6A1_HUMAN]	0,00	2,33	1	1
A2RUB1	Meiosis-specific coiled-coil domain-containing protein MEIOC OS=Homo sapiens GN=MEIOC PE=2 SV=3 - [MEIOC_HUMAN]	0,00	1,89	1	1
P02771	Alpha-fetoprotein OS=Homo sapiens GN=AFP PE=1 SV=1 - [FETA_HUMAN]	0,00	1,64	1	1
P11488	Guanine nucleotide-binding protein G(t) subunit alpha-1 OS=Homo sapiens GN=GNAT1 PE=1 SV=5 - [GNAT1_HUMAN]	0,00	3,14	12	1
A7E2F4	Golgin subfamily A member 8A OS=Homo sapiens GN=GOLGA8A PE=2 SV=3 - [GOG8A_HUMAN]	0,00	1,74	1	1
Q8N8K9	Uncharacterized protein KIAA1958 OS=Homo sapiens GN=KIAA1958 PE=1 SV=1 - [K1958_HUMAN]	0,00	0,98	1	1
Q05315	Galectin-10 OS=Homo sapiens GN=CLC PE=1 SV=3 - [LEG10_HUMAN]	0,00	9,15	1	2
P11226	Mannose-binding protein C OS=Homo sapiens GN=MBL2 PE=1 SV=2 - [MBL2_HUMAN]	0,00	5,24	1	1
Q9NRN9	Methyltransferase-like protein 5 OS=Homo sapiens GN=METTL5 PE=1 SV=1 - [METL5_HUMAN]	0,00	4,78	1	
Q9UJH8	Meteorin OS=Homo sapiens GN=METRN PE=2 SV=2 - [METRN_HUMAN]	0,00	4,78	1	
Q13459	Unconventional myosin-IXb OS=Homo sapiens GN=MYO9B PE=1 SV=3 - [MYO9B_HUMAN]	0,00	0,60	1	
E9PQ53	NADH dehydrogenase [ubiquinone] 1 subunit C2, isoform 2 OS=Homo sapiens GN=NDUFC2-KCTD14 PE=1 SV=1 - [NDUCR	0,00	5,26	2	
O15460	Prolyl 4-hydroxylase subunit alpha-2 OS=Homo sapiens GN=P4HA2 PE=1 SV=1 - [P4HA2_HUMAN]	0,00	2,24	1	
Q9Y5I2	Protocadherin alpha-10 OS=Homo sapiens GN=PCDHA10 PE=2 SV=1 - [PCDAA_HUMAN]	0,00	1,58	2	
Q9H6A9	Pecanex-like protein 3 OS=Homo sapiens GN=PCNX3 PE=1 SV=2 - [PCX3_HUMAN]	0,00	1,08	1	
P07237	Protein disulfide-isomerase OS=Homo sapiens GN=P4HB PE=1 SV=3 - [PDIA1_HUMAN]	0,00	1,57	1	
P35354	Prostaglandin G/H synthase 2 OS=Homo sapiens GN=PTGS2 PE=1 SV=2 - [PGH2_HUMAN]	0,00	2,98	1	
Q5H9R7	Serine/threonine-protein phosphatase 6 regulatory subunit 3 OS=Homo sapiens GN=PPP6R3 PE=1 SV=2 - [PP6R3_HUMAN	0,00	1,49	2	
Q96EY7	Pentatricopeptide repeat domain-containing protein 3, mitochondrial OS=Homo sapiens GN=PTCD3 PE=1 SV=3 - [PTCD3_	0,00	1,45	1	
Q14679	Tubulin polyglutamylase TTLL4 OS=Homo sapiens GN=TTLL4 PE=1 SV=2 - [TTLL4_HUMAN]	0,00	0,50	1	
O95155	Ubiquitin conjugation factor E4 B OS=Homo sapiens GN=UBE4B PE=1 SV=1 - [UBE4B_HUMAN]	0,00	0,69	1	
P25311	Zinc-alpha-2-glycoprotein OS=Homo sapiens GN=AZGP1 PE=1 SV=2 - [ZA2G_HUMAN]	0,00	4,03	1	
P52747	Zinc finger protein 143 OS=Homo sapiens GN=ZNF143 PE=1 SV=2 - [ZN143_HUMAN]	0,00	2,66	1	
Q8WTR7	Zinc finger protein 473 OS=Homo sapiens GN=ZNF473 PE=1 SV=1 - [ZN473_HUMAN]	0,00	2,18	1	

Supplemental table 3

Accession	Description	Score	Coverage	# Proteins
P02768	Serum albumin OS=Homo sapiens GN=ALB PE=1 SV=2 - [ALBU_HUMAN]	229,65	8,21	1
P02788	Lactotransferrin OS=Homo sapiens GN=LTF PE=1 SV=6 - [TRFL_HUMAN]	91,67	40,14	1
P60709	Actin, cytoplasmic 1 OS=Homo sapiens GN=ACTB PE=1 SV=1 - [ACTB_HUMAN]	64,95	48,53	8
P68871	Hemoglobin subunit beta OS=Homo sapiens GN=HBB PE=1 SV=2 - [HBB_HUMAN]	34,50	71,43	4
P06702	Protein S100-A9 OS=Homo sapiens GN=S100A9 PE=1 SV=1 - [S10A9_HUMAN]	34,36	67,54	1
P69905	Hemoglobin subunit alpha OS=Homo sapiens GN=HBA1 PE=1 SV=2 - [HBA_HUMAN]	31,96	49,30	1
P04406	Glyceraldehyde-3-phosphate dehydrogenase OS=Homo sapiens GN=GAPDH PE=1 SV=3 - [G3P_HUMAN]	29,40	36,72	2
P05164	Myeloperoxidase OS=Homo sapiens GN=MPO PE=1 SV=1 - [PERM_HUMAN]	23,65	11,54	1
P63267	Actin, gamma-enteric smooth muscle OS=Homo sapiens GN=ACTG2 PE=1 SV=1 - [ACTH_HUMAN]	20,77	21,81	5
P02042	Hemoglobin subunit delta OS=Homo sapiens GN=HBD PE=1 SV=2 - [HBD_HUMAN]	20,29	41,50	4
P04264	Keratin, type II cytoskeletal 1 OS=Homo sapiens GN=KRT1 PE=1 SV=6 - [K2C1_HUMAN]	19,65	12,89	12
P08246	Neutrophil elastase OS=Homo sapiens GN=ELANE PE=1 SV=1 - [ELNE_HUMAN]	17,53	22,85	1
P62805	Histone H4 OS=Homo sapiens GN=HIST1H4A PE=1 SV=2 - [H4_HUMAN]	16,58	40,78	1
P05109	Protein S100-A8 OS=Homo sapiens GN=S100A8 PE=1 SV=1 - [S10A8_HUMAN]	15,76	24,73	1
P13796	Plastin-2 OS=Homo sapiens GN=LCP1 PE=1 SV=6 - [PLSL_HUMAN]	14,40	8,61	3
P01023	Alpha-2-macroglobulin OS=Homo sapiens GN=A2M PE=1 SV=3 - [A2MG_HUMAN]	12,74	3,46	1
P68431	Histone H3.1 OS=Homo sapiens GN=HIST1H3A PE=1 SV=2 - [H31_HUMAN]	12,14	35,29	4
P06744	Glucose-6-phosphate isomerase OS=Homo sapiens GN=GPI PE=1 SV=4 - [G6PI_HUMAN]	11,76	5,73	1
P14780	Matrix metalloproteinase-9 OS=Homo sapiens GN=MMP9 PE=1 SV=3 - [MMP9_HUMAN]	11,57	7,07	1
P80188	Neutrophil gelatinase-associated lipocalin OS=Homo sapiens GN=LCN2 PE=1 SV=2 - [NGAL_HUMAN]	9,62	23,74	1
P06396	Gelsolin OS=Homo sapiens GN=GSN PE=1 SV=1 - [GELS_HUMAN]	9,49	3,58	1
P31946	14-3-3 protein beta/alpha OS=Homo sapiens GN=YWHAB PE=1 SV=3 - [1433B_HUMAN]	8,85	9,76	6
O60814	Histone H2B type 1-K OS=Homo sapiens GN=HIST1H2BK PE=1 SV=3 - [H2B1K_HUMAN]	8,75	19,05	14

Q71DI3	Histone H3.2 OS=Homo sapiens GN=HIST2H3A PE=1 SV=3 - [H32_HUMAN]	8,54	35,29	4	
P01024	Complement C3 OS=Homo sapiens GN=C3 PE=1 SV=2 - [CO3_HUMAN]	7,40	1,32	1	
P20742	Pregnancy zone protein OS=Homo sapiens GN=PZP PE=1 SV=4 - [PZP_HUMAN]	6,80	2,29	1	
P13645	Keratin, type I cytoskeletal 10 OS=Homo sapiens GN=KRT10 PE=1 SV=6 - [K1C10_HUMAN]	6,35	3,94	1	
P12814	Alpha-actinin-1 OS=Homo sapiens GN=ACTN1 PE=1 SV=2 - [ACTN1_HUMAN]	6,26	4,15	3	
P00558	Phosphoglycerate kinase 1 OS=Homo sapiens GN=PGK1 PE=1 SV=3 - [PGK1_HUMAN]	6,16	8,15	1	
P35527	Keratin, type I cytoskeletal 9 OS=Homo sapiens GN=KRT9 PE=1 SV=3 - [K1C9_HUMAN]	6,10	3,69	1	
P14618	Pyruvate kinase PKM OS=Homo sapiens GN=PKM PE=1 SV=4 - [KPYM_HUMAN]	6,10	4,52	1	
P04083	Annexin A1 OS=Homo sapiens GN=ANXA1 PE=1 SV=2 - [ANXA1_HUMAN]	6,04	8,96	1	
P49913	Cathelicidin antimicrobial peptide OS=Homo sapiens GN=CAMP PE=1 SV=1 - [CAMP_HUMAN]	5,92	12,94	1	
P29401	Transketolase OS=Homo sapiens GN=TKT PE=1 SV=3 - [TKT_HUMAN]	5,80	3,85	1	
P19823	Inter-alpha-trypsin inhibitor heavy chain H2 OS=Homo sapiens GN=ITIH2 PE=1 SV=2 - [ITIH2_HUMAN]	5,66	1,90	1	
P00338	L-lactate dehydrogenase A chain OS=Homo sapiens GN=LDHA PE=1 SV=2 - [LDHA_HUMAN]	5,36	9,34	4	3
P08311	Cathepsin G OS=Homo sapiens GN=CTSG PE=1 SV=2 - [CATG_HUMAN]	5,15	8,63	1	2
P06733	Alpha-enolase OS=Homo sapiens GN=ENO1 PE=1 SV=2 - [ENOA_HUMAN]	5,10	6,68	1	2
P24158	Myeloblastin OS=Homo sapiens GN=PRTN3 PE=1 SV=3 - [PRTN3_HUMAN]	5,04	8,20	1	2
Q96KK5	Histone H2A type 1-H OS=Homo sapiens GN=HIST1H2AH PE=1 SV=3 - [H2A1H_HUMAN]	4,78	21,88	15	2
P22894	Neutrophil collagenase OS=Homo sapiens GN=MMP8 PE=1 SV=1 - [MMP8_HUMAN]	4,57	3,43	1	1
P63104	14-3-3 protein zeta/delta OS=Homo sapiens GN=YWHAZ PE=1 SV=1 - [1433Z_HUMAN]	4,50	8,98	6	1
P20160	Azurocidin OS=Homo sapiens GN=AZU1 PE=1 SV=3 - [CAP7_HUMAN]	3,66	5,18	1	1
Q8WVE0	EEF1A lysine methyltransferase 1 OS=Homo sapiens GN=EEF1AKMT1 PE=1 SV=1 - [EFMT1_HUMAN]	3,32	5,61	1	1
O75594	Peptidoglycan recognition protein 1 OS=Homo sapiens GN=PGLYRP1 PE=1 SV=1 - [PGRP1_HUMAN]	3,27	7,65	1	1
P02765	Alpha-2-HS-glycoprotein OS=Homo sapiens GN=AHSG PE=1 SV=1 - [FETUA_HUMAN]	3,25	3,27	1	1
P02647	Apolipoprotein A-I OS=Homo sapiens GN=APOA1 PE=1 SV=1 - [APOA1_HUMAN]	3,09	5,99	1	1
P35579	Myosin-9 OS=Homo sapiens GN=MYH9 PE=1 SV=4 - [MYH9_HUMAN]	2,88	0,77	2	1
P02771	Alpha-fetoprotein OS=Homo sapiens GN=AFP PE=1 SV=1 - [FETA_HUMAN]	2,84	2,63	1	1
P37837	Transaldolase OS=Homo sapiens GN=TALDO1 PE=1 SV=2 - [TALDO_HUMAN]	2,75	3,86	1	1
Q9C0K3	Actin-related protein 3C OS=Homo sapiens GN=ACTR3C PE=2 SV=1 - [ARP3C_HUMAN]	2,72	5,24	3	1
P59665	Neutrophil defensin 1 OS=Homo sapiens GN=DEFA1 PE=1 SV=1 - [DEF1_HUMAN]	2,49	9,57	2	1
Q01518	Adenylyl cyclase-associated protein 1 OS=Homo sapiens GN=CAP1 PE=1 SV=5 - [CAP1_HUMAN]	2,48	2,74	1	1
P26038	Moesin OS=Homo sapiens GN=MSN PE=1 SV=3 - [MOES_HUMAN]	2,45	2,08	3	1
P07737	Profilin-1 OS=Homo sapiens GN=PFN1 PE=1 SV=2 - [PROF1_HUMAN]	2,45	17,14	1	2
P30740	Leukocyte elastase inhibitor OS=Homo sapiens GN=SERPINB1 PE=1 SV=1 - [ILEU_HUMAN]	2,10	2,64	1	1
P02774	Vitamin D-binding protein OS=Homo sapiens GN=GC PE=1 SV=1 - [VTDB_HUMAN]	1,98	1,69	1	1
Q9Y6V0	Protein piccolo OS=Homo sapiens GN=PCLO PE=1 SV=4 - [PCLO_HUMAN]	1,75	0,18	1	1
P59998	Actin-related protein 2/3 complex subunit 4 OS=Homo sapiens GN=ARPC4 PE=1 SV=3 - [ARPC4_HUMAN]	1,70	4,76	1	1
Q6UWY0	Arylsulfatase K OS=Homo sapiens GN=ARSK PE=1 SV=1 - [ARSK_HUMAN]	1,61	1,31	1	1
Q8NG11	Tetraspanin-14 OS=Homo sapiens GN=TSPAN14 PE=1 SV=1 - [TSN14_HUMAN]	1,27	2,96	1	1
P01008	Antithrombin-III OS=Homo sapiens GN=SERPINC1 PE=1 SV=1 - [ANT3_HUMAN]	0,00	3,88	1	2
Q9BXJ4	Complement C1q tumor necrosis factor-related protein 3 OS=Homo sapiens GN=C1QTNF3 PE=1 SV=1 - [C1QT3_HUMAN]	0,00	7,72	1	1
P51861	Cerebellar degeneration-related antigen 1 OS=Homo sapiens GN=CDR1 PE=1 SV=2 - [CDR1_HUMAN]	0,00	2,67	1	1
Q9Y6F8	Testis-specific chromodomain protein Y 1 OS=Homo sapiens GN=CDY1 PE=1 SV=1 - [CDY1_HUMAN]	0,00	1,11	2	1
P31146	Coronin-1A OS=Homo sapiens GN=CORO1A PE=1 SV=4 - [COR1A_HUMAN]	0,00	2,17	1	1
Q9P225	Dynein heavy chain 2, axonemal OS=Homo sapiens GN=DNAH2 PE=2 SV=3 - [DYH2_HUMAN]	0,00	0,50	1	1
A0FGR9	Extended synaptotagmin-3 OS=Homo sapiens GN=ESYT3 PE=1 SV=1 - [ESYT3_HUMAN]	0,00	0,79	1	1
Q9Y4F4	TOG array regulator of axonemal microtubules protein 1 OS=Homo sapiens GN=TOGARAM1 PE=1 SV=4 - [TGRM1_HUMAN]	0,00	0,52	1	1
Q01415	N-acetylgalactosamine kinase OS=Homo sapiens GN=GALK2 PE=1 SV=1 - [GALK2_HUMAN]	0,00	2,62	1	1
P80217	Interferon-induced 35 kDa protein OS=Homo sapiens GN=IFI35 PE=1 SV=5 - [IN35_HUMAN]	0,00	12,59	1	1
Q6ZN16	Mitogen-activated protein kinase kinase kinase 15 OS=Homo sapiens GN=MAP3K15 PE=1 SV=2 - [M3K15_HUMAN]	0,00	0,61	1	1
P43246	DNA mismatch repair protein Msh2 OS=Homo sapiens GN=MSH2 PE=1 SV=1 - [MSH2_HUMAN]	0,00	4,39	1	
Q7RTR0	NACHT, LRR and PYD domains-containing protein 9 OS=Homo sapiens GN=NLRP9 PE=1 SV=1 - [NLRP9_HUMAN]	0,00	1,21	1	
P37198	Nuclear pore glycoprotein p62 OS=Homo sapiens GN=NUP62 PE=1 SV=3 - [NUP62_HUMAN]	0,00	1,34	1	
Q149M9	NACHT domain- and WD repeat-containing protein 1 OS=Homo sapiens GN=NWD1 PE=1 SV=3 - [NWD1_HUMAN]	0,00	0,51	1	
Q96D21	GTP-binding protein Rhes OS=Homo sapiens GN=RASD2 PE=1 SV=1 - [RHES_HUMAN]	0,00	4,89	1	
Q9UGH3	Solute carrier family 23 member 2 OS=Homo sapiens GN=SLC23A2 PE=1 SV=1 - [S23A2_HUMAN]	0,00	4,15	1	
Q9UQD0	Sodium channel protein type 8 subunit alpha OS=Homo sapiens GN=SCN8A PE=1 SV=1 - [SCN8A_HUMAN]	0,00	0,61	1	
Q5SQN1	Synaptosomal-associated protein 47 OS=Homo sapiens GN=SNAP47 PE=1 SV=3 - [SNP47_HUMAN]	0,00	2,80	1	

Q8NBK3	Sulfatase-modifying factor 1 OS=Homo sapiens GN=SUMF1 PE=1 SV=3 - [SUMF1_HUMAN]	0,00	1,60	1	
Q9NZQ8	Transient receptor potential cation channel subfamily M member 5 OS=Homo sapiens GN=TRPM5 PE=2 SV=1 - [TRPM5_HUMAN]	0,00	0,60	1	
Q9BS34	Zinc finger protein 670 OS=Homo sapiens GN=ZNF670 PE=1 SV=1 - [ZN670_HUMAN]	0,00	3,08	1	

Supplementary table 4

Accession	Description	Score	Coverage	# Proteins
P02768	Serum albumin OS=Homo sapiens GN=ALB PE=1 SV=2 - [ALBU_HUMAN]	492,96	77,83	1
P0DOX5	Immunoglobulin gamma-1 heavy chain OS=Homo sapiens PE=1 SV=1 - [IGG1_HUMAN]	284,57	48,11	2
P01860	Immunoglobulin heavy constant gamma 3 OS=Homo sapiens GN=IGHG3 PE=1 SV=2 - [IGHG3_HUMAN]	135,50	50,93	1
P01859	Immunoglobulin heavy constant gamma 2 OS=Homo sapiens GN=IGHG2 PE=1 SV=2 - [IGHG2_HUMAN]	117,46	49,39	1
P01834	Immunoglobulin kappa constant OS=Homo sapiens GN=IGKC PE=1 SV=2 - [IGKC_HUMAN]	99,81	82,24	1
P0DOX7	Immunoglobulin kappa light chain OS=Homo sapiens PE=1 SV=1 - [IGK_HUMAN]	81,98	45,79	2
P60709	Actin, cytoplasmic 1 OS=Homo sapiens GN=ACTB PE=1 SV=1 - [ACTB_HUMAN]	57,24	50,40	8
P01861	Immunoglobulin heavy constant gamma 4 OS=Homo sapiens GN=IGHG4 PE=1 SV=1 - [IGHG4_HUMAN]	50,23	50,15	1
P02788	Lactotransferrin OS=Homo sapiens GN=LTF PE=1 SV=6 - [TRFL_HUMAN]	48,55	22,25	1
P06702	Protein S100-A9 OS=Homo sapiens GN=S100A9 PE=1 SV=1 - [S10A9_HUMAN]	41,06	67,54	1
P68871	Hemoglobin subunit beta OS=Homo sapiens GN=HBB PE=1 SV=2 - [HBB_HUMAN]	32,02	77,55	4
P0DOY2	Immunoglobulin lambda constant 2 OS=Homo sapiens GN=IGLC2 PE=1 SV=1 - [IGLC2_HUMAN]	25,50	74,53	4
P0CG04	Immunoglobulin lambda constant 1 OS=Homo sapiens GN=IGLC1 PE=1 SV=1 - [IGLC1_HUMAN]	22,63	65,09	3
P02042	Hemoglobin subunit delta OS=Homo sapiens GN=HBD PE=1 SV=2 - [HBD_HUMAN]	18,77	41,50	4
P68032	Actin, alpha cardiac muscle 1 OS=Homo sapiens GN=ACTC1 PE=1 SV=1 - [ACTC_HUMAN]	18,21	23,87	5
P04406	Glyceraldehyde-3-phosphate dehydrogenase OS=Homo sapiens GN=GAPDH PE=1 SV=3 - [G3P_HUMAN]	15,50	21,79	1
P00738	Haptoglobin OS=Homo sapiens GN=HP PE=1 SV=1 - [HPT_HUMAN]	13,83	15,27	2
P62805	Histone H4 OS=Homo sapiens GN=HIST1H4A PE=1 SV=2 - [H4_HUMAN]	13,50	40,78	1
P05109	Protein S100-A8 OS=Homo sapiens GN=S100A8 PE=1 SV=1 - [S10A8_HUMAN]	12,58	47,31	1
P69905	Hemoglobin subunit alpha OS=Homo sapiens GN=HBA1 PE=1 SV=2 - [HBA_HUMAN]	12,37	49,30	1
P13796	Plastin-2 OS=Homo sapiens GN=LCP1 PE=1 SV=6 - [PLSL_HUMAN]	9,63	9,89	3
P01717	Immunoglobulin lambda variable 3-25 OS=Homo sapiens GN=IGLV3-25 PE=1 SV=2 - [LV325_HUMAN]	8,24	18,75	4
P01599	Immunoglobulin kappa variable 1-17 OS=Homo sapiens GN=IGKV1-17 PE=1 SV=2 - [KV117_HUMAN]	7,92	13,68	1
O60814	Histone H2B type 1-K OS=Homo sapiens GN=HIST1H2BK PE=1 SV=3 - [H2B1K_HUMAN]	7,84	19,05	15
P01782	Immunoglobulin heavy variable 3-9 OS=Homo sapiens GN=IGHV3-9 PE=1 SV=2 - [HV309_HUMAN]	7,79	25,42	5
P05164	Myeloperoxidase OS=Homo sapiens GN=MPO PE=1 SV=1 - [PERM_HUMAN]	7,78	5,64	2
P04075	Fructose-bisphosphate aldolase A OS=Homo sapiens GN=ALDOA PE=1 SV=2 - [ALDOA_HUMAN]	7,61	8,79	1
P01619	Immunoglobulin kappa variable 3-20 OS=Homo sapiens GN=IGKV3-20 PE=1 SV=2 - [KV320_HUMAN]	7,27	21,55	1
A0A0C4DH25	Immunoglobulin kappa variable 3D-20 OS=Homo sapiens GN=IGKV3D-20 PE=3 SV=1 - [KVD20_HUMAN]	7,16	21,55	1
P06744	Glucose-6-phosphate isomerase OS=Homo sapiens GN=GPI PE=1 SV=4 - [G6PI_HUMAN]	6,98	5,73	1
A0A0C4DH42	Immunoglobulin heavy variable 3-66 OS=Homo sapiens GN=IGHV3-66 PE=3 SV=1 - [HV366_HUMAN]	6,81	18,97	9
P68104	Elongation factor 1-alpha 1 OS=Homo sapiens GN=EEF1A1 PE=1 SV=1 - [EF1A1_HUMAN]	6,23	8,66	3
P00338	L-lactate dehydrogenase A chain OS=Homo sapiens GN=LDHA PE=1 SV=2 - [LDHA_HUMAN]	5,93	6,63	4
P12814	Alpha-actinin-1 OS=Homo sapiens GN=ACTN1 PE=1 SV=2 - [ACTN1_HUMAN]	5,42	2,47	2
P08238	Heat shock protein HSP 90-beta OS=Homo sapiens GN=HSP90AB1 PE=1 SV=4 - [HS90B_HUMAN]	4,64	2,62	3
A0A075B6K5	Immunoglobulin lambda variable 3-9 OS=Homo sapiens GN=IGLV3-9 PE=3 SV=1 - [LV39_HUMAN]	4,62	13,91	2
P08246	Neutrophil elastase OS=Homo sapiens GN=ELANE PE=1 SV=1 - [ELNE_HUMAN]	4,58	3,75	1
A0A0C4DH72	Immunoglobulin kappa variable 1-6 OS=Homo sapiens GN=IGKV1-6 PE=3 SV=1 - [KV106_HUMAN]	4,35	13,68	4
P01871	Immunoglobulin heavy constant mu OS=Homo sapiens GN=IGHM PE=1 SV=4 - [IGHM_HUMAN]	4,01	6,84	2
P01593	Immunoglobulin kappa variable 1D-33 OS=Homo sapiens GN=IGKV1D-33 PE=1 SV=2 - [KVD33_HUMAN]	3,86	13,68	1
A0A0C4DH67	Immunoglobulin kappa variable 1-8 OS=Homo sapiens GN=IGKV1-8 PE=3 SV=1 - [KV108_HUMAN]	3,59	13,91	3
P02765	Alpha-2-HS-glycoprotein OS=Homo sapiens GN=AHSG PE=1 SV=1 - [FETUA_HUMAN]	3,56	3,27	1
P01700	Immunoglobulin lambda variable 1-47 OS=Homo sapiens GN=IGLV1-47 PE=1 SV=2 - [LV147_HUMAN]	3,54	11,11	1
P80188	Neutrophil gelatinase-associated lipocalin OS=Homo sapiens GN=LCN2 PE=1 SV=2 - [NGAL_HUMAN]	3,50	7,58	1

P14780	Matrix metalloproteinase-9 OS=Homo sapiens GN=MMP9 PE=1 SV=3 - [MMP9_HUMAN]	3,07	2,12	1
Q16513	Serine/threonine-protein kinase N2 OS=Homo sapiens GN=PKN2 PE=1 SV=1 - [PKN2_HUMAN]	2,96	2,95	1
P07900	Heat shock protein HSP 90-alpha OS=Homo sapiens GN=HSP90AA1 PE=1 SV=5 - [HS90A_HUMAN]	2,94	2,60	4
P02647	Apolipoprotein A-I OS=Homo sapiens GN=APOA1 PE=1 SV=1 - [APOA1_HUMAN]	2,84	5,99	1
P06312	Immunoglobulin kappa variable 4-1 OS=Homo sapiens GN=IGKV4-1 PE=1 SV=1 - [KV401_HUMAN]	2,68	7,44	1
A0A0A0MRZ8	Immunoglobulin kappa variable 3D-11 OS=Homo sapiens GN=IGKV3D-11 PE=3 SV=6 - [KVD11_HUMAN]	2,65	7,83	2
A0A075B6P5	Immunoglobulin kappa variable 2-28 OS=Homo sapiens GN=IGKV2-28 PE=3 SV=1 - [KV228_HUMAN]	2,59	10,83	7
P60174	Triosephosphate isomerase OS=Homo sapiens GN=TPI1 PE=1 SV=3 - [TPIS_HUMAN]	2,57	5,24	1
P04264	Keratin, type II cytoskeletal 1 OS=Homo sapiens GN=KRT1 PE=1 SV=6 - [K2C1_HUMAN]	2,56	1,86	1
P48741	Putative heat shock 70 kDa protein 7 OS=Homo sapiens GN=HSPA7 PE=5 SV=2 - [HSP77_HUMAN]	2,53	3,00	7
P06733	Alpha-enolase OS=Homo sapiens GN=ENO1 PE=1 SV=2 - [ENOA_HUMAN]	2,50	5,76	1
P59665	Neutrophil defensin 1 OS=Homo sapiens GN=DEFA1 PE=1 SV=1 - [DEF1_HUMAN]	2,48	9,57	2
A0A0A0MS15	Immunoglobulin heavy variable 3-49 OS=Homo sapiens GN=IGHV3-49 PE=3 SV=1 - [HV349_HUMAN]	2,44	7,56	1
P01023	Alpha-2-macroglobulin OS=Homo sapiens GN=A2M PE=1 SV=3 - [A2MG_HUMAN]	2,42	1,36	2
P01624	Immunoglobulin kappa variable 3-15 OS=Homo sapiens GN=IGKV3-15 PE=1 SV=2 - [KV315_HUMAN]	2,37	7,83	2
A0A0C4DH34	Immunoglobulin heavy variable 4-28 OS=Homo sapiens GN=IGHV4-28 PE=3 SV=1 - [HV428_HUMAN]	2,35	7,69	1
P01714	Immunoglobulin lambda variable 3-19 OS=Homo sapiens GN=IGLV3-19 PE=1 SV=2 - [LV319_HUMAN]	2,30	8,04	1
P02771	Alpha-fetoprotein OS=Homo sapiens GN=AFP PE=1 SV=1 - [FETA_HUMAN]	2,30	4,27	1
P31946	14-3-3 protein beta/alpha OS=Homo sapiens GN=YWHAB PE=1 SV=3 - [1433B_HUMAN]	2,26	9,76	7
P01825	Immunoglobulin heavy variable 4-59 OS=Homo sapiens GN=IGHV4-59 PE=1 SV=2 - [HV459_HUMAN]	2,24	7,76	6
P49913	Cathelicidin antimicrobial peptide OS=Homo sapiens GN=CAMP PE=1 SV=1 - [CAMP_HUMAN]	2,21	5,29	1
Q66K66	Transmembrane protein 198 OS=Homo sapiens GN=TMEM198 PE=1 SV=1 - [TM198_HUMAN]	2,18	2,50	1
P14618	Pyruvate kinase PKM OS=Homo sapiens GN=PKM PE=1 SV=4 - [KPYM_HUMAN]	2,15	1,51	1
P26038	Moesin OS=Homo sapiens GN=MSN PE=1 SV=3 - [MOES_HUMAN]	2,13	1,56	3
Q9BQE3	Tubulin alpha-1C chain OS=Homo sapiens GN=TUBA1C PE=1 SV=1 - [TBA1C_HUMAN]	2,12	2,00	3
Q00610	Clathrin heavy chain 1 OS=Homo sapiens GN=CLTC PE=1 SV=5 - [CLH1_HUMAN]	2,10	0,54	1
Q8NI35	InaD-like protein OS=Homo sapiens GN=PATJ PE=1 SV=3 - [INADL_HUMAN]	1,93	0,33	1
A0A0B4J1V0	Immunoglobulin heavy variable 3-15 OS=Homo sapiens GN=IGHV3-15 PE=3 SV=1 - [HV315_HUMAN]	1,87	5,88	3
P07437	Tubulin beta chain OS=Homo sapiens GN=TUBB PE=1 SV=2 - [TBB5_HUMAN]	1,74	5,41	9
O60292	Signal-induced proliferation-associated 1-like protein 3 OS=Homo sapiens GN=SIPA1L3 PE=1 SV=3 - [SI1L3_HUMAN]	1,72	0,73	1
A0A0B4J1U7	Immunoglobulin heavy variable 6-1 OS=Homo sapiens GN=IGHV6-1 PE=3 SV=1 - [HV601_HUMAN]	1,70	5,79	1
P02774	Vitamin D-binding protein OS=Homo sapiens GN=GC PE=1 SV=1 - [VTDB_HUMAN]	1,63	1,48	1
P27216	Annexin A13 OS=Homo sapiens GN=ANXA13 PE=1 SV=3 - [ANX13_HUMAN]	0,00	2,22	1
Q96G01	Protein bicaudal D homolog 1 OS=Homo sapiens GN=BICD1 PE=1 SV=3 - [BICD1_HUMAN]	0,00	1,13	1
Q8NG31	Kinetochore scaffold 1 OS=Homo sapiens GN=KNL1 PE=1 SV=3 - [KNL1_HUMAN]	0,00	0,51	1
Q14839	Chromodomain-helicase-DNA-binding protein 4 OS=Homo sapiens GN=CHD4 PE=1 SV=2 - [CHD4_HUMAN]	0,00	0,89	1
P0CG12	Chromosome transmission fidelity protein 8 homolog isoform 2 OS=Homo sapiens GN=CHTF8 PE=1 SV=1 - [CTF8A_HUMAN]	0,00	2,67	1
Q9H5Z1	Probable ATP-dependent RNA helicase DHX35 OS=Homo sapiens GN=DHX35 PE=1 SV=2 - [DHX35_HUMAN]	0,00	1,56	1
Q9Y6K1	DNA (cytosine-5)-methyltransferase 3A OS=Homo sapiens GN=DNMT3A PE=1 SV=4 - [DNM3A_HUMAN]	0,00	1,43	1
A6ND36	Protein FAM83G OS=Homo sapiens GN=FAM83G PE=1 SV=2 - [FA83G_HUMAN]	0,00	1,94	1
Q16676	Forkhead box protein D1 OS=Homo sapiens GN=FOXD1 PE=1 SV=1 - [FOXD1_HUMAN]	0,00	2,37	1
P16260	Graves disease carrier protein OS=Homo sapiens GN=SLC25A16 PE=1 SV=3 - [GDC_HUMAN]	0,00	7,23	1
P14866	Heterogeneous nuclear ribonucleoprotein L OS=Homo sapiens GN=HNRNPL PE=1 SV=2 - [HNRPL_HUMAN]	0,00	5,94	1
Q9P267	Methyl-CpG-binding domain protein 5 OS=Homo sapiens GN=MBD5 PE=1 SV=3 - [MBD5_HUMAN]	0,00	0,94	1
Q86YW9	Mediator of RNA polymerase II transcription subunit 12-like protein OS=Homo sapiens GN=MED12L PE=1 SV=2 - [MD12L_HU	0,00	0,89	1
Q9NXD2	Myotubularin-related protein 10 OS=Homo sapiens GN=MTMR10 PE=1 SV=3 - [MTMRA_HUMAN]	0,00	3,99	1
P35579	Myosin-9 OS=Homo sapiens GN=MYH9 PE=1 SV=4 - [MYH9_HUMAN]	0,00	0,77	2
Q8NEV4	Myosin-IIIa OS=Homo sapiens GN=MYO3A PE=1 SV=2 - [MYO3A_HUMAN]	0,00	1,05	1
Q8WVE0	EEF1A lysine methyltransferase 1 OS=Homo sapiens GN=EEF1AKMT1 PE=1 SV=1 - [EFMT1_HUMAN]	0,00	5,61	1
Q6P3X8	PiggyBac transposable element-derived protein 2 OS=Homo sapiens GN=PGBD2 PE=2 SV=1 - [PGBD2_HUMAN]	0,00	4,73	1
Q15269	Periodic tryptophan protein 2 homolog OS=Homo sapiens GN=PWP2 PE=2 SV=2 - [PWP2_HUMAN]	0,00	2,07	1
P24928	DNA-directed RNA polymerase II subunit RPB1 OS=Homo sapiens GN=POLR2A PE=1 SV=2 - [RPB1_HUMAN]	0,00	0,81	1
Q8TEQ0	Sorting nexin-29 OS=Homo sapiens GN=SNX29 PE=1 SV=3 - [SNX29_HUMAN]	0,00	3,69	1
Q6ZRS2	Helicase SRCAP OS=Homo sapiens GN=SRCAP PE=1 SV=3 - [SRCAP_HUMAN]	0,00	0,25	1
Q9ULQ1	Two pore calcium channel protein 1 OS=Homo sapiens GN=TPCN1 PE=1 SV=3 - [TPC1_HUMAN]	0,00	1,84	1
Q8NG11	Tetraspanin-14 OS=Homo sapiens GN=TSPAN14 PE=1 SV=1 - [TSN14_HUMAN]	0,00	2,96	1
P42681	Tyrosine-protein kinase TXK OS=Homo sapiens GN=TXK PE=1 SV=3 - [TXK_HUMAN]	0,00	4,36	1

P15498	Proto-oncogene vav OS=Homo sapiens GN=VAV1 PE=1 SV=4 - [VAV_HUMAN]	0,00	0,83	1
P52747	Zinc finger protein 143 OS=Homo sapiens GN=ZNF143 PE=1 SV=2 - [ZN143_HUMAN]	0,00	2,66	1

Supplementary table 5

Gene	Forward primer	Reverse primer
IFNA	GGTGACAGAGACTCCCCTGA	CAGGCACAAGGGCTGTATTTCTT
IRF7	GCTGGACGTGACCATCATGTA	GGGCCGTATAGGAACGTGC
IL33	GTGACGGTGTTGATGGTAAGAT	AGCTCCACAGAGTGTTCCTTG
GAPDH	CATGTTCCAATATGATTCCACC	GATGGGATTTCCATTGATGAC
HPRT1	GACCAGTCAACAGGGGACAT	CTTGCGACCTTGACCATCTT

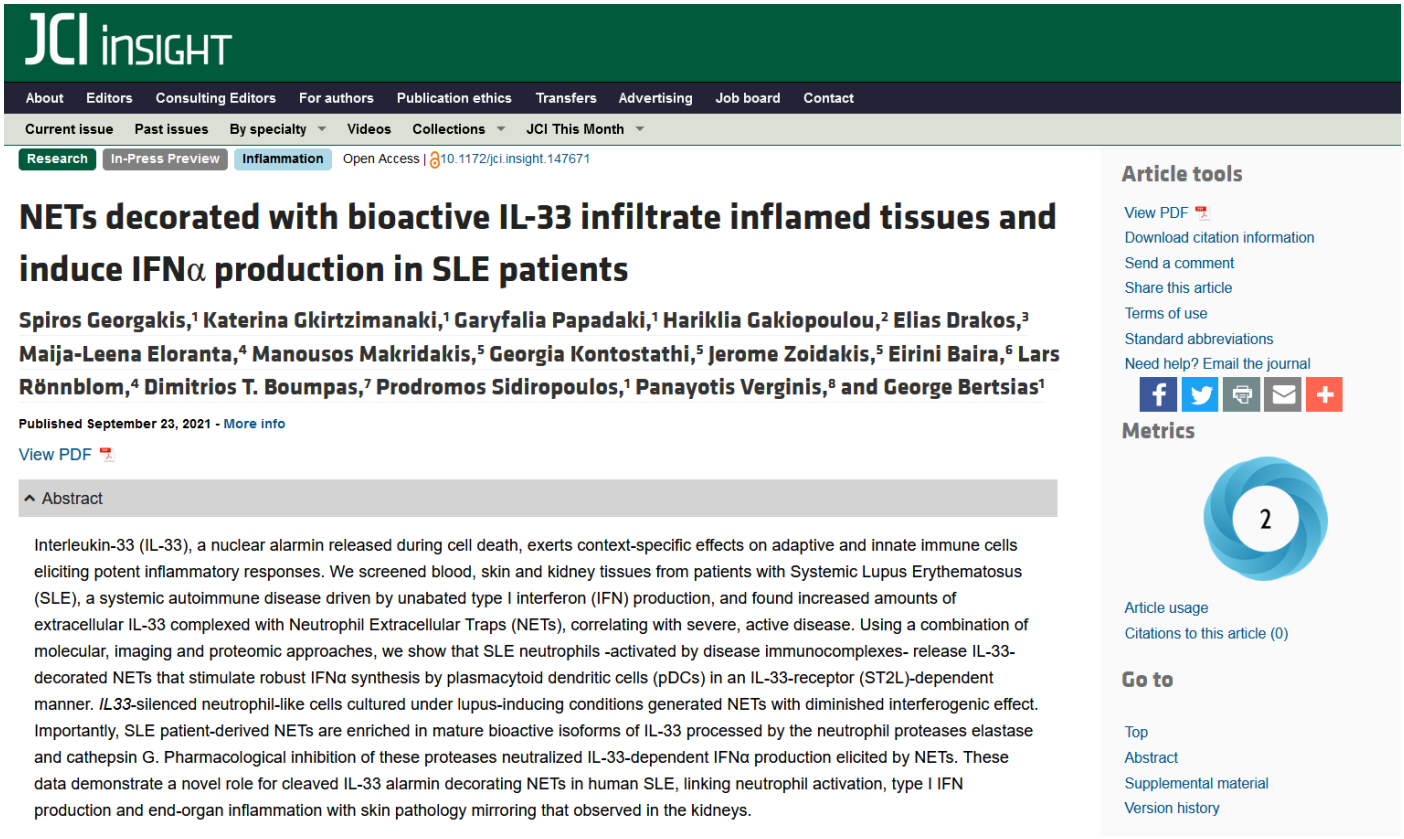

JCI insight

About Editors Consulting Editors For authors Publication ethics Transfers Advertising Job board Contact

Current issue Past issues By specialty Videos Collections JCI This Month

Research In-Press Preview Inflammation Open Access | 10.1172/jci.insight.147671

NETs decorated with bioactive IL-33 infiltrate inflamed tissues and induce IFNα production in SLE patients

Spiros Georgakis,[1] Katerina Gkirtzimanaki,[1] Garyfalia Papadaki,[1] Hariklia Gakiopoulou,[2] Elias Drakos,[3] Maija-Leena Eloranta,[4] Manousos Makridakis,[5] Georgia Kontostathi,[5] Jerome Zoidakis,[5] Eirini Baira,[6] Lars Rönnblom,[4] Dimitrios T. Boumpas,[7] Prodromos Sidiropoulos,[1] Panayotis Verginis,[8] and George Bertsias[1]

Published September 23, 2021 - More info

View PDF

Abstract

Interleukin-33 (IL-33), a nuclear alarmin released during cell death, exerts context-specific effects on adaptive and innate immune cells eliciting potent inflammatory responses. We screened blood, skin and kidney tissues from patients with Systemic Lupus Erythematosus (SLE), a systemic autoimmune disease driven by unabated type I interferon (IFN) production, and found increased amounts of extracellular IL-33 complexed with Neutrophil Extracellular Traps (NETs), correlating with severe, active disease. Using a combination of molecular, imaging and proteomic approaches, we show that SLE neutrophils -activated by disease immunocomplexes- release IL-33-decorated NETs that stimulate robust IFNα synthesis by plasmacytoid dendritic cells (pDCs) in an IL-33-receptor (ST2L)-dependent manner. *IL33*-silenced neutrophil-like cells cultured under lupus-inducing conditions generated NETs with diminished interferogenic effect. Importantly, SLE patient-derived NETs are enriched in mature bioactive isoforms of IL-33 processed by the neutrophil proteases elastase and cathepsin G. Pharmacological inhibition of these proteases neutralized IL-33-dependent IFNα production elicited by NETs. These data demonstrate a novel role for cleaved IL-33 alarmin decorating NETs in human SLE, linking neutrophil activation, type I IFN production and end-organ inflammation with skin pathology mirroring that observed in the kidneys.

Article tools

View PDF
Download citation information
Send a comment
Share this article
Terms of use
Standard abbreviations
Need help? Email the journal

Metrics

2

Article usage
Citations to this article (0)

Go to

Top
Abstract
Supplemental material
Version history

Clinical Immunology 216 (2020) 108445

Contents lists available at ScienceDirect

Clinical Immunology

journal homepage: www.elsevier.com/locate/yclim

Review Article

Update on the cellular and molecular aspects of lupus nephritis

Eleni Frangou[a], Spyros Georgakis[b,c,d], George Bertsias[b,c,d,*]

[a] Department of Nephrology, Limassol General Hospital, Limassol, Cyprus and Biomedical Research Foundation of the Academy of Athens, Athens, Greece
[b] Rheumatology, Clinical Immunology and Allergy, University of Crete Medical School, Greece
[c] Institute of Molecular Biology and Biotechnology, Foundation for Research and Technology - Hellas (FORTH), Heraklion, Greece
[d] University Hospital of Iraklio, Iraklio, Greece

ARTICLE INFO

Keywords:
Autoantibodies
Cytokines
Macrophages
Podocytes
Renal tubular epithelial cells
RNA sequencing

ABSTRACT

Recent progress has highlighted the involvement of a variety of innate and adaptive immune cells in lupus nephritis. These include activated neutrophils producing extracellular chromatin traps that induce type I interferon production and endothelial injury, metabolically-rewired IL-17–producing T-cells causing tissue inflammation, follicular and extra-follicular helper T-cells promoting the maturation of autoantibody-producing B-cells that may also sustain the formation of germinal centers, and alternatively activated monocytes/macrophages participating in tissue repair and remodeling. The role of resident cells such as podocytes and tubular epithelial cells is increasingly recognized in regulating the local immune responses and determining the kidney function and integrity. These findings are corroborated by advanced, high-throughput genomic studies, which have revealed an unprecedented amount of data highlighting the molecular heterogeneity of immune and non-immune cells implicated in lupus kidney disease. Importantly, this research has led to the discovery of putative pathogenic pathways, enabling the rationale design of novel treatments.

Clinical Immunology 206 (2019) 42–52

Contents lists available at ScienceDirect

Clinical Immunology

journal homepage: www.elsevier.com/locate/yclim

Cytokine targets in lupus nephritis: Current and future prospects

Christina Adamichou[a,b], Spyros Georgakis[b], George Bertsias[a,b,*]

[a] Rheumatology, Clinical Immunology and Allergy, University Hospital of Iraklio, Greece
[b] Laboratory of Rheumatology, Autoimmunity and Inflammation, University of Crete Medical School, Greece

ARTICLE INFO

Keywords:
Autoimmune diseases
Kidney
Lymphocytes
Autoantibodies
Biologics
Personalized medicine

ABSTRACT

Despite advancements in the care of lupus nephritis, a considerable proportion of patients may respond poorly or flare while on conventional immunosuppressive agents. Studies in murine and human lupus have illustrated a pathogenic role for several cytokines by enhancing T- and B-cell activation, autoantibodies production and affecting the function of kidney resident cells, therefore supporting their potential therapeutic targeting. To this end, there is limited post-hoc randomized evidence to suggest beneficial effect of belimumab, administered on top of standard-of-care, during maintenance therapy in lupus nephritis. Type I interferon receptor blockade has yielded promising results in preliminary SLE trials yet data on renal activity are unavailable. Conversely, targeting interleukin-6 and interferon-γ both failed to demonstrate a significant renal effect. For several other targets, preclinical data are encouraging but will require confirmation. We envision that high-throughput technologies will enable accurate patient stratification, thus offering the opportunity for personalized implementation of cytokine-targeting therapies.